Stony Brook University

Effect of Anionic Lipids upon the Topography of Membrane-Inserted Hydrophobic Helices

A dissertation Presented

By

Khurshida Shahidullah

to

The Graduate School

In Partial Fulfillment of the Requirements

For the Degree of

Doctor of Philosophy

in

Chemistry

Stony Brook University

December 2008

Stony Brook University
The Graduate School

Khurshida Shahidullah

We, the dissertation committee for the above candidate for the
Doctor of Philosophy degree,
hereby recommend acceptance of this dissertation.

Erwin London, Ph.D.
Dissertation Advisor
Professor
Department of Biochemistry and Cell Biology

Daniel P. Raleigh, Ph.D.
Chairperson of the dissertation committee
Professor
Department of Chemistry

Elizabeth Boon, Ph.D.
Third member of the dissertation committee
Assistant Professor
Department of Chemistry

Robert S. Haltiwanger, Ph.D.
Outside member
Professor and Interim Chair
Department of Biochemistry and Cell Biology

This dissertation is accepted by the Graduate School

Lawrence Martin
Dean of Graduate School

Abstract of the Dissertation

Effect of Anionic Lipids upon the Topography of Membrane-Inserted Hydrophobic Helices

by

Khurshida Shahidullah

Doctor of Philosophy

in

Chemistry

Stony Brook University

2008

To investigate the effect of lipid structure upon the membrane topography of hydrophobic helices, the behavior of hydrophobic peptides was studied in model membrane vesicles. To define topography, fluorescence and fluorescence quenching methods were used to determine the location of a Trp at the center of the hydrophobic sequence. For peptides with cationic residues flanking the hydrophobic sequence, the stability of the transmembrane (TM) configuration (relative to a *membrane-bound* non-TM state) increased as a function of lipid composition in the order: 1:1 (mol:mol) 1-palmitoyl-2-oleoyl phosphatidylcholine (POPC):1-palmitoyl-2-oleoyl phosphatidylethanolamine (POPE) ~ 6:4 POPC:cholesterol < POPC ~ dioleoylphosphatidylcholine (DOPC) < dioleoylphosphatidylglycerol (DOPG) ≤ dioleoylphosphatidylserine (DOPS), indicating that the anionic lipids DOPG and DOPS most strongly stabilized the TM configuration. TM-stabilization was near-maximal at 20-30mol% anionic lipid, physiologically relevant values. TM-stabilization by anionic lipid was observed for hydrophobic sequences with diverse set of sequences (including polyAla), diverse lengths (from 12-22 residues), and various cationic flanking residues

(H, R or K), but not when the flanking residues were uncharged. TM-stabilization by anionic lipid was also dependent on the number of cationic residues flanking the hydrophobic sequence, but was still significant with only one cationic residue flanking each end of the peptide. These observations are consistent with TM-stabilizing effects being electrostatic in origin. However, Trp located more deeply in 100mol%DOPS vesicles relative to 100mol%DOPG vesicles, and peptides in DOPS vesicles showed increased helix formation relative to DOPG and all other lipid compositions. These observations fit a model in which DOPS anchors flanking residues near the membrane surface more strongly than does DOPG, and/or increases the stability of the TM state to a greater degree than DOPG. TM-stabilization by anionic lipids was also observed for shifted TM helices (flanked on both sides by cationic residues) in which TM helix transverse movement within the bilayer was suppressed in 20 mol percent anionic lipid containing vesicles compare to the uncharged vesicles.

Topological consequence of hydrophilic mutations and anionic lipid upon the ErbB2 receptor(often over expressed in breast cancer) TM domain was also studied. Mutation at 664 that replaces a V residue with a hydrophilic residue pushed a part of the TM helix out of the membrane toward the N-terminus resulting in a shorter TM helix relative to the longer WT TM helix. Contrary to the artificial shifted TM sequences, 20% anionic lipid did not have any significant TM stabilizing effect upon the mutant ErbB2 shifted TM structures. ErbB2 have an abundance of positively charged residues only at the C-terminal end which can interact with the anionic lipid but the helix shift happened in the opposite direction so the shifted structures was unaffected in the presence of anionic lipids. However, helix shift toward the C-terminus induced by the hydrophilic mutation near the C-terminus region in uncharged vesicles was greatly suppressed in anionic lipid containing vesicles. Hence, TM helix shift can not happen toward the cytoplasmic side of the membrane where the TM protein juxtamembrane (JM) region rich in positively charged residues tend to reside due to their affinity for anionic lipid in cytofacial membrane.

This work is dedicated to

My dear husband Syed Shahidullah

Table of Contents

List of Abbreviations

TM	Transmembrane
JM	Juxtamembrane
pLA	poly Leucine Alanine peptide
HPLC	High performance liquid chromatography
MALDI-TOF	Matrix assisted laser desorption ionization time of flight
DOPC	Dioleylphosphatidylcholine
DEuPC	Dierucoylphophatidylcholine
POPC	Palmitoylphosphatidylcholine
POPE	Palmitoylphosphatidyethanolamine
DOPG	Dioleylphosphatidylglycerol
DOPS	Dioleylphosphatidylserine
λmax	Fluorescence emission maximum
10-DN	10-doxylnonadecane
WT	wild type

List of Figures

List of Tables

Acknowledgement

I would like to thank all the people who have helped me and inspired in the completion of this doctoral study.

First, I would like to express my deep and sincere gratitude to my advisor Dr. Erwin London. He believed in me and gave me the chance to learn and eventually master the principles of peptide-lipid interactions and fluorescence techniques. His enthusiasm, inspiration and constant guidance had helped me navigate through my doctoral study. He was always accessible for any help with my research and very understanding about personal issues such as impending motherhood in my case which made my life as a PhD student and a mother little easier.

I would like to thank my colleagues at London lab for providing a stimulating and fun environment to learn and grow. I am thankful to Shyam for his helpful suggestions, discussions and friendship. Thanks to Greg for training me when I joined the lab. I deeply appreciate Omar and Megha's help and friendship. I am also grateful to Jie, Bing, Lindsay, Hui-Ting, Priya and Mi-Jin for their help.

I wish to thank my mother for her help in taking care of my children and my house during my doctoral research. Especially during the first year her help was crucial. I also like to thank my father, brothers and sisters for their love. I am grateful to my siblings (Lucy, Shakil, Jessy and Nishi) as well as Anna and Hira for their help with my kids. I wish to thank my relatives and family friends in New York for their moral support.

Most importantly my deepest gratitude to my husband for the sacrifices he made in order for me to pursue my PhD degree. This dissertation would not have been possible without his support, guidance and encouragement.

Lastly, my two kids Sabiq and Keyan have been a great source of joy and motivation during this long journey.

Chapter 1

Introduction

Integral membrane proteins are embedded in biological membrane and perform a variety of biological functions such as relaying signals and transporting molecules across the membrane. It is estimated that integral membrane proteins comprise one third of the total proteins encoded by the cellular genome[1]. The most common type of integral membrane proteins are transmembrane (TM) proteins that span the membrane with hydrophobic α-helices of 15-25 amino acids in length[2; 3; 4].

Transmembrane (TM)/non-TM equilibrium

How does a membrane protein (MP) find its way into the membrane? Constitutive MP's tend to insert into the membrane co-translationaly. In this process during protein synthesis the ribosome attaches itself transiently to a complex of membrane proteins referred to as a translocon. Newly synthesized proteins get inserted into the membrane through the translocon tunnel [5; 6; 7]. Non-constitutive membrane proteins such as toxins and antimicrobial peptides bypass the translocon and insert into the membrane from solution [7; 8; 9]. Even though the insertion pathway may involve a translocon , MP's are thought to be equilibrium structures[10; 11]. So the energetics of membrane insertion can be analyzed by a thermodynamic model where membrane protein can interact with aqueous solvent, membrane interfacial region, and a hydrophobic membrane interior mostly composed of hydrocarbon chain. (Figure 1.1). Even though both the membrane surface-bound and non bound helices are non-transmembrane(TM) structures there are two clearly distinct equilibria that govern TM stability. The first is the equilibrium between the unbound and membrane bound non-TM states (governed by K1) and the second is the equilibrium between the TM and bound non-TM state (governed by K2). In case of unbound non-TM state (non-TM state 1) K2 might not be affected by K1 but overall insertion is affected because the amount of the TM state is affected by the amount of the surface bound non-TM state. In contrast, there is only one equilibrium (K2) when the non-TM state is always surface bound (non-TM 2) and thus when a helix will interconvert between TM and non-TM states can lead to a better understanding of the structure/function relationship of membrane-inserted hydrophobic helices.

Background and Significance of TM/non-TM equilibrium

The equilibrium between TM and non-TM topographies is especially significant for post translational membrane insertion of proteins and protein toxins. Bacterial protein toxins form the most widely studied examples of proteins with this behavior. Helix 8 and 9 of diphtheria toxin TM domain undergo TM/non-TM interconversion that is thought to be essential for translocation [12; 13]. This type of interconversion is also common in membrane inserted segments of β-barrel toxins, including anthrax protective antigen [14], and cholesterol dependant cytolysins [15; 16]. Interconversion between TM and non-TM state is unlikely for TM helices flanked on both sides of the bilayer by large soluble domains. However it can occur in helical hairpins connected by short hydrophilic link (e.g. helix 8 and 9 of hairpin of diphtheria toxin and helices in some colicins)[12; 13; 17] or in the case of proteins with hydrophobic anchoring tail sequences capped at one end with short hydrophilic sequences. Most notable examples of proteins with short tail anchoring sequence include Bcl family proteins (have a key role in apoptosis) [18], and a number of endoplasmic reticulum enzymes. The tail sequences of these proteins are involved in post translational membrane insertion[19]. TM/non-TM equilibria is also important for LAT protein (involved in signal transduction)[20], posttranslational insertion of polio virus 3A protein [21], and antimicrobial peptides [22]. TM/non-TM equilibria can be especially important in determining the fate of proteins with borderline hydrophobic sequences such sequences may be abundant in nature as indicated by the genomic analysis [23].

Techniques for Distinguishing between TM/non-TM topography

TM helices have been studied in detergent, membrane mimetic systems (micelles, bicelles or lipid bilayer) and in cell based systems using a wide variety of biochemical and spectroscopic techniques, each having its own advantages and disadvantages which will be discussed in the later in this section. Unlike soluble proteins TM helices of membrane proteins are to a large degree independently folding units [24]. As a result, much insight about the membrane protein folding and structure has come from the studies of individual hydrophobic helices [25; 26; 27]. A widely used approach to gain highly detailed information about TM helix behavior, including their conformation and membrane

orientation, is NMR. Bechinger and colleagues have used solid state NMR to investigate the TM stability of helical hydrophobic sequences containing pH sensitive Histidines by measuring the molecular alignment of samples relative to the magnetic field[28; 29; 30; 31]. Drawbacks of the NMR approach are low sensitivity, which necessitates a large amount of materials and the fact that an isotope is required in the helix of interest. Optical techniques such as FT-IR (fourier transform infrared spectrocopy) [32; 33] and oriented circular dichroism (OCD) [34; 35; 36]are also used to determine the helix alignment in bilayers. Samples placed in an uniaxially oriented bilayer are hit with incident light at normal and oblique angles with respect to the bilayer plane. In OCD, the presence or absence of a negative band around 208nm indicates a surface or a transmembrane helix respectively. In polarized ATR-FTIR spectroscopy, membrane alignment of helices is determined by the dichroic ratio (R), a ratio of molecular absorption due to parallel versus perpendicular incident light. Unlike NMR, FT-IR and OCD method do not require any isotope level and the sensitivity is higher. However, FT-IR and OCD methods can not distinguish a mixture of two different conformations from an average one. Fluorescence spectroscopy is a highly sensitive and widely used technique to measure various aspects of helix behavior. Polarity-sensitive fluorescent probe are routinely used to determine the location and orientation of TM helices in lipid bilayer [26; 37; 38; 39]. Fluorescent properties of these probes (intensity and or wavelength) change in response to the polarity of the local environment. Thus these parameters can be used to monitor helix behavior. Fluorescence quenching is another spectroscopic parameter to examine TM helix behavior [39; 40; 41].Quenching is a loss fluorescence intensity of fluorophore that is near a quencher molecule due to the decrease in quantum yield of fluorophore. Using tryptophan (trp) fluorescence quenching Deber and Liu [42]observed that membrane association of hydrophobic helices can be modulated by anionic lipid in bilayers. In addition, heterogeneous TM topography can be identified by using two different quenchers designed to quench various Trp location [43].One disadvantage of this system is that you need to place a fluorescent probe in the hydrophobic sequence, which may perturb the structure.

There are also biological methods that can be used to characterize TM/non-TM topography. The glycosylation mapping technique developed by von Heijne and colleagues quantified the efficiency of membrane integration of TM segments into mammalian cell mediated by Sec 61 translocon [44]. In this approach, a test hydrophobic sequence of interest flanked by N-linked glyscosylation sites is engineered into a carrier protein, and degree of membrane integration is quantified by singly versus doubly glycosylated sites (Figure 2). If the test segment is secreted and so delivered to the luminal space then both glyscosylation acceptor sites are glycosylated. In contrast, if it is inserted into the membrane in a TM form, then only a single site become glycosylated (Figure 1.2). Singly and doubly glycosylated species are quantified by SDS-PAGE. This translocon-based assay is powerful and gives biologically relevant results. Using this approach, a complete biological hydrophobicity scale was derived that predicts the contribution of each of the 20 amino acid residues to the TM/non-TM equilibrium[44]. In addition, it was found that the position of a residue within the hydrophobic sequence greatly affected the TM insertion of the sequence. They did a scan where two identical amino acid residues were moved symmetrically from the center of the sequence toward the end, and found that aromatic residues (Trp, Tyr) and charged residues (Lys, Arg) greatly reduced membrane insertion when placed toward the center of the hydrophobic sequence [45].

However, there are some limitations to this technique. First, there is no control over the experimental conditions like lipid composition and pH. This is unlike the model membrane system which will be discussed in the next paragraph. Another caveat is that the TM helix integration event taking place in the translocon might not reflect the true thermodynamic equilibrium. Thus, the results might not be applicable to topography changes that take place after the release of a protein from translocon.

Lipid model membrane based studies of amino acid hydrophobic tendency could be used to generate similar scale but data so far is incomplete[28; 46; 47]. However, it has been a valuable aproach because additional information about TM helix behavior under different pH and lipid bilayer width was gained by using this system. Recently,

Aisenbrey et al came up with a method to measure the tendency of amino acid residues to be in the interface or in the membrane interior which can yield a more complete and exact scale [33]. Both model membrane and translocon based results regarding the hydrophobicity of amino acids mostly coincide. For instance, position dependent effects on TM stability due to polar and charged residues in hydrophobic helices detected in the translocon system have also been seen in model membranes [46].

Amino Acid composition of Hydrophobic Helices and TM stability

Amino acid sequence is an important determinant of the stability of TM helices. TM helices are primarily composed of hydrophobic amino acids (Leu, Val, Ile) because they can avoid unfavorable interaction with water by being within the non-polar membrane interior. Polar and ionizable residues are less abundant in TM segments due to the unfavorable energetics for exposure of hydrophilic residues to a non-polar environment [23; 48; 49].

However, with the growth of membrane protein databases there is more evidence of hydrophilic residues being very common within the TM domain of membrane proteins. Studies conducted in our lab with model hydrophobic helices shows that a single polar (Ser, Pro, His) or ionizable residue (Lys,Asp) can be tolerated in the core of hydrophobic (poly Leu) sequences without perturbing the TM conformation [47; 50]. In contrast, using a test sequence composed of poly Leu-Ala Hessa et al found that a single charged or polar residue when placed in the middle of the hydrophobic sequence can destabilize the TM state sufficiently to perturb the fraction of TM helix formation[51]. Thus a TM segment containing an internal polar or charged residue can adopt a stable TM state only if the other residues in the sequence are sufficiently hydrophobic.

Charged residues in TM segments can also be tolerated if required by specific protein function. Though the topography of S4 helix, an Arg rich sequence, in the of voltage-sensitive K+ channel, is still controversial it is believed to be a TM helix located within the lipid bilayer [52]. Polar and charged amino acid residues are also evident within the TM segment of other membrane pumps and ion channels [53; 54].

This brings up the topic of the minimum hydrophobicity requirement for a sequence to be able to insert into lipid bilayer in TM form. A model peptide with a hydrophobic stretch of all Leu residues (16-24) can incorporate into lipid bilayer[55; 56; 57; 58], which is consistent with the strong hydrophobicity of leucine in all thermodynamic scales. On the other hand, polyalanine stretches seem to be at the threshold of minimum hydrophobicity needed to form a stable transbilayer helix, and several studies [30; 59; 60; 61]have shown that poly Ala sequences (18-23 residues) can not form stable TM helix *in vitro*.

Using translocon-based glyscosylation studies it was shown that for a transmembrane segment of typical length (19 residues) composed of Leu and Ala residues, 5 Leu residues are required for stable membrane insertion [44]. This threshold prediction agrees nicely with Wimley and White octanol scale [7; 62]. A similar observation was also reported in model membrane studies. Using a poly Leu-Ala containing alpha-helical segment of 24 residues Lewis et al found that Leu/Ala ratios of greater than 7/17 are required for stable transmembrane insertion [27]. Needless to say stable membrane insertion of a hydrophobic sequence can also be affected by other parameters like sequence length and flanking residues and helix-helix interaction, which will be discussed in following sections.

Helix length and TM topography

Helix length is another important parameter that can control TM stability. Studies in bacterial and eukaryotic systems have shown that quite short sequences can actually form transmembrane helices [63; 64]. Though short TM helices are common in membrane proteins [65; 66; 67] they have not been studied in great detail. Behavior of short TM helices might be of interest in the length dependent sorting of TM sequences within the membrane compartments. TM segments of Golgi proteins are generally shorter (15 residues) than those of plasma membrane proteins (18-20 residues) as a result it has been proposed that membrane proteins with shorter hydrophobic sequence are retained in the Golgi in order to minimize hydrophobic mismatch[68; 69; 70; 71]. Since short hydrophobic

sequences tend to form TM states with moderate stability [55; 72] it is important to define how sequence controls their TM/non-TM equilibrium.

What is the minimum length of a hydrophobic sequence that can form a stable TM structure and how is it affected by the sequence? A study conducted in our lab revealed a weak dependance of minimum length on the sequence hydrophobicity [58]. Minimum length for TM formation in the case of all Leu sequence was 11-12 residues as opposed to 13 residues for moderately hydrophobic Leu-Ala sequences [55; 58]. These observations regarding minimum helix length and its dependence on hydrophobicity coincide nicely with the results obtained under in vivo conditions using glyscosylation mapping [67; 73].In one study, synaptobrevin2, a C-terminal tail anchoring protein was shown to insert into membrane with as few as 12 leucines [67].

Transverse positioning of helical sequences

Hydrophilic residues can alter the position of a TM helix within the bilayers, causing a transverse shift so that the hydrophilic residue can locate at or closer to the bilayer surface [44; 55; 74]as shown in Figure 1.3A. The TM helix can either move vertically or pivot around an anchoring point as a result of a change in transverse position. These movements can affect the protein function. Unlike soluble proteins, membrane proteins are positioned in a fixed plane relative to the membrane surface and two separate sequences might only interact properly when they are located on the same plane (Figure 1.3B). Also, a swinging motion of the TM helix might be amplified further away from the bilayer and it could effect the interaction of TM flanking domains. Unlike TM/non-TM interconversion, a switch between two different TM states can occur even when a TM helix is flanked on both sides by soluble domains and so it may be more common.

There are several examples in which transverse shifts in TM helix position appear to have an important role in function. It is well documented that vertical movement of TM helices in membranes turn bacterial chemoreceptors on and off [75; 76; 77]. Other examples include integrins [78] and fibroblast growth factor receptor 3 (FGFR3) [79]. Shifts

in TM helix position can also change the position of the juxtamembrane (JM) domains which can also affect protein function. For example, in cases in which ubiquitination involves the juxtamembrane Lys residues at the end of a TM sequence might be affected by altered JM position induced by TM helix shift [80; 81; 82]. It has also been suggested that proteolytic digestion by enzyme γ-secretase can be altered as result of change in substrate helix shift)[83; 84; 85]. This action can have important consequences because among other things this enzyme digests APP to form Aβ protein (involved in Alzheimer's disease)[83; 84; 85].

Pioneering studies using an earlier version of the glyscosylation mapping technique have reported the tendency of several hydrophilic residues to induce shifts the TM helix position [86; 87; 88; 89]. The earlier glycosylation mapping technique engineered several potential glycosylation acceptor sites downstream of test hydrophobic sequence into a model protein and based on the fact that ER enzyme oligosaccharide transferase (OST) can only glycosylate certain distance from the membrane, this technique was used to measure the TM helix boundary. Using this method, Monné et al found that hydrophilic mutations (Asp, Glu) within in the first turn of α-helices (but not at the center of the helices) induced a change in TM helix membrane boundary such that the hydrophilic residues located closer to the membrane surface[87]. It was also reported that Asp and Lys when placed on the opposite face of helix to prevent a salt bridge formation, the helix was partially pushed out of the membrane[86]. But when placed on the same side of the helix it did not induce any shift probably due to salt bridge formation[86]. Moreover, aromatic residues (Trp and Phe) at the center of the hydrophobic poly-Leu sequence induced a shift in TM helix position to locate them closer to the surface whereas Trp and Phe at the flanking poly-Leu sequence favored a shift increase their membrane insertion[89]. This is consistent with the tendency of Trp and Tyr to locate at the edge of the lipid bilayer[86].

A more detailed study of transverse helix shifting potential for the complete series of amino acid residues was reported recently from our lab for artificial helices in monounsaturated phosphatidylcholine vesicles using a fluorescence approach [90]. Highly

polar residues such as Asp, Gln, Glu had a greater tendency to move the TM helix position than the moderately polar or non-polar residues. Also, the TM helix shift was greater for charged form of the ionizable residues relative to their uncharged form[90].Both the glycosylation and fluorescence approaches had similar observation on the extent of helix shift being dependent on the nature of the hydrophilic residue.

JM (juxtamembrane) residues and Lipid Composition

Protein topology might also be dynamically controlled by lipid composition in some cases. For example the different lipid composition encountered by eukaryotic membrane proteins upon movement from one membrane compartment to another (e.g. ER to plasma membrane) might regulate the topology in each compartment. Anionic lipids are an integral part of biological membranes and may have an especially large impact on topography. There is enough evidence to suggest that interactions between anionic lipid head groups and positively charged residues of proteins or peptides can promote membrane association and or transport [42; 91; 92; 93].

The cytoplasmic end of the TM segments are often flanked by positively charged Lys and Arg residues and according to "positive inside rule"and these charged JM residues have been proposed to act as a topological determinant of TM helix orientation [94; 95; 96]. In addition, positively charged residues favored TM insertion into the membrane by sec61 translocon when placed at the cytoplasmic end of a transmembrane segment rather than the luminal end. It has been proposed that interaction between the negatively charged lipid headgroup in the cytofacial side of the membrane and the positively charged JM residues contribute to enhanced TM stability [51; 97]. In these translocon based experiments, the lipid composition is not controlled but the cytofacial leaflet probably contains anionic lipids. Despite that the role of anionic lipid and charged JM residues interaction in controlling TM non-TM topography has not been studied very well. Because lipid composition can be varied in lipid bilayers, model membrane should be ideal for such studies.

Charged JM residues can also alter the behavior of TM helices in the absence of anionic lipids. In neutral vesicles, charged flanking residues actually destabilized the TM state of a short hydrophobic sequence to a greater degree then when they are uncharged [58]. This makes sense because in the TM state they experience a local environment more hydrophobic than the aqueous solution and this environment is energetically unfavorable for charged residues.

Flanking JM residues can also have a significant effect on TM helix behavior in terms of helix-helix association and hydrophobic mismatch. Lew et al [98] noted that interaction between flanking residues can modulate helix association. Polypeptide sequences containing Leu residues flanked by LysAsp associated under physiological conditions in which the peptides had no net charge but not at low pH when Asp was protonated so that the peptide was cationic. This shows electrostatic repulsion between positively charged Lys residues can reduces helix-helix interaction in polypeptide sequences. In addition, flanking JM residues can affect how a TM helix responds to mismatch. Killian and colleagues reported that under condition of positive mismatch Lys flanked peptides tilted more than the Trp flanked ones, suggesting that these residues anchor differently at the membrane interface [99; 100; 101]. Lys-flanked sequences tolerated negative mismatch better than the Trp-flanked sequences mainly due to the long side chain of Lys which can snorkel[102; 103; 104]. Snorkeling refer to the fact that Arg and Lys residues have long side chains and they can stretch their side chain allowing the charged terminal group to reach into the lipid head group while keeping the C^{α} atom within the membrane[87].

Helix-helix association

One way for the membrane proteins to overcome the energetic cost of burying a hydrophilic residue into the membrane is by forming hydrogen bonds with a similar residue on another helix. This drives helix-helix association (oligomerization). Hence, helix-helix association can be an important determinant of TM stability. Studies in model membranes by the Degrado lab [105] as well as in biological membranes using the TOXCAT system (Figure 1.4) by Engelman and colleagues[106] observed that an

asparagine residue can drive association of transmembrane domains. Strong hydrogen bonding between membrane helices are thought to drive this interaction. Subsequent studies by these labs noted that highly polar and ionizable residues (Asp, Glu, His) within the TM sequence stabilized the formation of oligomers more than the weakly polar residues (Ser, Thr, Tyr) [107; 108]. Moderately polar side chains have been shown to favor transmembrane self-association/dimerization through H-bond. TOXCAT analysis of random library of sequences revealed that motif rich in serine and threonine such as xSxxSsxT or SXxxSSxxT tend to form dimers [109].

In addition, TM sequence context can [47] also play a significant role in the helix-helix association. It was shown that polar residues (Asp and Asn) introduced in the hydrophobic core of the TM segment of M13 bacteriophage coat protein promoted helix-helix association whereas interfacially placed Asp and Asp did not promote helix association [110]indicating that hydrogen bonding by polar residues can be modulated by other factor like the depth of the polar residues in the membrane.

Hydrophobic Mismatch

Hydrophobic mismatch can be defined as the difference between the hydrophobic thickness of the lipid bilayer and the length of the hydrophobic sequence that spans the bilayer. Hydrophobic mismatch can be of two types: positive mismatch occurs when hydrophobic length of the protein is longer than the hydrophobic thickness of the bilayer and the opposite situation leads to negative mismatch. Consequences of positive and negative mismatch are shown in Figure 1.5. Studies by Ren et al using lipids of various acyl chain lengths had shown that polyLeu helix TM insertion can be modulated by hydrophobic mismatch and cholesterol content [74]. Subsequent studies also showed that while a polyLeu sequence of 11 residues formed a surface bound non-TM sate in DOPC (a lipid with 18 carbon atom long acyl chain), 15,19,and 23 residue poly Leu sequences were able to adopt stable TM structure [55]. In addition, the longer sequence (23 residues) had a tendency to form oligomers under condition of positive mismatch. Therefore, hydrophobic mismatch can significantly affect the stability of the TM conformation giving rise to a non-TM topography or helix-helix association.

Transmembrane segments of membrane proteins usually vary from 15-24 residues [48; 49; 111] and membrane proteins encounters bilayer of different thicknes. Plasma membrane is generally thought to be thicker than the endoplasmic reticulum (ER) due to the higher cholesterol content[112]. So, it is not surprising that TM domains encounter hydrophobic mismatch. The behavior of membrane proteins has been shown to be affected by hydrophobic mismatch in several cases. For example, diphtheria toxin T domain adopts a non-TM structure (bilayer surface bound) in 18 carbon atom long acyl chain bilayer but in thinner bilayer with16 carbon long acyl chains it adopts a TM structure[12]. Mismatch can also affect the function of membrane proteins. Cytrochrome oxidase c activity is optimal in lipid bilayers with 18 carbon acyl chain but declines under positive or negative mismatch [113]. The effect of mismatch upon membrane protein conformation often may be less than expected because there is evidence suggesting that lipid bilayer sometimes adjusts its acyl chains to match the length of membrane protein [114; 115; 116].

Goal of this work: TM topography and lipid composition

As the studies above show the amino acid composition of TM segments is one major determinant of the topography and TM stability of membrane-inserted helices. Much less is known about the effect of lipid. Understanding how sequence and lipid composition can cause the TM helix to interconvert between different topographical states will improve our ability to predict membrane protein structure and function.

To do this, model hydrophobic helices were used to define the TM topography as a function of sequence and lipid composition. Model hydrophobic α-helices have been extensively used for sequence-structure studies of TM proteins because of their versatility. Our lab has investigated the principles of membrane protein structure by applying fluorescence and fluorescence quenching methods to studies of hydrophobic helices. In my study, these methods were used to define the structures of model membrane-inserted hydrophobic helices. The effect of sequence hydrophobicity (altered by varying Leu/Ala ratio) and bilayer lipid composition upon TM stability was

characterized. Also, hydrophobic sequences of different lengths were used to investigate if lipid composition affected the TM stability in the same fashion regardless of the TM length. The effect of lipid change upon the ability of hydrophilic residues to shift TM helix position was also studied. These latter studies included measuring the consequences of a hydrophilic mutation at the C-terminus of the TM domain of the ErbB2 receptor.

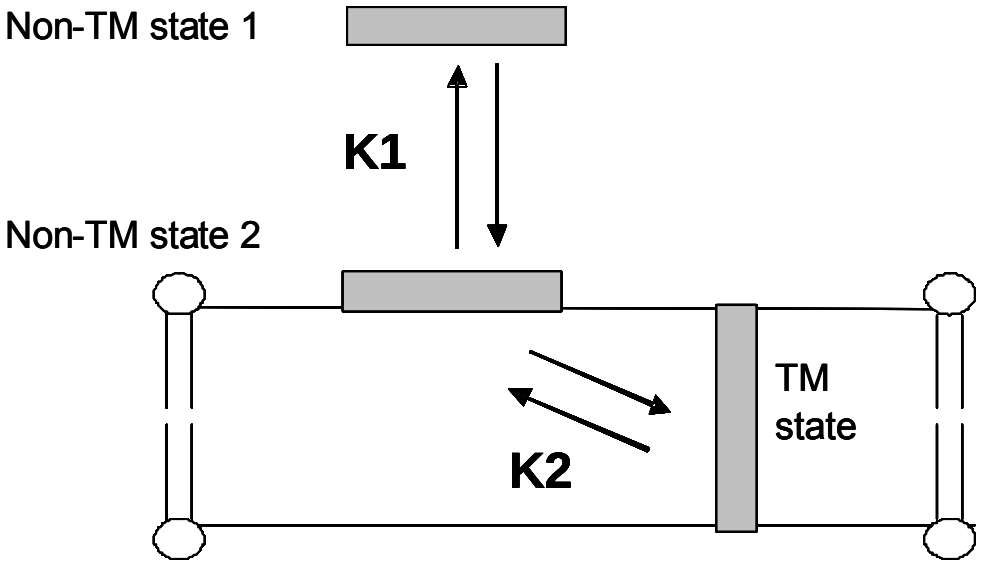

Figure1.1: Schematic model depicting the equilibrium between different transmembrane conformations. The grey rectangles represent transmembrane (TM) helices. K1 is equilibrium constant between the membrane surface bound helix (non-TM state 2) and non-bound helix in aqueous solution (non-TM state 1). K2 represents the equilibrium constant between the bilayer inserted TM state and non-TM state 2.

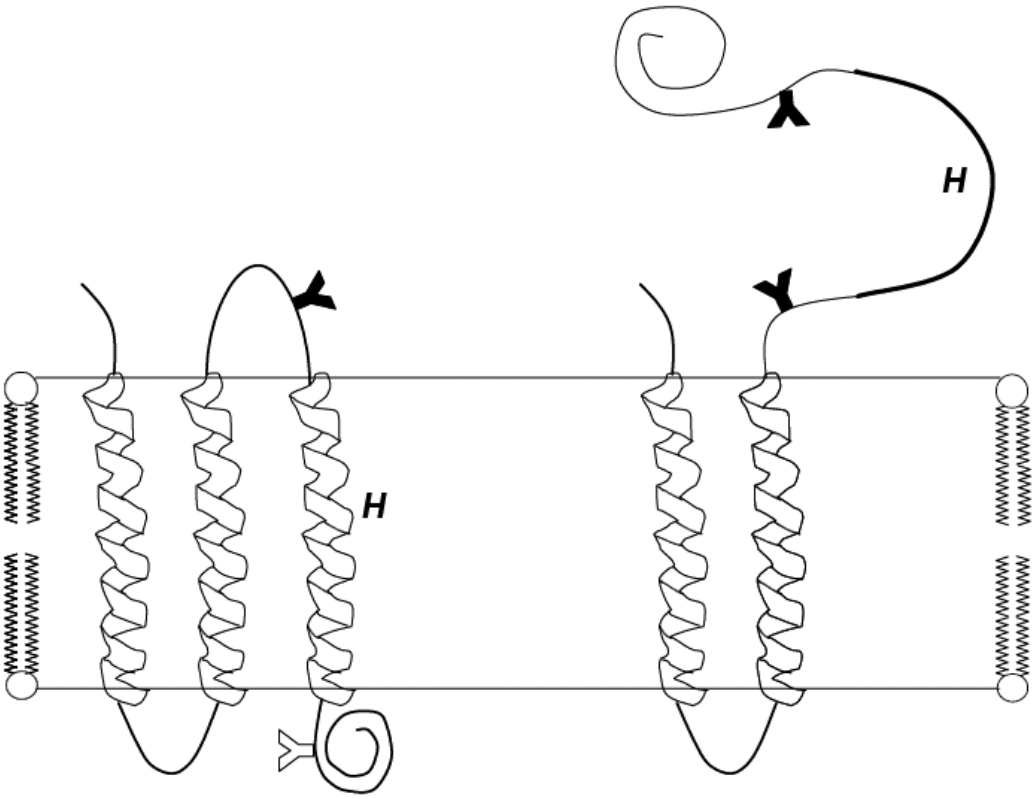

Figure 1.2. Schematic figure depicting the membrane integration of putative hydrophobic helices using glyscosylation mapping. Integration of hydrophobic segment H leads to one glyscosylation site (filled Y) and one unglycosylated sites (open Y) whereas translocation of the sequence allows both sites to be glycosylated (filled Y). Singly, and doubly glycosylated sites can be quantified by SDS-PAGE. Adapted from Hessa et al [44].

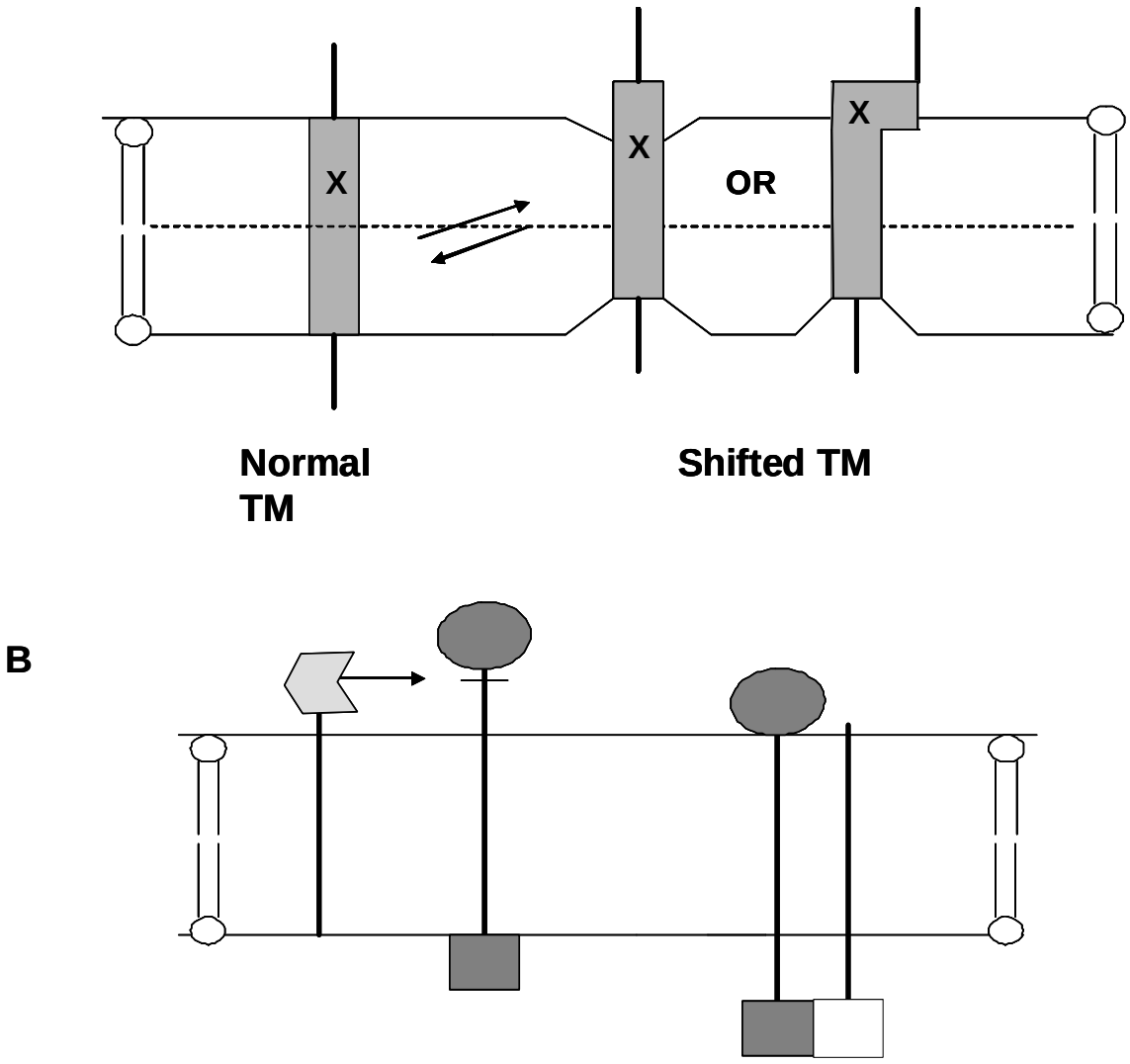

Figure 1.3: (A) Helix transverse shift induced by a hydrophilic residue X. Grey rectangle represent the helix. Dotted line represents the center of the lipid bilayer. (B) Control TM protein-protein interaction by helix shift. As depicted on the left a protease (light grey) can only recognize the substrates only at one of two transverse positions (dark grey). As depicted on the right side, domain of clear protein can only interact with the grey protein that has the right transverse position in the membrane.

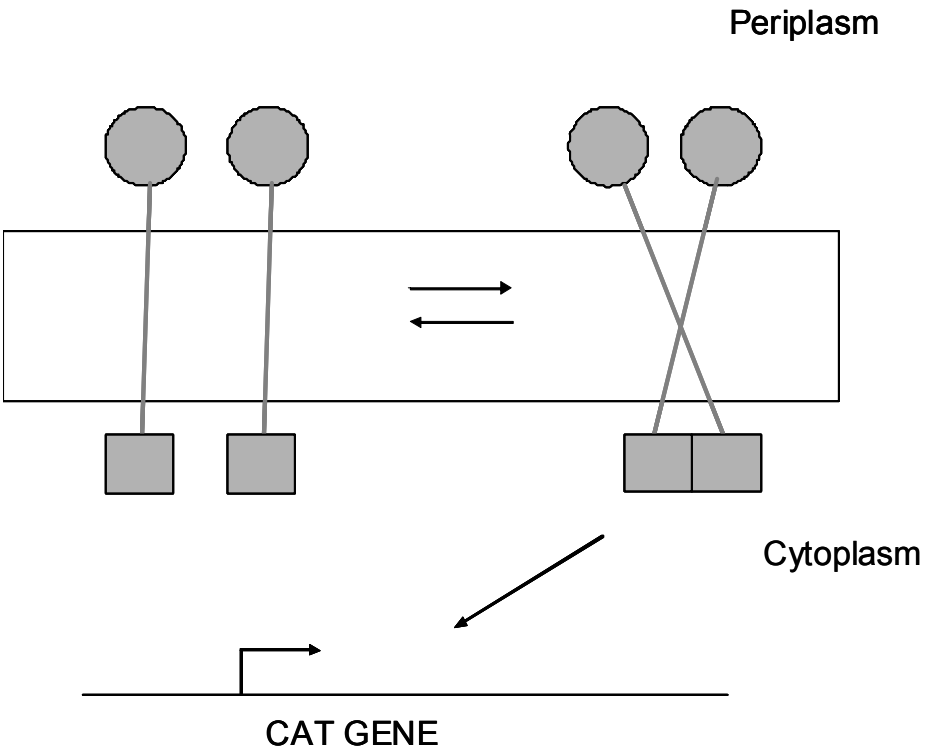

Figure 1.4.Schematic presentation of the TOXCAT system for detecting transmembrane helix association. The maltose binding protein (MBP, circles) is fused to the C-terminal of TM segment and the N-terminal is fused to ToxR(squares), a transcription factor that is only active when dimeric. If the TM segment dimerizes the ToxR monomers form a dimer and it induces the transcription of the chloramphenicol transferase (CAT) gene. Adapted from Russ et al 1999.

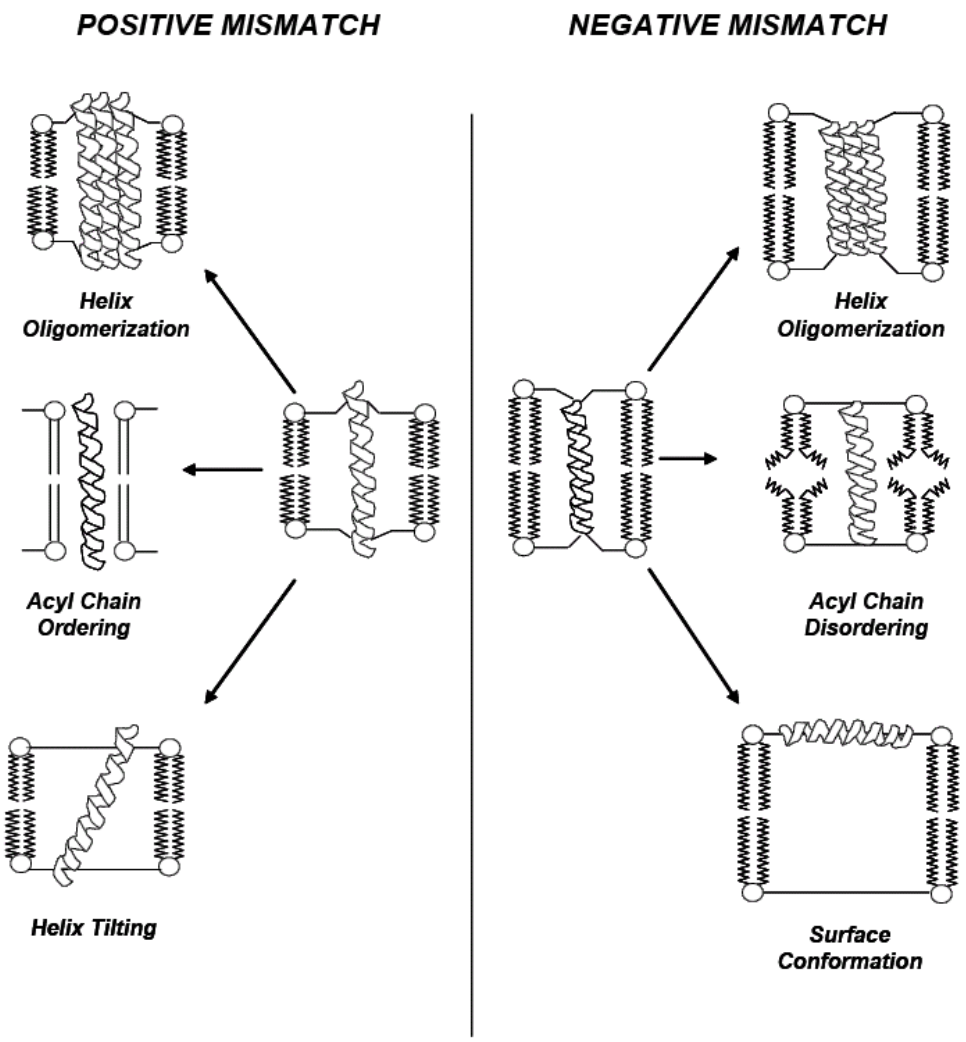

Figure 1.5: Schematic model of some possible consequences of hydrophobic mismatch when hydrophobic segment is longer (left) or shorter (right) than the hydrophobic bilayer thickness. Adapted from Killian 1998.

Chapter 2

Materials and methods

Materials. All the artificial peptides were purchased from Anaspec Inc.(San Jose, CA).The peptides were purified via reversed-phase HPLC using a C18 column using a 2-propanol/water gradient containing 0.5% (v/v) trifluoroacetic acid as described previously [117]. The ErbB2 peptides were bought fro Keck Facility at Yale University and purified by a C4 HPLC column using a (60:40) (2-propanol: acetonitrile)/water gradient containing 0.5% (v/v) trifluoroacetic acid. The peptides were dried under N_2, redissolved in 1:1 (v/v) 2-propanol/water, and stored at 4°C. Peptide purity was confirmed by MALDI-TOF (Proteomics Center, Stony Brook University) and generally was ~90% or greater. Estimated purity was lower (about 80%) only for $^{KK}pL_{11}A_4$(D10) and $^{KK}pL_9A_6$(D10). The concentrations of purified peptides were measured by absorbance spectroscopy using a Beckman DU-650 spectrophotometer, using an extinction coefficient for Trp of 5560 M^{-1} cm^{-1} at 280 nm. Phosphatidylcholines (1,2-diacyl-*sn*-glycero-3-phosphocholines), [diC14:1Δ9cPC (dimyristoleoylphosphatidylcholine); diC16:1Δ9cPC; diC18:1Δ9cPC, (dioleoylphosphatidylcholine, DOPC); diC20:1Δ11cPC; diC22:1Δ13cPC, (dierucoylphosphatidylcholine); and diC24:1Δ15cPC; 1,2-dioleoyl-*sn*-glycero-3-[phospho-L-serine] sodium salt (DOPS), 1,2-dioleoyl-*sn*-glycero-3-[phospho-*rac*-(1-glycerol)] sodium salt (DOPG), 1-palmitoyl-2-oleoyl-*sn*-glycero-3-phosphoethanolamine (POPE), 1-palmitoyl-2-oleoyl-*sn*-glycero-3-phosphocholine (POPC) and cholesterol were purchased from Avanti Polar Lipids (Alabaster, AL). Lipids were stored in chloroform at -20^0 C. Lipid concentrations were determined by dry weight. Acrylamide was purchased from Sigma-Aldrich Chemical Co.(St. Louis, MO). 10-doxylnonadecane (10-DN) was custom-synthesized (contact authors for availability) by Molecular Probes (Eugene, OR). It was stored as a 6 mM stock solution [determined using extinction coefficient = 12 M^{-1} cm^{-1} at 422 nm [43]]in ethanol at -20°C.

Model Membrane Vesicle Preparation. Model membranes (unilamellar) were prepared using the ethanol-dilution method [55; 74]. Peptides dissolved in 1:1 (v/v) 2-propanol/water and lipids dissolved in chloroform were mixed and then dried under a stream of N_2. Samples were then further dried under high vacuum for 1h. Then, 10 μL (for 800 μL samples) or 30 μL (for 2 mL samples) of 100% ethanol was added to dissolve the dried peptide/lipid film. To disperse the lipid-peptide mixtures 790 or 1970

μL, respectively, of PBS (10 mM sodium phosphate and 150 mM NaCl, pH 7), was added to the samples while vortexing. For samples prepared at low or high pH, the pH of the PBS was first adjusted using glacial acetic acid, for pH 3.8-5.5, or 2 M NaOH, for pH 9.0. The final concentrations were 2 μM peptide and 200 μM lipid, or 500 μM lipid except for pH titration experiments using peptides incorporated into DOPS vesicles in which, due to the difficulty of dissolving DOPS in ethanol, the final concentrations used were 1 μM peptide and 100 μM lipid.

Fluorescence Measurements. Fluorescence data were obtained on a SPEX τ2 Fluorolog spectrofluorometer operating in steady-state mode. Measurements were taken on samples in semimicro quartz cuvettes (1-cm excitation path length and 4-mm emission path length), except in the titration experiments, in which a 1-cm excitation and 1-cm emission path-length cuvette was used. A 2.5-mm excitation slit width and 5-mm emission slit width (band pass of 4.5 and 9 nm, respectively) were used for all experiments. Trp fluorescence emission spectra were measured over the range of 300-375 nm. Fluorescence from background samples containing lipid but lacking peptide was subtracted from the reported values. All measurements were made at room temperature.

pH Titration Experiments. As described above, 2 mL samples containing peptide incorporated into vesicles were prepared using PBS adjusted to about pH 4, and their Trp fluorescence emission intensity was measured at 330 and 350 nm. Sample pH was increased by adding 1-8 μL aliquots of either 0.25 or 2 M NaOH. After each aliquot was added and the sample mixed, it was incubated for 2 min (control experiments show this to be a sufficient time for equilibration of pH across the bilayer [47; 98] and then fluorescence was remeasured. The total volume of NaOH added by the end of the titration experiment (by which pH was 11.4-11.6) was about 70 μL. Intensities were corrected for background fluorescence using control samples lacking peptide. The pH dependence of the ratio of fluorescence intensity at 350 nm and 330 nm (F_{350}/F_{330}) was calculated. The data was fitted to a sigmoidal curve (Slidewrite Program, Advanced Graphics Solutions, Encinitas, CA), and apparent pKa values were estimated from the pH at the inflection point of the F_{350}/F_{330} ratio vs. pH curve.

Acrylamide Quenching Measurements. Fluorescence intensity and emission spectra were first measured for model membrane-incorporated peptides or background samples. After addition of a 50 μL aliquot of acrylamide from a 4 M stock solution in water and a 5min incubation period, fluorescence was remeasured. (This is sufficient time for acrylamide to equilibrate across the bilayer [43].) Fluorescence intensity was measured at an excitation wavelength of 295 nm and an emission wavelength of 340 nm. This excitation wavelength was chosen to reduce the resulting inner filter effect due to acrylamide absorbance. Corrections to intensity were made both for dilution by the addition of acrylamide and for the residual inner filter effects [43]. Fluorescence emission spectra were recorded using an excitation wavelength of 280 nm, despite the stronger inner-filter effect arising from acrylamide at 280 nm, because the overall intensity was greater than when an excitation wavelength of 295 nm was used. Controls show that emission spectra have very similar wavelength maxima using either excitation wavelength [43].

10-DN-Quenching Measurements. To measure quenching in samples containing 10mol% 10-DN, samples containing model membrane-incorporated peptides or background samples without peptide were prepared in which 10 mol % of each of the lipids present was replaced by an equivalent mole fraction of 10-DN. Fluorescence intensity and emission spectra were measured for samples with and without 10-DN. Fluorescence intensity was measured using an excitation wavelength of 280 nm and an emission wavelength of 330 nm. Emission spectra were recorded using an excitation wavelength of 280 nm.

Calculation of the Acrylamide/10-DN Quenching Ratio (Q Ratio). The ratio of quenching by acrylamide to quenching by 10-DN was used to estimate Trp depth in the bilayer. This ratio was calculated from the formula Q ratio = $[(F_o/F_{acrylamide}) - 1]/[(F_o/F_{10\text{-}DN}) - 1]$, where F_o is the fluorescence of the sample with no quencher present and $F_{acrylamide}$ and $F_{10\text{-}DN}$ are the fluorescence intensities in the presence of acrylamide or 10-DN, respectively [43].

Circular Dichroism (CD) Measurements. Circular dichroism spectra were recorded on a Jasco J-715 CD spectrophotometer at room temperature using a 1-mm path-length quartz cuvette. Unless otherwise noted, samples were prepared using 5 μM or 10μM peptide and 500μM lipid. The spectra were obtained from at least 50 scans. Backgrounds from samples lacking peptide were subtracted. Estimation of helical content was done using DICROWEB an online server for secondary structure analysis from CD data.

Chapter 3

Affect of lipid composition upon the topography of membrane-inserted hydrophobic helices

INTRODUCTION

The fact that interior of the bilayer is hydrophobic leads to the expectation that helical TM sequences should be composed of hydrophobic amino acids. On the other hand, TM sequences can contain a significant number of hydrophilic residues if required by helix-helix interactions or specific functions, as is evident for membrane pumps and ion channels in which numerous charged and polar residues are tolerated within generally non-polar TM segments [53; 54].

Nevertheless, too many hydrophilic residues in the hydrophobic core can lead to a less stable TM topography resulting in the formation of a non-TM state in aqueous solution or membrane-bound but located close to the membrane surface (non-TM sate 1 and 2 in Figure 1) [45; 47; 50]. The equilibrium between TM and non-TM topographies can be functionally significant. The hydrophobic helices of diphtheria toxin T domain undergo TM/non-TM interconversion thought to be essential for translocation across membranes [12; 13]. This interconversion also occurs in the membrane-inserting segments of beta-barrel toxins, including anthrax toxin protective antigen[14] and cholesterol-dependent cytolysins [15; 16]. It is also believed to be important for some Bcl family proteins (involved in apoptosis)[18], a number of tail-anchored endoplasmic reticulum enzymes, [19] polio virus 3A protein [21], and antimicrobial peptides [22]. This equilibrium can also play an important role in the fate of TM helices with borderline hydrophobicity. Moderately hydrophobic sequences are not uncommon in membrane proteins as observed by genomic analysis[23].

TM topography can be regulated by lipid composition. For example, it has been reported that bacterial lipid composition affects the topography of TM helices in complex membrane proteins [118; 119]. Certain bacterial cytolysins require cholesterol to form a TM state [120], and the T domain of diphtheria toxin forms a TM state more easily in bilayers composed of lipids with short acyl chains[12]. The question of modulation of TM protein topography and function by lipid composition is also interesting in eukaryotic membranes because the lipid environment of many membrane proteins varies as they cycle between various internal membranes and the plasma membrane. Nevertheless, little is known

mechanistically about what effect the structural diversity of membrane lipids has in controlling TM topography.

In this report, we studied the effect of lipid composition on hydrophobic helix behavior using synthetic peptides incorporated into model membrane vesicles ("liposomes"). Synthetic hydrophobic peptides, frequently Lys-flanked polyLeu or polyLeu-Ala helices, have been successfully utilized as models for hydrophobic α-helical TM domains by our lab and many others [27; 28; 30; 121; 122; 123; 124]. In this report fluorescence spectroscopy was used to study the lipid composition-dependence of the TM stability of these and closely related sequences. We found that physiological membrane concentrations of anionic lipids greatly stabilize the TM conformation of the hydrophobic helices flanked by cationic residues. In addition, there was a marked difference between topography in the presence of two different anionic lipids. This was true for peptide sequences with diverse hydrophobic sequences, short or long hydrophobic lengths, and various cationic flanking residues. It is likely that these properties are important for the function of these lipids.

RESULTS

Distinguishing TM and non-TM Topographies

The effect of lipid composition upon the topography of a variety of bilayer-inserted hydrophobic sequences was studied. Structures of different lipids used in this study are shown in figure 3.1. The peptides had hydrophobic cores with a variety of lengths and hydrophobicities, and their hydrophobic sequences were flanked by ionizable hydrophilic residues (Table 3.1). The peptides also contained a Trp in the center of the hydrophobic sequence. Measurement of Trp location within the membrane allows identification of membrane topography [47; 50; 55; 74]. Since Trp emission is sensitive to the polarity of its surrounding environment, one method to measure Trp location is from its fluorescence emission λmax. For the peptides in this study, in a fully TM orientation a Trp residue at the center of the sequence locates at the center of the highly non-polar core of the lipid bilayer and exhibits a highly blue-shifted λmax near 320-325 nm [58; 90]. When a peptide adopts a membrane-bound non-TM orientation, its hydrophobic core moves close to the more polar bilayer surface, and Trp λmax exhibits a strong red shift, falling in the range of 335-345nm [58; 90]. Intermediate values of Trp λmax can be indicative of mixed populations of TM and non-TM topographies, but can also be observed when a conformation forms in which Trp is at an intermediate depth [43; 58].

To confirm TM topography using a more direct method, dual fluorescence quenching was also used to measure Trp depth. In this method, Trp fluorescence quenching is compared using two molecules: 10-doxylnonadecane (10-DN), a bilayer inserted quencher that quenches Trp deeply buried within the membrane strongly, and acrylamide, a water soluble quencher that quenches Trp most strongly when the Trp is exposed to aqueous solution. The ratio of acrylamide quenching to 10-DN quenching (quenching ratio or Q-ratio) exhibits a linear relationship with Trp depth [43]. A low quenching ratio of <0.1-0.2 is indicative of a Trp located near the bilayer center and a high Q-ratio ≥1 is observed for a Trp located close to the bilayer surface. Intermediate Q-ratios can be observed for mixed populations of deep and shallow Trp, or when a conformation forms in which Trp is at an intermediate depth [43; 58].

A third method to define the topography of hydrophobic helices is to measure how Trp fluorescence is affected by bilayer width. Studies have shown that Trp at the center of hydrophobic sequence give the most blue shifted fluorescence when a hydrophobic sequence length matches the width of the bilayer[50; 74]. Hydrophobic helices that can form a TM configuration are sensitive to hydrophobic mismatch, which is the difference between the length of a hydrophobic helix and the width of the hydrophobic core of the bilayer. Such sequences exhibit Trp emission that is sensitive to bilayer width. Trp emission red shifts in wide bilayers due to negative mismatch-induced destabilization of the TM state, and formation of a significant amount of a non-TM state [50; 74]. Emission also red shifts in very thin bilayers, partly due to positive mismatch [55]. In contrast, when a hydrophobic helix is bound to membrane in a non-TM location close to the bilayer surface it emits red-shifted fluorescence with a λmax that is insensitive to bilayer width [50].

The Stability of the TM Topography of Hydrophobic Helices with Varying Hydrophobicities: Effect of Bilayer Width

First, the membrane topography of a series of peptides containing Leu/Ala-rich hydrophobic cores was measured. Hydrophobicity was varied by varying the content of Leu and Ala residues from 15 Leu 0 Ala (most hydrophobic, $^{KK}pL_{15}(D10)$) to 7 Leu 8 Ala (most hydrophilic, $^{KK}pL_7A_8(D10)$) (Table 3.1, sequences 1-5). To allow evaluation of peptide topography the peptides also contained a single Trp at the center of the hydrophobic sequences. An Asp was also present at the center of the hydrophobic sequence so that the hydrophobicity of the peptides could be controlled with pH.

Trp emission λmax was measured as a function of bilayer width by incorporating the peptides into vesicles composed of phosphatidylcholines containing monounsaturated acyl chains of various lengths (Figure 3.1). Under low pH conditions (+), in which the Asp residue should be uncharged (see below), most of the peptides exhibited a U-shaped dependence of λmax on bilayer width with a minimum λmax ~320-325 nm, indicative of a TM topography in bilayers with an intermediate width (e.g. with 18:1 acyl chains). The exception was the most hydrophilic peptide tested ($^{KK}pL_7A_8(D10)$) which showed a red

shifted λmax (335-340 nm) that was not very dependent on bilayer width. This indicates that $^{KK}pL_7A_8$(D10) does not form a TM state in these vesicles at low pH. (Instead, the peptide is bound to the bilayer surface, see below.)

Under high pH conditions (Δ), in which the Asp residue should be charged (see below), all of the peptides exhibited red shifted fluorescence that was not very dependent on bilayer width. This indicates that when the Asp residue is charged the peptides are not hydrophobic enough to form a TM topography. The Trp λmax values observed in most cases (335-345 nm) were indicative of peptides bound to the bilayer surface. The $^{KK}pL_7A_8$(D10) peptide exhibited even more highly red-shifted fluorescence (λmax ~350 nm, off scale in Figure 1) indicative of peptide that is dissolved, or at least largely dissolved, in aqueous solution.

Most subsequent experiments were carried out at pH 4 so that the Asp residue would be uncharged. However, when DOPS vesicles were used, pH was generally kept at 5.5 so that the PS carboxyl group would not be protonated, and PS would retain a net negative charge [125; 126]. This was not necessary for PG which ionizes at a somewhat lower pH than PS [127].

Effect of Lipid Structure Upon the Stability of The TM Topography of Hydrophobic Helices With Varying Hydrophobicities: Vesicles with No Net Charge

Next, the Trp fluorescence of these peptides was measured in a variety of lipids and lipid mixtures with different polar headgroups. Phospholipids containing 16 or 18 carbon atom long acyl chains, which are common in biological membranes, were used. The phospholipids used had a least one 9-10 cis double bond in one of their acyl chains so that the lipid bilayers would be in the normal liquid disordered state [128].

Figure 3.2 shows Trp emission λmax (Figure 3.2A) and Q-ratios (Figure 3.2B, raw quenching data is in Table 3.2) for these peptides when incorporated into lipid vesicles with various compositions lacking a net electric charge (DOPC, POPC, 1:1 POPC/POPE mol:mol, and 6:4 mol:mol POPC/cholesterol). In all cases, the most

hydrophobic peptide ($^{KK}pL_{15}$(D10)) exhibited a blue-shifted λmax and low Q-ratio value typical for TM helices with a Trp at the center of the bilayer, while the red shifted λmax and high Q-ratio values were observed for the least hydrophobic peptide ($^{KK}pL_7A_8$(D10)) corresponding to a fully non-TM state [46; 50]. The peptides with intermediate numbers of Ala showed intermediate λmax and Q-ratio values that tended to increase as the number of Ala increased, consistent with progressively less stable TM orientation as the hydrophobicity of the peptides decreased. It should be noted that previous studies show similar effects of the Leu to Ala ratio upon the stability of the TM topography [27; 45].

For vesicles without net charge, the behavior of most of the peptides was only slightly dependent upon lipid structure (Figure 3.2). The main exception was the $^{KK}pL_7A_8$(D10) peptide, which exhibited highest λmax (345-355nm) and Q-ratio values in POPC/POPE and POPC/cholesterol vesicles. These values indicate that a significant fraction of this peptide was either very shallowly located or not even membrane-bound in vesicles composed of these lipids.

The value of the pKa of the Asp residue also yields information concerning the location of these peptides. Because a charged Asp residue is energetically unfavorable in a hydrophobic environment [46; 47; 50], the pKa of an Asp residue in the center of a TM helix is much higher than in a state in which the Asp residue is located more shallowly in the membrane or fully exposed to aqueous solution, as in the case of a peptide located at the bilayer surface or dissolved in aqueous solution [47]. In fact, previous studies showed that the presence of a charged Asp buried within the lipid bilayer is so energetically unfavorable that ionization of an Asp in the middle of a TM helix is accompanied by conversion to the non-TM state[47], i.e. the TM/non-TM and Asp ionization equilibria are linked.

As shown in Figure 3.1 there were changes in Trp fluorescence due to ionization of the Asp residue, so that the Asp pKa values could be determined from wavelength shifts in the emission spectra as a function of pH. Figure 3.3A gives apparent Asp pKa values for the peptides determined by this method as a function of the number of Ala

residues when the lipids used have no net charge. Asp pKa decreased as the hydrophobicity of the peptide decreased (i.e. as the number of Ala increased). This suggest that when the Asp is protonated the stability of the TM state decreases as peptide hydrophobicity decreases, consistent with the λmax and quenching data. On the average, pKa values were slightly lower for vesicle compositions containing POPE or cholesterol. This is consistent with a slightly lower stability of the TM state relative to a non-TM configuration in these lipids as compare to that in DOPC or POPC vesicles.

Effect of Lipid Structure Upon the Stability of The TM Topography of Hydrophobic Helices With Varying Hydrophobicities: Zwitterionic vs. Anionic Lipid Vesicles

In contrast to the results above, lipid charge had a large effect on the stability of the TM state. Generally, λmax was more blue shifted (Figure 3.4A) and the Q-ratio was lower (Figure 3.4B) when peptides were incorporated into vesicles composed of anionic lipids (DOPG or DOPS) than when incorporated into vesicles composed of zwitterionic and/or uncharged lipids. [This is most obvious for the least hydrophobic peptides, $^{KK}pL_9A_6(D10)$ and $^{KK}pL_7A_8(D10)$.] This behavior indicates that the TM state is significantly more stable in the vesicles composed of these anionic lipids.

It is noteworthy that Trp located more deeply in vesicles composed of DOPS than in vesicles composed of DOPG, with λmax and Q-ratio values in DOPS indicative of full formation of a TM state with the Trp at the bilayer center even in the case of the relatively hydrophilic $^{KK}pL_7A_8(D10)$ peptide. Additionally, pKa data indicated that the depth of the Asp group was deeper for peptides in DOPS vesicles than in DOPG vesicles (Figure 3.3B). The decrease in pKa as peptide hydrophobicity decreased was less in DOPS vesicles than in DOPG vesicles. Although the pKa of the Asp residues is much higher in anionic lipid vesicles than in vesicles lacking a net charge (compare Figure 3.3A and 3.3B) this may not be related to a difference in TM stability in anionic and zwitterionic vesicles. Instead, it reflects the well-known high proton concentrations close to the surface of anionic vesicles arising from the attraction of protons by the anionic charge on the lipid [126].

Importantly, the observation that Trp depth in DOPG vesicles was intermediate between the deep value observed in DOPS vesicles and the shallower values observed in vesicles lacking a net charge did not appear to involve the formation of a mixture of TM and non-TM topographies by peptides in DOPG vesicles but rather the formation of a single topography with an intermediate Trp and Asp depth. This reason for this statement is that we did not observe any large quencher-induced shifts in λmax. Such shifts are characteristic of co-existing populations with deep and shallow Trp depths because the relatively selective quenching of the deep population by 10-DN induces a large red shift of λmax while the quenching of the shallow population by acrylamide induces a large blue shift [43]. Instead of this, we observed only very small quencher-induced shifts (Table 3.3), behavior characteristic of cases in which there is an intermediate Trp depth [50; 90]. This suggests that the difference between peptide behavior in the DOPG vesicles and DOPS vesicles arises from the way the TM state is anchored in the lipid bilayer (Figure 3.8).

It should also be noted that the differences between peptide behavior in DOPG and DOPS vesicles were not due to the difference in solution pH used in the λmax and Q-ratio experiments for these lipids. Control experiments showed that the λmax and Q-ratio values for peptides in DOPG vesicles was the same at pH 3.8 and 5.5, and that differential behavior of peptides in DOPG and DOPS vesicles could also be observed at neutral pH (Table 3.4).

The Role of Cationic Flanking Residues in the Stabilization of the TM Conformation in Anionic Vesicles: Electrostatic Origin of Stabilization

The stabilization of the TM state observed for peptides inserted into anionic lipid vesicles could be due to electrostatic interactions between the charged residues and anionic lipids. To study this, we used a series of peptides lacking an Asp residue so that the charge of flanking residues could be varied without the complication of changes due to Asp ionization (Table 3.1, sequences 7-9). The peptides chosen had an inherently borderline TM stability due to their short hydrophobic segments [58]. To investigate the

role of electrostatic effects, the effect of pH upon the stability of the TM state was compared in both zwitterionic and anionic vesicles when the peptides were flanked on both ends of the hydrophobic sequence by 2Lys ($^{KK}pL_{12}$), 2His ($^{HH}pL_{12}$), or 1Lys plus 1His residue ($^{KH}pL_{12}$).

Figure 3.5 illustrates the dependence of λmax and quenching upon flanking residue type and lipid composition at pH 5.5 and pH 9 for these peptides. Lys residues are charged at both of these pH values [47], while His residues should be largely protonated at pH 5.5 and largely deprotonated at pH 9. Consistent with this, in both anionic and zwitterionic vesicles Figure 3.5 shows that there were pH-dependent changes in both Trp λmax and Q-ratio for a His-flanked peptide, but none for a peptide flanked only by Lys.

[In fact, for the $^{HH}pL_{12}$ peptide a change in fluorescence intensity upon pH titration detects one His pKa slightly above 5.5 and a pH-dependent shift in the Trp emission wavelength detects another pKa close to pH 7.5 for peptides incorporated into DOPC vesicles. In DOPS vesicles, the change in fluorescence intensity upon pH titration detects one His pKa near 6.5 and a pH-dependent shift in the Trp emission wavelength detects another close to pH ~8-8.3 (data not shown).]

Figure 3.5 also shows that at pH 5.5 Trp λmax blue shifted and Q-ratio were significantly lower in DOPS vesicles than in DOPC vesicles for all three peptides. This indicates that relative to topography in DOPC vesicles, in DOPS vesicles the TM state is stabilized relative to the non-TM state both when the flanking residues are charged Lys or charged His. This rules out stabilization of the TM state requiring a specific Lys-PS interaction. At pH 9, the λmax and Q-ratio data was similar to that at pH 5.5 for the Lys_2-flanked peptide, but for the His_2-flanked peptide there was no blue shift or decrease in Q-ratio in DOPS vesicles relative to that in DOPC vesicles. This indicates that when the His is not charged, DOPS does not stabilize the TM state, and thus the stabilization of the TM state is likely to be electrostatic in origin. In contrast, as noted above for the Lys-flanked peptide the λmax and Q-ratio data at pH 9 is similar to that at pH 5.5.

Figure 3.5 also shows that the behavior of the peptide with a hydrophobic core flanked by one His and one Lys exhibited intermediate behavior at high pH, with differences both in λmax and Q-ratio in DOPS vesicles relative to DOPC vesicles that were smaller than those for the peptide flanked by two Lys but larger than those for the peptide flanked by two His. This is expected as the peptide with one His and one Lys should carry a charge of +1 on each end at high pH, intermediate between that of the Lys_2(+2) and His_2(0) flanked peptides.

The Effect of Lipid Composition on the Stability of the TM State for Longer Helical Sequences

The studies above used peptides with relatively short, 12-17 residue hydrophobic cores. In these peptides the charged residues flanking the hydrophobic core would be somewhat more buried within the bilayer in the TM state than in the case of the longer ~20 residue hydrophobic sequences common in many TM proteins. The increased exposure of charged residues to a hydrophobic environment in the short peptides would tend to increase the free energy of the TM state for such sequences. Thus, it was possible that the stabilizing effects of anionic lipids upon peptide topography found above were specific to short hydrophobic helices.

To determine whether lipids have similar effects for longer hydrophobic sequences, peptides with hydrophobic cores of 18-22 residues long were studied. These sequences had weakly hydrophobic cores composed of Ala with or without a few Leu (Table 3.1, sequences 10-14). When these peptides were inserted into DOPS vesicles highly blue-shifted λmax and low Q-ratio values were generally observed (with the exception of $^{KK}pA_{22}$ peptide which showed a somewhat more red shifted λmax and high Q-ratio), showing that a TM state predominated. In contrast, a non-TM state predominated in the presence of vesicles composed of DOPC (Table 3.5). This shows that stabilization of the TM state by DOPS is not restricted to short hydrophobic sequences. It should also be noted that stabilization of the TM configuration in DOPS vesicles relative to DOPC vesicles was similar for peptides with flanking Lys and Arg residues, indicating they interact similarly with DOPS.

Fluorescence properties indicated that in most cases the non-TM state formed in the presence of DOPC vesicles for these longer and less hydrophilic peptides was predominantly not vesicle-bound. First, Trp λmax, was close to that for free Trp and significantly more red shifted than for Trp located at the membrane surface [59]. Second, there was very little, if any, quenching of Trp fluorescence by the membrane-bound quencher 10-DN (Table 3.2)[43].

An exception to this behavior was observed for the $^{KK}pL_4A_{18}$ peptide, which was slightly more hydrophobic than the other long peptides. It exhibited λmax and Q-ratio values indicating that the peptide was bound to the DOPC vesicles, similar to the behavior of the shorter hydrophobic sequences described above (Table 3.5). Also similar to the behavior of shorter hydrophobic sequences, the incorporation of cholesterol appeared to inhibit its binding to PC-containing vesicles, while λmax and Q-ratio values for this peptide incorporated into anionic lipids was lower than that in DOPC, with values in DOPG vesicles that were not as low as in DOPS vesicles. This shows that many of the effects of lipid structure upon topography described above are not restricted to shorter hydrophobic helices.

Behavior of Helical Peptides in Biologically Relevant Amounts of Anionic Lipids

The studies above used pure DOPS and DOPG vesicles. We were interested in whether anionic lipid effects would be similar in vesicles containing more physiologically relevant anionic lipid contents of 20-30mol%. Figure 3.6 shows that, as judged from Trp depth measured by Q-ratio, the stabilization of the TM state in vesicles composed of 30 mol%DOPS/70 mol% DOPC was almost as great as that in pure DOPS vesicles for a variety of peptides. [It should be noted that at the sample pH used peptide Asp residues were still protonated at lower anionic lipid contents, with a pKa value of ~ 6.5 at 30mol% DOPS (data not shown).]

Similarly, only a low mol% of DOPG was necessary to stabilize the TM state, with a significant degree of stabilization by as little as 5mol% DOPG (Figure 3.7). The

mol% DOPG need to maximally stabilize the TM state (20 mol%) was similar for a peptide with four flanking Lys at each end of the hydrophobic sequence ($^{KKKK}pL_{11}A_4(D10)$) and a peptide with a less hydrophobic core, and only two flanking Lys at each end ($^{KK}pL_7A_8(D10)$), as judged by both Q-ratio (Figure 3.7A) and λmax (Figure 3.7B). It is noteworthy that for the latter peptide the increased stability of the TM state reached a plateau at 20mol% DOPG even though it has not formed a state with Trp as deep as in DOPS vesicles (see Discussion).

Secondary Structure Shows Increased Helix Content When Peptides Are Inserted into Phosphatidylserine Vesicles.

The secondary structures of the peptides used above were evaluated by circular dichroism. Secondary structure was evaluated at different pH values and in different lipid compositions (Table 3.6). In all cases, the peptides had a largely helical structure. In the presence of DOPC vesicles, helix content was generally in the range 65-75%, which corresponds to helix formation by almost all of the residues in the hydrophobic core of the peptides. The more weakly hydrophobic peptides exhibited a helix content at the lower end of this range. For Asp-containing peptides helix content in DOPC vesicles was not greatly affected by whether a peptide formed a TM state (at low pH) or non-TM state (at high pH). There was also little dependence of helix content upon lipid composition, with the striking exception of DOPS vesicles, in which there was an increase in helix content to 80-90%. Because DOPG vesicles did not induce a significant increase in helix content, this increase cannot be due simply to DOPS being anionic (see Discussion).

DISCUSSION

Role of Negative Lipid in TM Stability: Electrostatic Interactions

It is well known that, relative to zwitterionic lipids, anionic lipids enhance the binding of cationic polypeptides to membranes [42; 93]. The results in this report demonstrate that anionic lipids also stabilize the TM topography of hydrophobic α-helices with flanking cationic residues relative to the non-TM topography. This is not simply a matter of enhanced binding to the membrane, because an enhancement of the amount of peptide in a TM state by anionic lipid is observed in cases in which a peptide is fully bound to zwitterionic vesicles. Thus, there are two effects of anionic lipids upon polypeptide-membrane interaction, as summarized in Figure 3.8A.

Several lines of evidence are consistent with this being a result of Coulombic type electrostatic interactions. First, stabilization depends on lipid having a negative charge and peptide having a positive charge. Second, stabilization of the TM state is observed with more than one type of anionic lipid. Third, stabilization is not specific for the type of charged residue. Finally, the effect increases with the number of positive charges on the peptide, as shown by the observation that stabilization of TM topography was greater when there were two flanking positive charges than when there was one flanking positive charge.

Presumably, interactions between positively charged residues and anionic lipid head groups decrease the free energy of the peptides in the TM state relative to that when the bilayer is uncharged. However, the free energy of a membrane-bound non-TM state should also be decreased by electrostatic interactions. The TM topography may be preferentially stabilized because cationic residues are further from the hydrophobic core of the bilayer in the non-TM state than when in the TM state, so that the electrostatic interactions stabilize the free energy of the non-TM state to a lesser degree than they do that of the TM state.

The electrostatic interaction between peptide and lipid is probably stronger than in bulk aqueous solution because charged amino acid residues located near or at the

boundary between the non-polar/polar regions of the bilayer should experience a local environment with a lower effective dielectric coefficient than in bulk water. Consistent with this, it has been reported that free energy is higher for charged residues near the membrane bilayer in ER translocon system [45; 51].

It should be noted that hydrophobic peptides that equilibrate between fully soluble and fully TM states may be useful for evaluating the effect of different residues upon the relative stability of these two states via experiments in which various substitutions are made in these sequences. This could provide a hydrophobicity scale that would complement other types of scales, and which would be particularly useful for biological cases in which there is post-translational equilibration of hydrophobic sequences between TM and soluble states.

The Origin of the Difference Between Peptide Topography in DOPS and DOPG

One of the most striking observations in this report was that there was a substantial difference between peptide topography in DOPS vesicles and DOPG vesicles. This is an interesting observation because the functional significance of the different types of anionic phospholipids is a long standing mystery in biology. The difference between DOPG and DOPS vesicles is puzzling in terms of a simple electrostatic interaction. Both PG and PS should have a net -1 charge on their polar headgroups at the experimental pH studied. However, PS has two negative charges, one on the phosphate and one on the carboxyl, and one possibility is that the PS headgroup can orient so as to allow both charges to interact with cationic residues. Another possibility is that differences in hydrogen bonding or other polar interactions between peptide and lipid are affected by the difference in PS and PG headgroup structure. Studies have shown that changes in lipid composition that affect the dipoles near the interfacial region can disrupt the binding of helical peptides to a lipid bilayer[129].

The nature of the difference in polypeptide topography in DOPS and DOPG vesicles is also of interest. As noted in the results, the fluorescence behavior for peptides in which topography in DOPS and DOPG was compared does not fit a model in which

topography in DOPG is simply explained by the presence of a co-existing TM state similar to that in DOPS vesicles and a non-TM state similar to that in DOPC vesicles. An alternative that does fit the data is that there are two different TM states in DOPS and DOPG vesicles which differ in the degree of positional anchoring of the TM helix. We have previously proposed that in the absence of heteroaromatic residues at the boundary of the hydrophobic sequence, decreasing TM peptide core hydrophobicity (by substituting Leu with Ala) decreases anchoring of the sequence at a precise position in membranes, such that there is decreased burial of one or the other end of the hydrophobic core of the peptide within the bilayer [58]. A greater degree of peptide anchoring in DOPS vesicles could also explain the difference between peptide behavior in DOPG and DOPS vesicles (Figure 3.8B). Notice that, as illustrated in Figure 3.8, a loss of precise anchoring would be associated with a shallower Trp depth, consistent with the shallower Trp depth observed in DOPG vesicles. This model is also consistent with the observation of less helical structure in DOPG vesicles than in DOPS vesicles. A poorly-anchored hydrophobic sequence would have additional residues exposed to aqueous solution, and such residues would not need to be constrained in a helical structure. It should be noted that sensitivity of anchoring to lipid structure might be sequence dependent. Heteroaromatic residues have a distinct energetic preference for the polar/non-polar boundary of the bilayer [45; 51; 130; 131] and their presence at the end of the hydrophobic segment might compensate for anchoring that would otherwise be weak. In any case, our report points to cationic residue-PS interaction as a novel factor controlling TM peptide anchoring, and worthy of further study.

The hydrophobicity of the core sequence may also be important for determining how well a TM state is anchored. Trp location for the $^{KK}pL_7A_8$(D10) peptide as DOPG levels in the membrane increased was found to plateau at a depth that was shallower than observed for the peptides with a more hydrophobic (Leu-rich) core. This is consistent with the idea that the unfavorable energetics of exposing Leu in the latter peptides to aqueous solution, relative to the cost of exposing Ala, also anchors the TM topography in a constant position relative to the bilayer.

A second, but less likely possibility for the shallow Trp depths observed for peptides in DOPG vesicles relative to in DOPS is that there is greater stabilization of the TM state in DOPS vesicles than in DOPG vesicles, but that the stabilization is not easily detected by fluorescence. It is possible that when incorporated into DOPG vesicles the Trp residue in the non-TM state locates more deeply than when incorporated into vesicle lacking a net charge, so that there is only a moderate difference between Trp depth in the TM and non-TM states, and their co-existence cannot be detected easily via quencher-induced λmax shifts. It is also possible that a relatively deeply penetrating non-TM state co-exists with the poorly anchored TM state described above, and these two states might have similar average Trp depths.

Effect of POPE and Cholesterol upon the Stability of the Surface Bound Non-TM Topography

Cholesterol and POPE appeared to disfavor the surface associated non-TM state relative to the state in which the peptides are dissolved in solution. A possible explanation arises from the fact that cholesterol and POPE have headgroups that are smaller than those of other lipids, so that they may pack more tightly in the headgroup region of the bilayer, which could make it more energetically difficult for a peptide to penetrate into the polar headgroup region. It has been proposed that the strength of the interaction of Apo-I protein (a primary constituent of high density lipoprotein) and other peptides with phospholipids is impaired at higher concentrations of cholesterol due to this type of effect [132; 133]

Physiological Significance of Stabilization of TM Topography by Negatively Charged Lipids

Electrostatic interactions between anionic lipids and cationic residues have important biological consequences. The preferential interaction of water soluble positively charged peptides and peripheral proteins with anionic lipids has been extensively characterized in numerous cases [42; 93; 134]. Antimicrobial peptides, which are generally cationic, are believed to disrupt the microbial membrane by interacting with negatively charged lipids [135; 136]. Preferential interactions between sites on TM proteins

and anionic lipids have also been documented, and the anionic lipid may often have an important structural and functional role [137; 138; 139; 140; 141]. There is already evidence that anionic lipids affect TM protein orientation in cells. In cell membrane, TM helices orient such that the more cationic of their flanking hydrophilic sequences tends to orient towards the cytoplasmic surface of membrane (positive-inside rule), and studies have found that anionic phospholipids control orientation by what appears to be an electrostatic interaction with cationic residues[142; 143].

In this regard, the ability of DOPS to promote helix formation may be important for determining peptide behavior in DOPS vesicles and in real membranes. It is interesting to note that the ability of cationic residues on the cytofacial side of the membrane to form a helical continuation of a hydrophobic helix structure has been shown to be important for the formation of a TM topography during membrane insertion in the translocon [51]. The cytofacial surface of the endoplasmic reticulum membrane presumably contains a significant amount of PS, and thus PS might play a role in this process.

Stabilization of the TM state by anionic lipids may be particularly important for proteins that undergo post-translational changes in topography. As noted in the introduction, a number of proteins have hydrophobic sequences that post-translationally convert from a non-TM to TM state. Stabilization of the TM state might be most important for determining the structure of the hydrophobic sequences in such proteins when they are semi-hydrophobic, i.e. have a hydrophobicity at the borderline necessary for stability in the TM state. For example, although several studies have shown polyAla sequences do not form stable TM helices in vitro [30; 59; 60; 61], the results in our study suggest this would not necessarily be the case in natural membranes containing moderate amounts of anionic lipids. Other sequences with borderline hydrophobicity may not be rare. Genomic analysis has revealed that there are numerous semi-hydrophobic sequences with borderline hydrophobicity in both prokaryotes and eukaryotes [23].

Furthermore, TM state stabilizing effects were observed at levels of anionic lipid ($\leq$20%) within the physiological level believed to be present on the cytofacial leaflet. It

should be interesting in future studies to investigate the effect of anionic lipids upon membrane proteins with natural semi-hydrophobic sequences in order to determine whether anionic lipids, and/or the type of anionic lipid present, have a significant effect on topography.

Table 3.1. Sequences of the hydrophobic peptides used in this study. Notice that for simplicity the names do not explicitly mention the Trp at the center of the hydrophobic sequence.

Sequence	Name	Sequence
1	$^{KK}pL_{15}(D10)$	Acetyl-KKLLLLLLLDWLLLLLLLKK-amide
2	$^{KK}pL_{13}A_2(D10)$	Acetyl-KKLALLLLLDWLLLLLLALK$_2$-amide
3	$^{KK}pL_{11}A_4(D10)$	Acetyl-KKLALALLLDWLLLLALALKK-amide
4	$^{KK}pL_9A_6(D10)$	Acetyl-KKLALALALDWLLALALALKK-amide
5	$^{KK}pL_7A_8(D10)$	Acetyl-KKLALALAADWALALALALKK-amide
6	$^{KKKK}pL_{11}A_4(D10)$	Acetyl-KKKKLALALLLDWLLLLALALKKKK-amide
7	$^{KK}pL_{12}$	Acetyl-KKGLLLLLLWLLLLLLKKA-amide
8	$^{KH}pL_{12}$	Acetyl-KHGLLLLLLWLLLLLLHKA-amide
9	$^{HH}pL_{12}$	Acetyl-HHLLLLLLWLLLLLLHH-amide
10	$^{KK}pA_{18}$	Acetyl-KKAAAAAAAAAWAAAAAAAAAK2-amide
11	$^{RR}pA_{18}$	Acetyl-RRAAAAAAAAAWAAAAAAAAALRR-amide
12	$^{KK}pL_2A_{18}$	Acetyl-KKLAAAAAAAAAWAAAAAAAAALK2-amide
13	$^{KK}pL_4A_{18}$	Acetyl-KKLAAAAAAAAALWLAAAAAAAAALK2-amide
14	$^{KK}pA_{22}$	Acetyl-KKAAAAAAAAAAAWAAAAAAAAAAAK2-amide

Table 3.2. Quenching of Trp fluorescence by acrylamide and 10-doxylnonadecane (10-DN). F/Fo is the ratio of fluorescence in the presence of the quencher to that in its absence. Q-ratio is defined in Materials and Methods. Q-ratio values shown are for the average from 3-6 samples, and their standard deviation.

Peptide	pH	Lipid	F/Fo Acrylamide	F/Fo 10-DN	Q ratio
$^{KK}pL_{15}$(D10)	3.8	DOPC	1.09±0.06	3.74±0.48	0.035±.024
		POPC	1.09±0.09	4.05±0.5	0.029±.031
		POPC+chol	1.13±0.03	4.09±0.17	0.042±0.01
		POPC/POPE	1.17±0.02	4.65±0.62	0.046±0.01
		DOPG	1.08±0.12	3.46±0.88	0.032±0.05
	5.5	DOPS	1.13±0.08	4.34±0.1.6	0.040±0.03
$^{KK}pL_{13}A_2$(D10)	3.8	DOPC	1.28±0.09	2.7±0.22	0.16±0.055
		POPC	1.28±0.04	2.77±0.50	0.156±0.05
		POPC+chol	1.43±0.05	3.62±0.21	0.165±0.02
		POPC/POPE	1.46±0.05	3.23±0.30	0.206±0.043
		DOPG	1.30±0.02	3.04±0.29	0.148±0.02
	5.5	DOPS	1.24±0.10	3.87±0.31	0.086±0.03
$^{KK}pL_{11}A_4$(D10)	3.8	DOPC	1.19±0.13	2.23±0.07	0.15±0.01
		POPC	1.22±0.26	2.46±0.50	0.152±0.03
		POPC/POPE	1.24±0.05	1.94±0.23	0.258±0.08
		POPC+chol	1.36±0.15	3.21±0.10	0.161±0.07
		DOPG	1.28±0.01	3.00±0.57	0.139±0.04
	5.5	DOPS	1.08±0.02	2.84±0.21	0.043±0.01
		30% DOPS	1.12±0.03	2.58±0.23	0.076±0.02
$^{KK}pL_9A_6$(D10)	3.8	DOPC	1.33±0.15	1.86±0.11	0.384±0.18
		POPC	1.28±0.15	1.9±0.14	0.309±0.05
		POPC/POPE	1.34±0.16	1.88±0.16	0.385±0.19
		POPC+chol	1.363±0.02	2.04±0.26	0.348±0.09
		DOPG	1.26±0.04	2.49±0.07	0.172±.008
	5.5	30% DOPS	1.31±0.07	2.53±0.07	0.206±0.05
		DOPS	1.14±0.03	2.76±0.22	0.078±0.02
$^{KK}pL_7A_8$(D10)	3.8	DOPC	1.73±0.07	1.88±0.17	0.838±0.18
		POPC	1.3±0.12	1.35±0.09	0.841±0.40
		POPC/POPE	2.55±0.15	1.3±0.13	5.216±2.4
		POPC+chol	2.54±0.26	1.27±0.07	5.74±1.81
		DOPG	1.40±0.14	1.83±0.19	0.482±0.30
	5.5	30% DOPS	1.22±0.08	2.37±0.23	0.161±0.06
		DOPS	1.12±0.10	2.31±0.07	0.095±0.005
$^{KK}pL_{12}$	5.5	DOPC	1.54±0.19	1.38±0.03	1.413±0.50
	9	DOPC	1.97±0.06	1.66±0.15	1.46±0.34

	5.5	DOPS	1.06±0.05	1.78±0.39	0.074±0.07
	9	DOPS	1.10±0.16	2.92±0.32	0.052±0.09
	5.5	30% DOPS	0.137±0.06	0.504±0.03	0.272±0.06
$^{KH}pL_{12}$	5.5	DOPC	1.50±0.05	1.81±0.05	0.663±0.08
	9	DOPC	1.56±0.05	2.07±0.07	0.526±0.10
	5.5	DOPS	1.06±0.09	2.18±0.19	0.048±0.008
	9	DOPS	1.22±0.01	1.8±0.12	0.278±0.04
	5.5	30% DOPS	1.16±0.03	1.98±0.14	0.16±0.04
$^{HH}pL_{12}$	5.5	DOPC	1.64±0.14	1.84±0.22	0.76±0.26
	9	DOPC	1.38±0.19	1.85±0.17	0.452±0.24
	5.5	DOPS	1.13±0.11	2.49±0.17	0.077±0.08
	9	DOPS	1.19±0.11	1.43±0.15	0.439±0.16
	5.5	30% DOPS	1.21±0.09	1.91±0.20	0.233±0.11
$^{KK}pA_{22}$	5.5	DOPC	6.18±2.25	1.14±0.06	36.88
		DOPS	1.48±0.07	1.62±0.01	0.785±0.13
$^{KK}pA_{18}$	5.5	DOPC	3.49±1.3	1.06±0.04	39
		DOPS	1.31±0.06	1.8±0.10	0.387±0.09
$^{KK}pL_2A_{18}$	5.5	DOPC	2.32±0.21	1.13±0.12	10
		DOPS	1.11±0.06	1.79±0.26	0.143±0.05
$^{KK}pL_4A_{18}$	5.5	DOPC	1.78±0.09	1.84±0.26	0.933±0.31
		DOPG	1.41±0.06	1.57±0.09	0.718±0.16
		DOPS	1.24±0.04	1.95±0.19	0.254±0.05
		POPC/chol	1.23±0.14	0.636±0.29	1.94±0.91
$^{KKKK}pL_{11}A_4$(D10)	4	DOPC	1.27±0.07	1.45±0.18	0.605±0.29
		30% DOPG	1.31±0.09	3.54±0.22	0.12±0.04
		100%PG	1.26±0.22	3.35±0.43	0.112±0.09

Table 3.3. Effect of quenchers on Trp emission λmax. The parameter Δλmax is defined by the absolute value of the difference between λmax in the presence of 10-DN and that in the presence of acrylamide, with the quenchers present at the same concentrations as for Q-ratio measurements. Large Δλmax values that are consistent with large fractions of each of two co-existing populations with very different depths in the membrane are shown in bold. Average values from data from 3-6 samples are shown. The λmax values for individual samples generally differed from the average by no more than ±1 nm.

Peptide	Lipid	pH	λmax (nm)	$\lambda max_{10\text{-}DN}$ (nm)	$\lambda max_{acrylamide}$ (nm)	Δλmax (nm)
$^{KK}L_{15}$(D10)	DOPC	4	323	322	322	1
	POPC	4	324	321	323	2
	POPC/40%chol	4	328	329	326	3
	POPC/POPE	4	325	326	325	2
	DOPG	4	322	321	323	2
	DOPS	5.5	320.5	321	320	1
$^{KK}L_{13}A_2$(D10)	DOPC	4	326.7	325.5	327	1.5
	POPC	4	328.5	327	330	3
	POPC/40%chol	4	330	330	330	0
	POPC/POPE	4	331	330	329	1
	DOPG	4	326	325	326	1
	DOPS	5.5	324	324	324	0
$^{KK}L_{11}A_4$(D10)	DOPC	4	324	324	323	1
	POPC	4	326	326	325	1
	POPC/40%chol	4	327	326	327	1
	POPC/POPE	4	327	330	327	3
	DOPG	4	324	322	324	2
	DOPS	5.5	321	321	321	0
$^{KK}L_9A_6$(D10)	DOPC	4	327.5	335.8	324	**8**
	POPC	4	328	334	327	**7**
	POPC/40%chol	4	331	345	327	**18**
	POPC/POPE	4	331	338	324	**14**
	DOPG	4	325	326	325	1
	DOPS	5.5	321	323	321	2
$^{KK}L_7A_8$(D10)	DOPC	4	335	336	332	4
	POPC	4	334	338	333	5
	POPC/40%chol	4	353	355	353	2
	POPC/POPE	4	346	343	341	2
	DOPG	4	329	329.5	328	1.5
	DOPS	5.5	325	327	324	3
$^{KK}L_{12}$	DOPC	5.5	335	348	325	**23**
	DOPC	9	335	348	325	**23**
	DOPS	5.5	322	326	322	4
	DOPS	9	322	325	322	3
$^{KH}L_{12}$	DOPC	5.5	326	327	326	1
	DOPC	9	326	325	324	1
	DOPS	5.5	324	325	323	2
	DOPS	9	324	325	323	2

$^{HH}L_{12}$	DOPC	5.5	326	329	327	2
	DOPC	9	327	328	326	2
	DOPS	5.5	324	326	324	2
	DOPS	9	327	328	327	1
$^{KK}L_4A_{18}$	DOPC	5.5	335	336	333	3
	DOPG	5.5	332	333	331	2
	DOPS	5.5	325	327	325	2
$^{KK}L_2A_{16}$	DOPC	5.5	357	357	356	1
	DOPS	5.5	327	336	325	**11**
$^{KK}A_{18}$	DOPC	5.5	360	360	360	0
	DOPS	5.5	327	335	325	**10**
$^{RR}A_{18}$	DOPC	5.5	356	359	356	3
	DOPS	5.5	327	333	325	**8**
$^{KK}A_{22}$	DOPC	5.5	358	358	359	1
	DOPS	5.5	334	335	334	1
$^{KKKK}L_{11}A_4$(D10)	DOPC	4	331	340	327	**13**
	DOPG	4	323	322	323	1

Table 3.4. Comparison of λmax and Q-ratio values for peptides incorporated into lipid vesicles at various pH. Samples contained 2 μM peptide and 200 μM lipid. The sample buffer used at pH 7 was PBS. Average values from data from three samples are shown. The λmax values for individual samples generally differed from the average by no more than ±1 nm.

Peptide	pH	Lipid	λmax (nm)	Δλmax (nm)	Q-ratio
$^{KK}pL_{11}A_4$(D10)	3.8	DOPG	324	1.7	0.173±0.03
	5.5	DOPG	324	2	0.208±0.03
$^{KK}pL_7A_8$(D10)	3.8	DOPG	329	1.8	0.616±0.3
	5.5	DOPG	331	2	0.574±0.18
$^{KK}pL_{12}$	7	DOPC	332	22	1.097±0.18
	7	DOPG	328	1	0.683±0.33
	7	DOPS	325	1.5	0.152±0.03

Table 3.5. Q-ratio and λmax values for peptides with medium-to-long hydrophobic segments. Q-ratio is defined in Materials and Methods. nd = not determined. Q-ratio and λmax values shown are the average from three samples. Standard deviation is shown for the Q-ratio. The λmax values for individual samples generally differed from the average by no more than ±1 nm.

peptide	DOPC		DOPS		DOPG		POPC/40%chol	
	Q-ratio	λmax	Q-ratio	λmax	Q-ratio	λmax	Q-ratio	λmax
$^{KK}pA_{18}$	36.7±3	358	0.387±0.09	327	nd	nd	nd	nd
$^{RR}pA_{18}$	5.63± 1.6	356	0.135±0.03	327	nd	nd	nd	nd
$^{KK}pL_2A_{18}$	10± 1	357	0.143±0.05	327	nd	nd	nd	nd
$^{KK}pA_{22}$	36.9± 5	360	0.785±0.13	334	nd	nd	nd	nd
$^{KK}pL_4A_{18}$	0.933±.31	335	0.254±0.05	325	0.718±0.16	332	1.94±0.91	349

Table 3.6. Helix content of membrane-associated peptides in different lipids as determined by circular dichroism. Samples contained 5 or 10 μM peptide in vesicles composed of 500 μM lipid. The remainder of the secondary structure was largely unordered.

Peptide	Lipid	Peptide:Lipid Ratio (mol:mol)	pH	% Helix Content
$^{KK}pL_7A_8(D10)$	DOPC	1:50	4	65
	DOPC	1.50	9	68
	POPC/40%Chol	1:50	4	58
	POPC/POPE	1:50	4	67
	DOPG	1.50	4	68
	DOPG	1:50	5.5	69
	DOPS	1:50	5.5	90
$^{KK}pL_{13}A_2(D10)$	DOPC	1.50	4	71
	DOPC	1:50	9	74
	POPC/40%Chol	1:50	4	66
	POPC/POPE	1.50	4	68
	DOPG	1:50	4	70
	DOPS	1:50	5.5	85
	DOPC	1:100	4	68
	DOPS	1:100	5.5	80
$^{KK}pL_9A_6(D10)$	DOPC	1:50	4	73
	DOPC	1.50	9	74
	DOPS	1:50	5.5	89
	DOPC	1:100	4	70
	DOPS	1:100	5.5	94
$^{KK}pL_{11}A_4(D10)$	DOPC	1:50	4	78
	DOPC	1:50	9	72
$^{KK}pL_4A_{18}$	DOPC	1:50	4	60
	POPC/40%Chol	1:50	4	61

	DOPG	1:50	4	67
	DOPS	1:50	5.5	83
	DOPC	1:100	4	63
	DOPS	1:100	4	86
$^{KK}pA_{18}$	DOPC	1:50	4	71
	DOPS	1.50	5.5	79
$^{KK}pA_{22}$	DOPC	1:50	4	65
	DOPS	1:50	5.5	85
$^{KKKK}pL_{11}A_4$(D10)	DOPC	1.50	4	67
	DOPG	1:50	4	65
^{HH}L12	DOPC	1:50	5.5	76
	DOPS	1:50	5.5	90
	DOPC	1:100	5.5	80
	DOPS	1:100	5.5	90

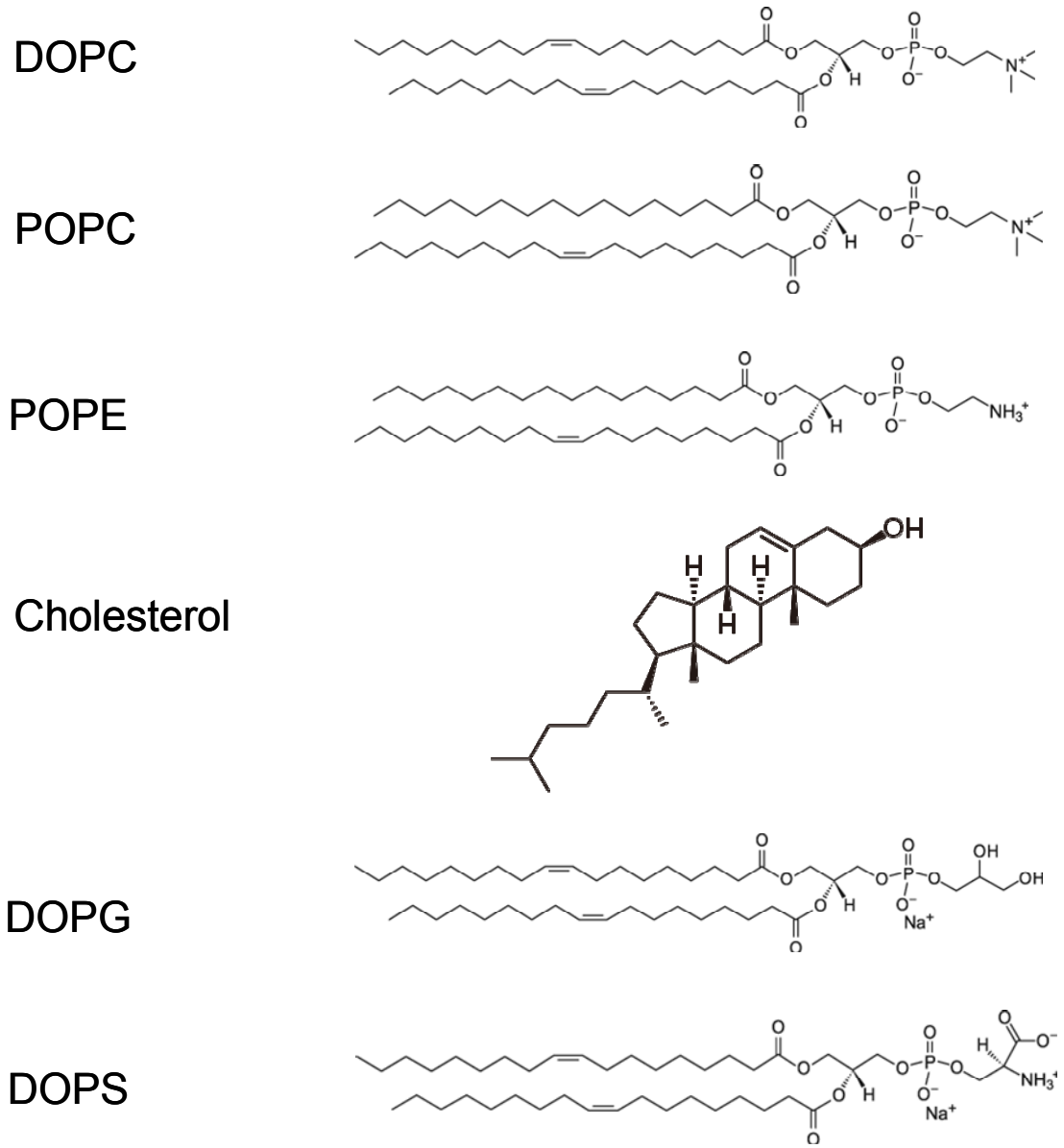

Figure 3.1. At physiological pH (7.4) DOPC, POPC and POPE headgroups are zwitterionic hence carries no net charge. On the contrary, DOPG and DOPS headgroup have net -1 charge at physiological pH.

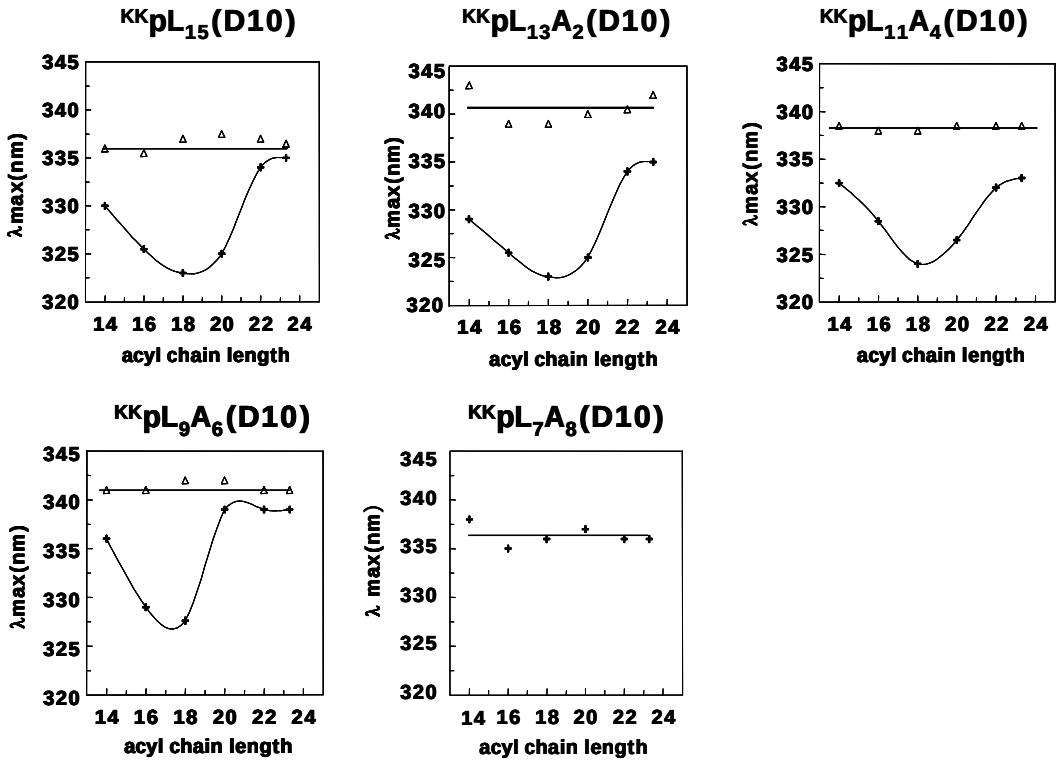

Figure 3.2: Trp emission λmax of peptides incorporated into lipid vesicles composed of di-unsaturated phosphatidylcholines with various acyl chain lengths. The vesicles were prepared at pH 3.8 (+) or 8.5 (Δ), values below and above the pKa of Asp residue, respectively. Samples in this and subsequent figures contained 2μM peptide and vesicles contained 200μM lipid unless otherwise noted**.** (A) $^{KK}pL_{15}(D10)$. (B) $^{KK}pL_{13}A_2(D10)$. (C) $^{KK}pL_{11}A_4(D10)$**.** (D) $^{KK}pL_9A_6(D10)$. (E) $^{KK}pL_7A_8(D10)$**.** In the case of $^{KK}pL_7A_8(D10)$ only the pH 3.8 curve is shown, as at pH 8.5 the peptide is not membrane bound and its λmax is off scale (350 –355 nm). The λmax values reported are average from at least three samples, and values for individual samples usually differ from the average value by no more than ±1 nm.

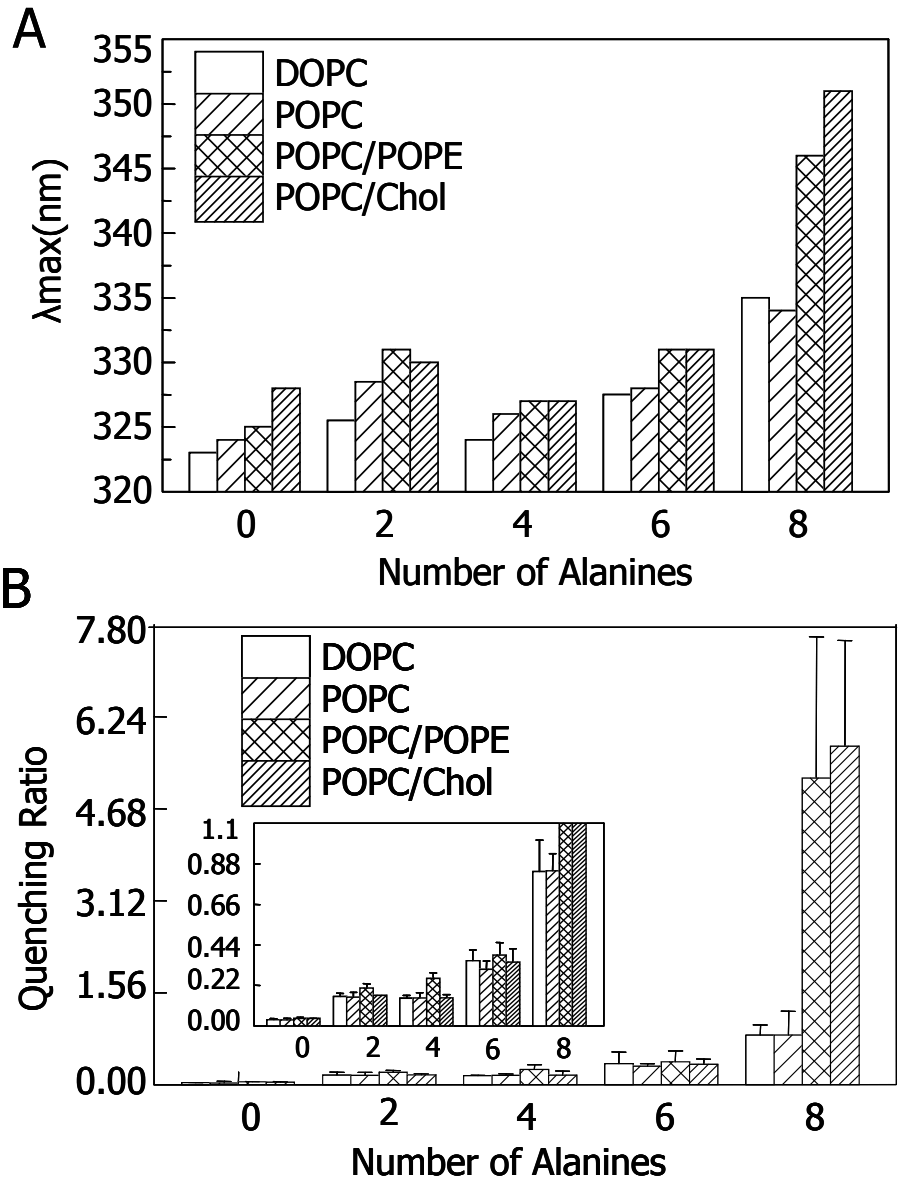

Figure 3.3: Effect of lipid structure upon the stability of TM state measured by λmax and quenching ratio for peptides incorporated into lipid vesicles without net charge. (A) λmax. (B) Q-ratio. All samples were prepared at pH 4. POPC/POPE mol ratio is 1:1 and POPC/cholesterol mol ratio is 3:2. In panel B, the off-scale values are: for POPC/POPE vesicles 5.2 ± 2.4, for POPC/cholesterol vesicles 5.74 ± 1.8 and the standard deviation for POPC is ± 0.4. The λmax values and Q-ratio reported are average from at least three samples. Standard deviations for Q-ratios are shown and the λmax values in individual samples generally within ±1 nm of the average values.

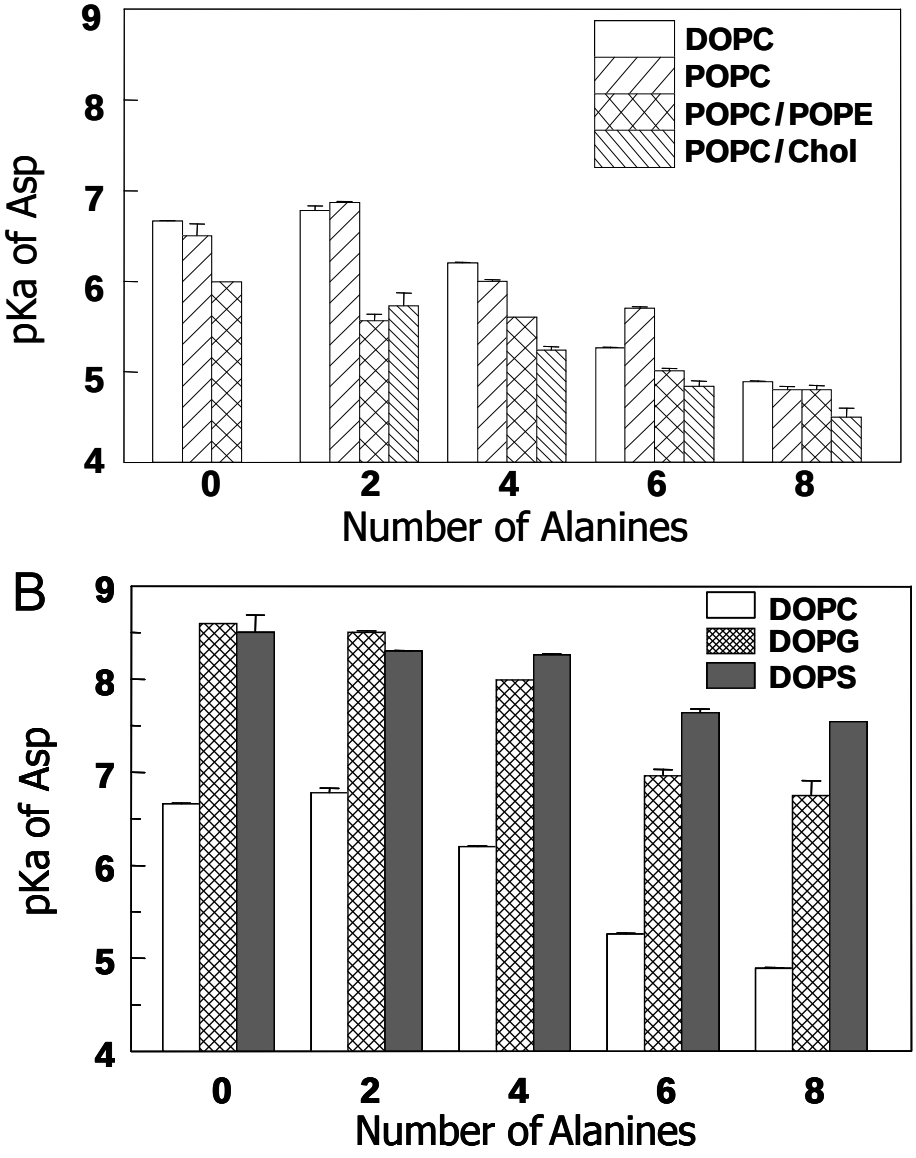

Figure 3.4: Apparent Asp pKa of peptides in (A) Lipid vesicles with no net charge. (B) Lipid vesicles composed anionic lipids. (pKa values for DOPC vesicles are also shown in B. for purposes of comparison.) pKa values were estimated from the change in the ratio of fluorescence emission intensity at 330 nm to that at 350 nm as pH was increased in samples containing a 1:100 peptide:lipid mole ratio. Values shown are the average pKa from duplicates and their range. The pKa values have not been corrected for the difference in the quantum yield of Trp fluorescence when the peptide Asp is in the ionized and unionized states. Correcting for this variable does not shift pKa measured by more than ±0.2 units.

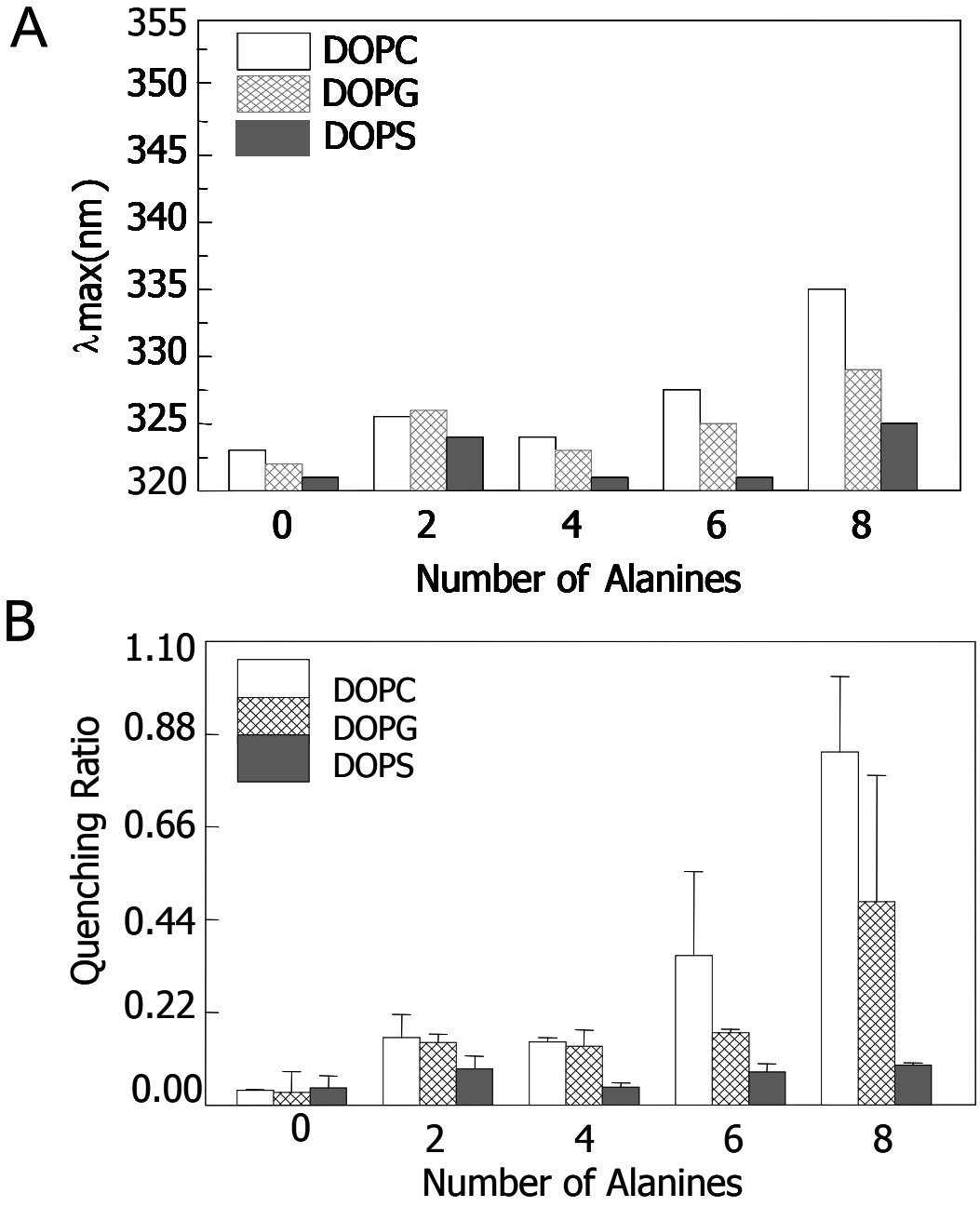

Figure 3.5: Effect of lipid structure upon the stability of TM state measured by λmax and Q-ratio for peptides incorporated into anionic lipid vesicles. Values for the zwitterionic lipid DOPC are shown for comparison. (A) λmax. (B) Q-ratio. Samples were prepared at pH 4 except for those containing DOPS vesicles, which were prepared at pH 5.5 to maintain anionic charge on the PS headgroup. The results shown are for the average from three samples. Standard deviations are shown for Q-ratios. λmax values in individual samples were generally within ±1 nm of the average value.

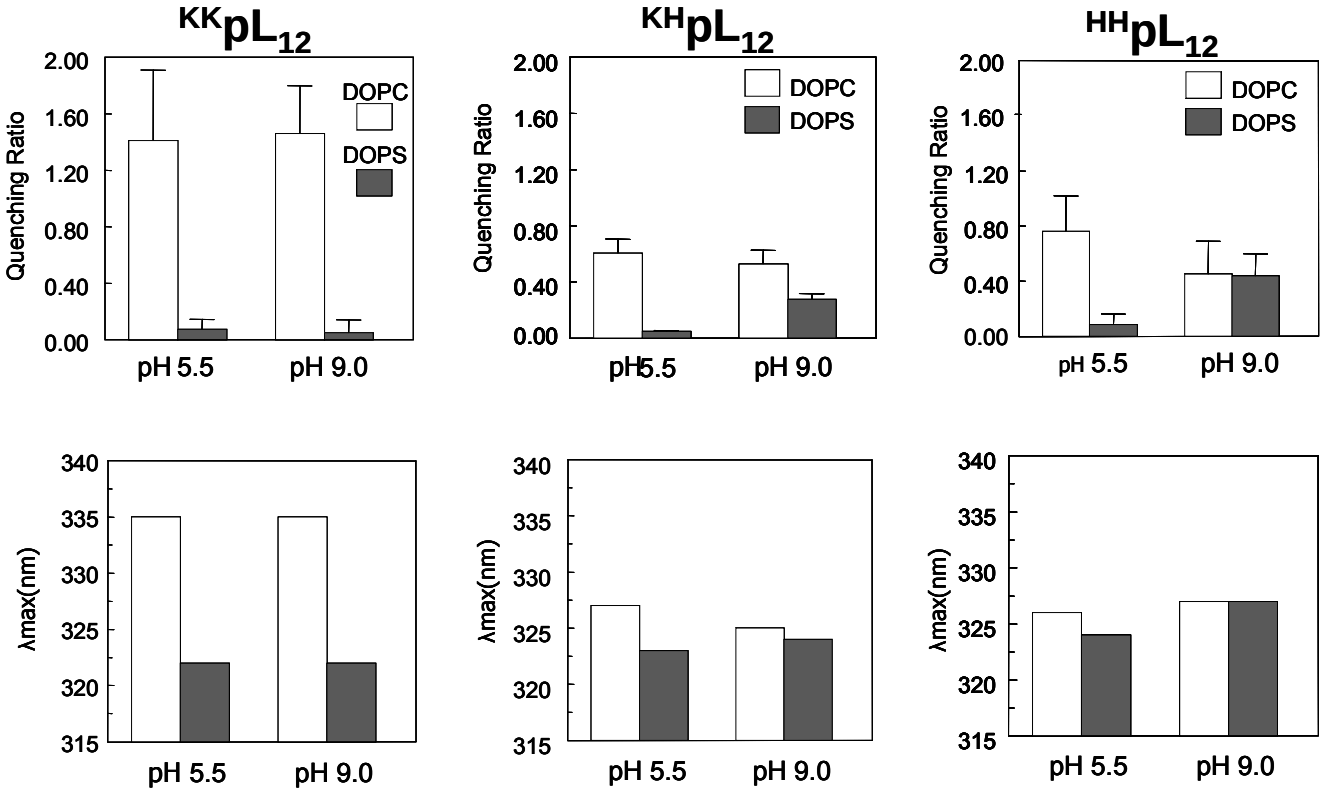

Figure 3.6: Q-ratio and λmax for peptides with short hydrophobic sequences $^{KK}pL_{12,}$ $^{HH}pL_{12,}$ $^{KH}pL_{12}$ are shown when they are incorporated into vesicles composed of DOPC (open bars) or DOPS (filled bars) at pH 5.5 and pH 9.0. The results shown are for the average from three samples. Standard deviations are shown for Q-ratios. λmax values in individual samples were generally within ±1 nm of the average value.

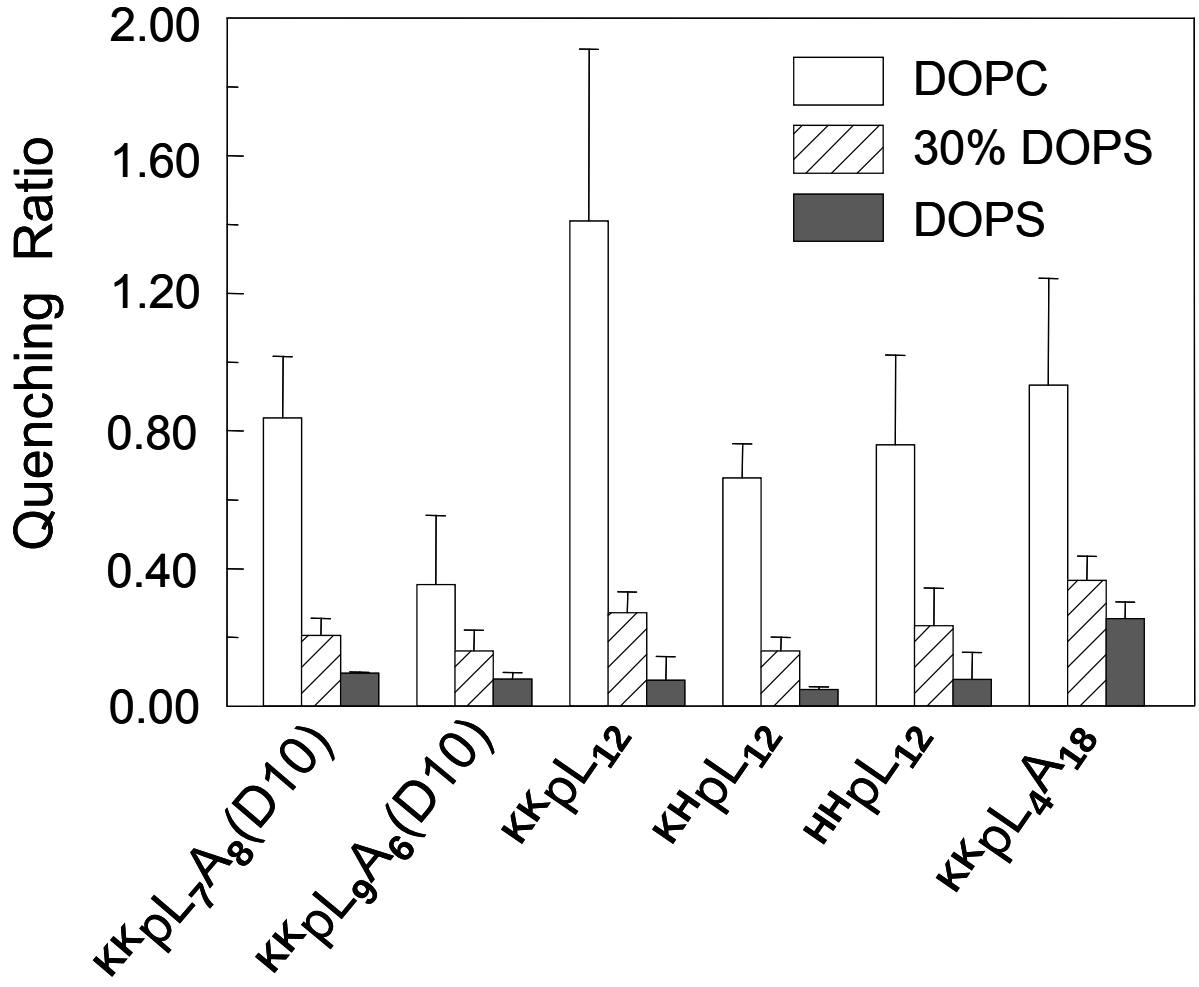

Figure 3.7: Comparison of Q-ratio for peptides with different lengths and varying flanking residues in 30mol%DOPS/70mol%DOPC vesicles to that in pure DOPC or pure DOPS vesicles. Samples containing DOPS were prepared at pH 5.5; those containing only DOPC were prepared at pH 4.0. The results shown are for the average from three samples. Values shown are average from at least three samples and standard deviation.

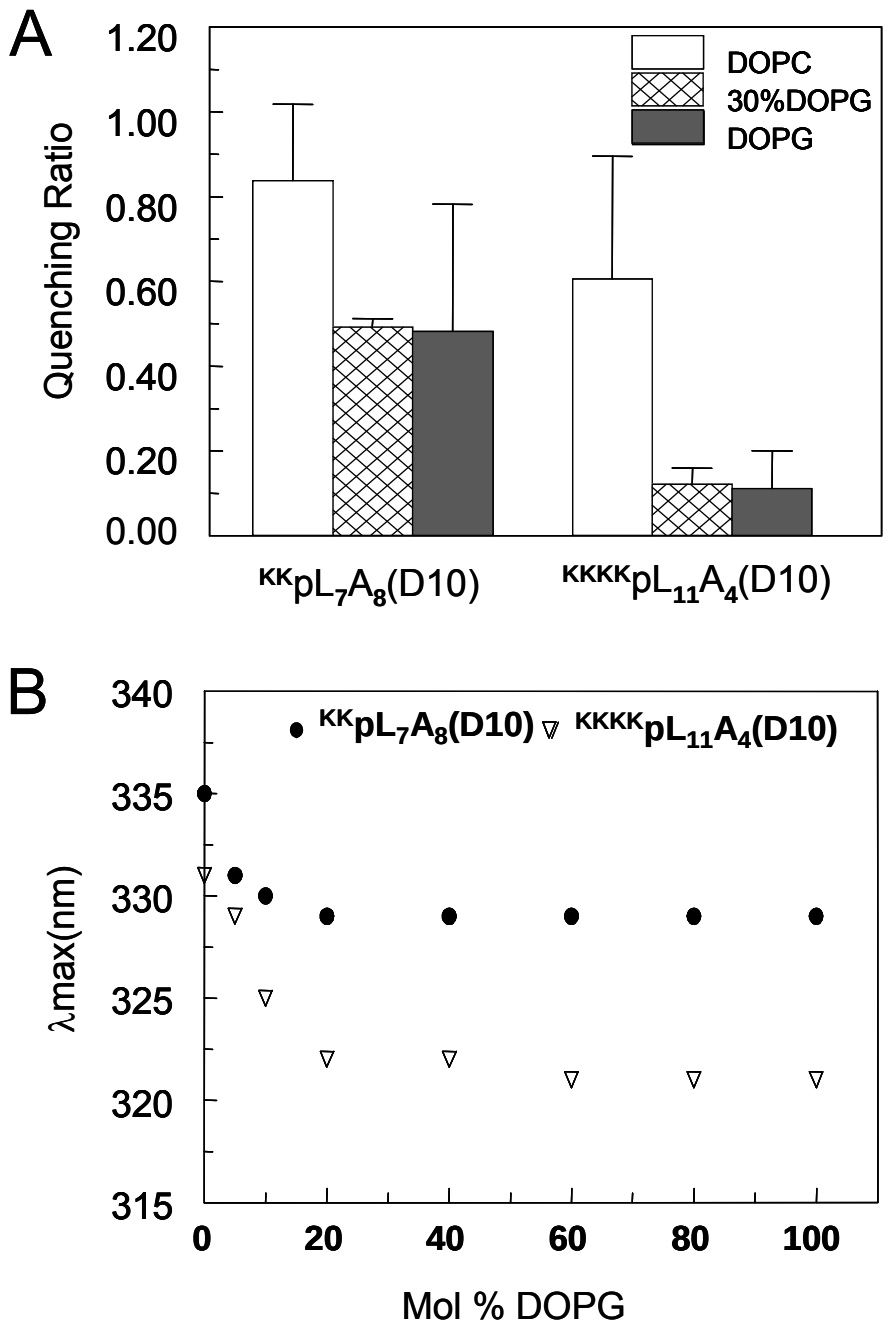

Figure 3.8: Effect of the vesicle DOPG content upon Q-ratio and λmax for vesicle-associated $^{KKKK}pL_{11}A_4(D10)$ and $^{KK}pL_7A_8(D10)$ peptides. (A) Q-ratios at pH 4.0. Values reported are the average from at least three samples and standard deviation. (B)Trp emission λmax at pH 4.0. The results shown are for the average from two samples. λmax values in individual samples were generally within ±1 nm of the average value.

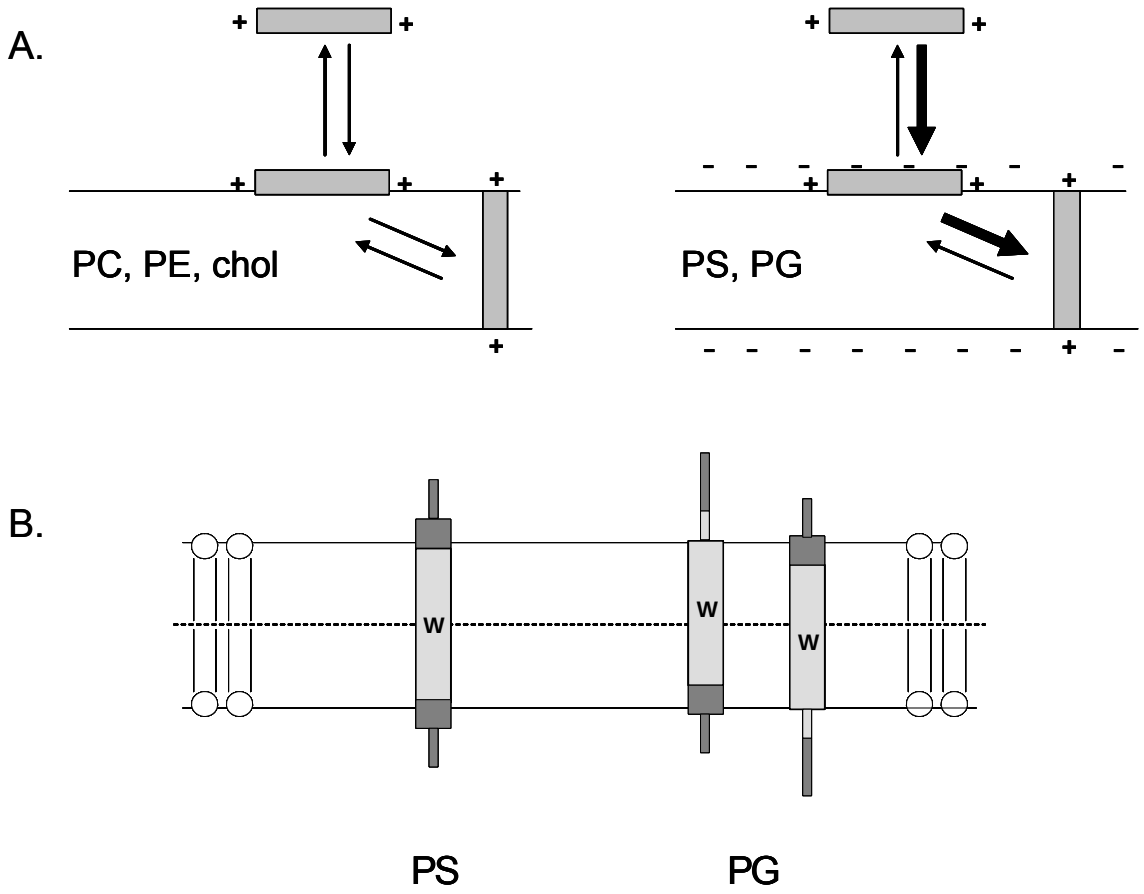

Figure 3.9: Schematic illustration of the proposed difference in peptide topography in DOPG and DOPS-containing vesicles. (A) Effect of anionic lipid on membrane association and topographical equilibria. Notice that anionic lipid enhances both binding of polypeptides to membrane and the formation of the TM topography when the polypeptide is membrane-bound. (B) Difference between topography in DOPG and DOPS vesicles. Trp location is indicated by the "W". The hydrophobic core of the peptide is shown by light gray shading and the hydrophilic flanking segments by dark gray shading. Helical sequences are indicated by thick rectangular regions and disordered sequences by thin rectangular regions. In addition to the topographical difference illustrated here may be a lesser degree of formation of the TM topography in the presence of DOPG-containing vesicles.

Chapter 4

Transverse Shift and Anionic Lipid

INTRODUCTION

Transmembrane segment of membrane proteins are usually thought of as a fixed stretch of 20-25 hydrophobic amino acid residues. However, with the advancement in our knowledge of membrane protein structure it is evident that the membrane-buried residues can be flexible and diverse. Studies conducted in our lab using both artificial helices [46; 50] and TM segment of polio virus 3A protein [21] showed that a TM helix can sometimes exist in two positions with different membrane boundaries, as shown in figure 4.1. This type of transverse shift can result in a significant movement of TM helix position. The presence of a highly hydrophilic residue within a poly-Leu-Ala hydrophobic sequence has been shown to shift the position of a TM helix up to 6Å [90] so that the hydrophilic residue can locate at or near the bilayer surface.

The notion that changes in TM helix tranverse position might control protein function was proposed long time ago[144] and there are several examples where a shift in helix position plays an important role in protein function. In the case of bacterial chemoreceptor it is well documented that vertical movement of TM helix can control the signaling state of the receptor[75; 76; 77] Similarly, in integrins, transmembrane signaling is modulated by the transverse movement of the TM helix within the membrane[78; 145]. Helix shift is also functionally important for fibroblast growth factor receptor 3 (FGFR3)[79].

Anionic lipids, an integral part of biological membranes, are often found to be involved in a wide range of biological phenomenan including membrane protein insertion and translocation [6; 146; 147] and hormone or toxin penetration[148; 149]. It is well documented that electrostatic interactions with charged membrane promote insertion and or transport of membrane proteins with cationic residues or polybasic clusters[91; 92; 93; 150] Although most biomembranes are known to contain ~ 20% anionic lipids in inner leaflet recent study in intact cell have noted that the distribution of phosphatidylserine (PS) within the cellular organelles can vary [151; 152]. This uneven distribution of surface charge potential can influence how proteins are targeted and retained in sub cellular compartments. So, interactions with lipids have a key role in stabilizing the structure of membrane protein within their lipid bilayer environment.

Von Heijne and colleagues first reported that hydrophilic residues within the hydrophobic helices can change the position of the TM helix within the membrane using glyscosylation mapping [86; 87; 88; 89]. Our lab extended such studies in lipid bilayer system, and measured helix transverse shift for the whole series of hydrophilic residues using membrane inserted peptides with a KKLALA**X**ALALAWLALALALALAKK sequence (X is the hydrophilic residue). The shift was found to be dependant on the identity of the hydrophilic residue. The extent of shift induced by hydrophilic residue at pH 7 in increasing order: L<G~Y<T<R~H<S<P<K<Q~E<N<D [90]. The order correlated nicely with a combination of amino acid hydrophobicity and the ability to snorkel. In previous chapter I have reported that anionic lipid can stabilize the non-TM topography of borderline hydrophobic sequences through an interaction between helix flanking cationic residues and the anionic lipid head group. In this chapter, studies were done to investigate whether the same type of head group specific interaction will exert any effect upon the TM sequences that would have a tendency to form a shifted TM state.

RESULTS

Defining the Topography of Membrane-Inserted Hydrophobic Helices Using Fluorescence Emission λmax, Fluorescence Quenching and Bilayer width

To define the topography, fluorescence properties of a trp residue located at the center of the hydrophobic sequence was used as a prob [47; 55]. Trp is sensitive to the polarity of the local environment. When a helical sequence form a TM structure it is accompanied by blue-shifted trp emission λmax (320-325nm) and when a sequence adopts a non-TM surface bound topography the trp experiences a more polar environment resulting in a strong red shifted trp λmax (335-345nm)[58; 90]. Intermediate values of trp λmax are indicative of a mixed population of TM and non-TM topography or a shifted-TM state wherein only a part of hydrophobic sequence is form the spanning segment such that a polar residue can locate close to the bilayer surface (Figure 4.1)[50; 90].

Interpretation of λmax results can be complemented with a more direct measurement of trp depth. To do this a dual fluorescence quenching method[43] developed in our lab was used to determine the trp depth within the bilayer. This method uses two quenchers of trp fluorescence: 10-doxylnonadecane (10-DN), a membrane inserted quencher which preferentially quenches the fluorescence of membrane-buried trp, and acrylamide, a water soluble quencher mainly quenches the fluorescence of aqueous solution exposed trp. The ratio of acrylamide quenching to 10-DN quenching (Q ratio) correlates linearly with the trp depth in the bilayer. Low Q ratio (<0.1-0.2) is a characteristic of trp near or close to bilayer center while a high Q ratio (≥ 1) indicate a trp location near the bilayer surface[43]. An intermediate value for Q ratio is observed for peptides adopting a mixed orientation with shallow and deep trp depth, or for peptide adopting a shifted TM conformation.

Changing bilayer width to induce hydrophobic mismatch between lipid bilayer and helix length is another method to define the TM topography of membrane inserted helices. For a trp located at the center of a hydrophobic sequence, trp fluorescence is generally most blue shifted when trp is at the center of the widest bilayer in which the TM configuration is stable [46; 55; 74]. For this reason, the bilayer width at which the trp

fluorescence is most blue shifted can distinguish short, medium and long TM helices (Figure 4.2). Trp emission red shifts in wider bilayers due to negative mismatch-induced destabilization of the TM state, and formation of a significant amount of a non-TM state [50; 74]. Emission also red shifts in very thin bilayers, partly due to positive mismatch [55] This positive mismatch induced red shift arises because in thinner bilayer trp is closer to the bilayer surface since the distance between bilayer center and the surface is reduced as bilayer width decreases (Figure 4.3). Also, in thinner bilayer the helix tends to tilt to minimize exposure to aqueous solution and it has been proposed that this promotes oligomerization. In an oligomeric state a trp may be shielded from the apolar membrane environment thus giving a red shifted λmax [47; 98].

Behavior of Shifted-TM Hydrophobic Helices in Anionic Lipid Containing Vesicles: Investigated by Bilayer width variation and Trp depth

The peptide used in this study consisted of a 25 residue long poly-Leu-Ala sequence with a 21-residue hydrophobic core containing a trp at the center of the sequence and a single variable (X) residue located 5 residues away from the N-terminal end of the hydrophobic sequence (Table 4.1). All the sequences were flanked by two JM lysine residues on both N and C-terminus. These sequences were originally studied by a former student in our lab to study how different hydrophilic residues can control transverse position of transmembrane helices [90]. Peptides with X=L, R,Q,Y,E were selected by me because they represented the transverse shifting tendency of different types of hydrophilic residues. In order to study the effect of bilayer width upon the helix topography, lipids with different acyl chain length were needed. Since, anionic lipids (PG/PS) with different acyl chain lengths are not available commercially, 20mol% of readily available 18 carbon anionic lipids were combined with mono-unsaturated phosphatidylcholine (PC) of different chain lengths to get negatively charged vesicles with different bilayer widths. Resulting bilayer thickness should be the average of two types of lipid chain lengths (Table 4.2).

pLA_{10} (X=L) peptide

As mentioned in earlier in this chapter, the change in the trp emission λmax as a function of lipid bilayer thickness can tell us about the length of the membrane spanning segment of the peptide. A decrease in length of the membrane spanning sequence, due to helix shift, can easily be detected because TM state of a short helix gets destabilized (causes λmax red shifts) in much thinner bilayer than for longer helices as shown in figure 4.2[90]. To see lipid effects helix shift peptides were incorporated into both uncharged bilayers composed of phosphatidylcholine (PC) lipids and partially charged bilayers containing (80:20) mol:mol zwitterionic lipid and anionic lipid. Figure 4.4 compares the effect of bilayer width on the trp emission λmax (A) and trp depth (B) in these two types of bilayer for the "parental" poly-Leu-Ala peptide sequence (X=L) at pH 7.0. The λmax profile for this peptide (Figure 4.4A) shows that the "effective TM length" is longer in anionic lipid containing vesicles. "Effective TM length" is defined as the bilayer width (in acyl chain length units) at which trp fluorescence is most blue shifted because there is a close match between the bilayer thickness and length of the hydrophobic sequence[90]. In uncharged bilayers (dotted line) the minimum is about 19.5 carbons (shown by an arrow) and the minimum goes up to 20.5-21 carbons (arrow) in 20% DOPS or 20% DOPG containing bilayers (solid lines). This increase in effective TM length combined with the blue shifted λmax in thicker bilayer indicates that TM conformation is stabilized by anionic lipids. A smaller quenching ratio (Q ratio) in 20% anionic lipid containing vesicle compare to 100%DOPC vesicle (Figure 4.4B) confirms the observation of enhanced TM stability in wider bilayers. This could be due better anchoring of the poly-Leu-ala sequence in negatively charged vesicles (Figure 4.9 and discussion) because both the λmax and Q ratio values confirm that pLA_{10} is in fully TM state in both types of bilayers.

$pLAQ_7$Peptide (X=Q)

Peptide containing glutamine (Q) residue shows a large shift in the helix position when incorporated into uncharged vesicles as judged by the shortening of the effective TM length to about 17 carbons (+, Figure 4.5A) compared to the parental pLA sequence (+, Figure 4.4A). This is consistent with the hydrophilic nature of the glutamine residue

which gives it a strong tendency to locate near the membrane surface. The TM topography starts to become destabilized in much thinner bilayer than X=L peptide which is also consistent with the behavior of short TM sequences (+,Figure 4.4A, Figure 4.5A)[58]. However, the TM stability increases when the peptide is incorporated into 20% anionic lipid containing vesicle as seen from both the change in λmax profile (solid lines, Figure 4.5A) and smaller Q ratio (Figure 4.5B).

pLAR$_7$Peptide (X=R)

Arginine is a charged residue and has a long side chain which can snorkel [103]so this sequence does not shift as much as Q showing an effective TM length of 18 carbons in uncharged bilayers(Figure 4.6A, +). There is 1 carbon increase in the λmax minimum (indicated by arrow in Figure 4.6A) in 20% anionic lipid containing vesicles relative to all PC vesicles indicating TM stabilization. Trp depth is also deeper in negatively charged bilayer and it seems deepest in 20%PS containing vesicles (Figure 4.6B).

pLAE$_7$Peptide (X=E)

Glutamate is an ionizable residue and it also induces a large helix shift in uncharged bilayers at pH 7.0 (effective TM length is 17 carbons, +,Figure 4.7A). As observed for other sequences in this chapter, effective TM length increases in the presence of anionic lipid to about 18.5 carbon atoms (arrow Figure 4.7A) showing that shifted TM structure is suppressed in preference to a normal TM topography when the peptide is incorporated into anionic lipid containing vesicles. This is evident from both λmax result (Figure 4.6A) and trp fluorescence quenching (Figure 4.7B). It has been shown that E is partially charged at pH 7.0[90]but pKa of E might be different in anionic lipid containing vesicles as observed in chapter 3. λmax result at pH 9.0 still showed an increase in effective TM length in the presence of anionic lipids but not as much as pH 7.0. This indicate that pKa of E is probably slightly higher in 20% anionic lipid containing vesicles than PC vesicles.

LAY_7Peptide (X=Y)

Finally, the effect of tyrosine residue, which is known to prefer the bilayer interfacial region, was tested. It does not induce much transverse helix shift in uncharged bilayers (effective TM length is 19 carbon atoms). The λmax profile (dotted line Figure 4.8A) is actually not much different from the parental X=L sequence (Figure 4.4A). Both had had long effective TM length (18.5-19 carbon atoms). Again there is TM length increase by 1 carbon atom indicating stabilization of TM state in the presence of negatively charged lipids (Figure 4.8).

Characterizing TM topography using quencher induced λmax shift (Δ λmax)

Shifted TM structures mostly exist in equilibrium with other TM conformations so quencher induced shift in Trp λmax is another parameter for defining the TM topography. When a membrane-inserted peptide forms coexisting deep and shallow structures, its Trp emission λmax would be the average of blue and red shifted spectra resulting from the deep and shallow conformation respectively. If that's the case acrylamide preferentially quenches the shallow Trp which give rise to a blue shift. On the other hand, 10-DN quenches the deep Trp resulting in a red shifted λmax. The difference in λmax (Δλmax) in the presence of acrylamide and 10-DN can be up to 15 nm[90]. But for a homogeneous population with an intermediate trp depth the difference in λmax is very small. Table 4.3 showed that the Δλmax values for X= Q,E and R containing peptides in DOPS vesicles is very small (~1nm) compare to the DOPC (4.3-5.7 nm) vesicles indicating the existence of a single species and a mixed species in charged bilayers and uncharged bilayers respectively. For more hydrophobic sequences like, X=L and X=Y, the Δλmax values were small regardless of the nature of the lipid bilayers. These observations indicate that strong electrostatic interaction between the flanking cationic residues and anionic lipid headgroup can stabilizes the TM conformation in preference to the shifted-TM topography.

DISCUSSION

Better anchoring of TM sequences having cationic JM residues in negatively charged lipid vesicles

All these peptide sequences are flanked by two positively charged JM Lys residues at each ends. This was designed originally to prevent peptide aggregation. In previous chapter I have reported that anionic lipid was able to preferentially stabilize the TM structure of hydrophobic helices relative to the surface bound non-TM structure through an interaction between the JM cationic residues and negatively charged lipid headgroup. This electrostatic interaction reduced the free energy of the TM state hence making it more stable. Interaction between the flanking residues and anionic lipid headgroup can also anchor the existing TM topography within the membrane. For instance, increased TM stability of the pLA sequence in anionic lipid containing bilayer can be explained by the better anchoring of the flanking Lys residues to the charged bilayer. This is not uncommon. It has been proposed that TM sequences containing moderately hydrophobic core (alternating Leu and Ala residues) can not anchor very strongly in neutral PC bilayers such that the TM state is not strongly fixed in its position[58]. It is evident that small amount of negative charge in the bilayer can anchor these type TM helices to the bilayer (Figure 4.9). Increased TM stability in case of pLA and $pLAY_7$ in the presence of anionic lipid is probably due to the anchoring of the flanking Lys residues since these helices form a normal TM structure in uncharged bilayers.

Hydrophobic helices resist negative mismatch in the presence of anionic lipid

It is interesting to notice from the λmax curves of the hydrophobic sequences in this study that in the (dotted lines) uncharged bilayers and charged bilayers (solid lines) there is a large difference toward the right side of the plot accompanying the increase in bilayer thickness. This difference is more dramatic for the shifted sequences that have a shorter TM length. When the bilayer lipid acyl chain length is longer than the length of the TM segment negative mismatch occurs. Under moderate negative mismatch the TM sequence can oligomerize to prevent exposure of the hydrophobic sequence of the peptide

or equilibrate between surface and TM conformation resulting in a red shifted λmax. In case of extreme negative mismatch the peptide pops up to the surface giving a strongly red shifted λmax. For instance, 22 carbons represent the widest bilayer in this study and Trp λmax was most red in this bilayer. But λmax curves representing anionic lipid containing bilayer do not go up as much as the PC bilayer. There is evidence that flanking Lys residues form a continuation of the transmembrane helix and this may facilitate favorable electrostatic interaction with the negatively charged lipid headgroups [97; 153]. This is probably the reason the hydrophobic helices are able to maintain stable TM conformation under negative mismatch condition in the presence of negative lipid.

Difference between PG and PS

In previous chapter, I reported a marked difference between DOPG and DOPS lipid in terms of their ability to stabilize the TM conformation of hydrophobic helices relative to the non-TM conformation. However, for those studies I used 100% anionic lipid bilayer while in this study I used 20% anionic lipid containing bilayer. May be the difference between PG and PS is not easily detectable with this smaller amount of anionic lipid. Nevertheless, in some cases, such as, with X=R and X=E there was a difference between PG and PS containing vesicles in terms of quenching ratio and λmax in vesicles with 19 carbon atoms long acyl chains. The same difference in PG and PS behavior seen in chapter 3 can be applied here as well. DOPS probably has a larger effect on anchoring of the sequences to the membrane than the DOPG.

Table 4.1. List of hydrophobic peptides used in this study.

Peptide	Primary Sequence
pLA_{10}	Acetyl-KKLALALALALAWLALALALALAKK-amide
$pLAY_7$	Acetyl-KKLALAYALALAWLALALALALAKK-amide
$pLAQ_7$	Acetyl-KKLALAQALALAWLALALALALAKK-amide
$pLAR_7$	Acetyl-KKLALARALALAWLALALALALAKK-amide
$pLAE_7$	Acetyl-KKLALAEALALAWLALALALALAKK-amide

Table 4.2 : The average lipid acyl chain length resulting from 80:20 mixture of PC and DOPS lipids. All the lipids used in this study contain monounsaturated acyl chains so that the bilayer remains in the fluid Ld state at room temperature. DNPC, a 24 carbon acyl chain lipid has a relatively high melting temperature. To ensure its fluidity at room temperature we made vesicles with 33% DEuPC and 66% DNPC.

Lipid	Acyl chain length	Average acyl chain length with 20% DOPS
DMoPC	14	14.8
DPoPc	16	16.4
DOPC	18	18
DiEPC	20	19.6
DEuPC	22	21.2
66%DNPC/33% DEuPC	23.3	22.2

Table 4.3: Quencher induced shift in Trp emission λmax for peptides at pH 7.0. Δ λmax is the absolute difference between λmax in the presence of acrylamide and λmax in the presence of 10-DN. The Δ λmax values for hydrophilic residues in DOPC and DOPS vesicles are highlighted for comparison.

Peptide	DOPC		(80:20) DOPC/20%DOPG		(80:20) DOPC/20%DOPS	
	λmax(nm)	Δ λmax(nm)	λmax(nm)	Δ λmax(nm)	λmax(nm)	Δ λmax(nm)
pLA_{10}	325	1.4	324	2.7	323	1
$pLAY_7$	321	1.4	322	.7	320	1
$pLAQ_7$	327.5	**4.8**	324	2	323	**0.6**
$pLAR_7$	324	**5.7**	322	.7	320	**1**
$pLAE_7$	326	**4.3**	324	2.7	322	**1**

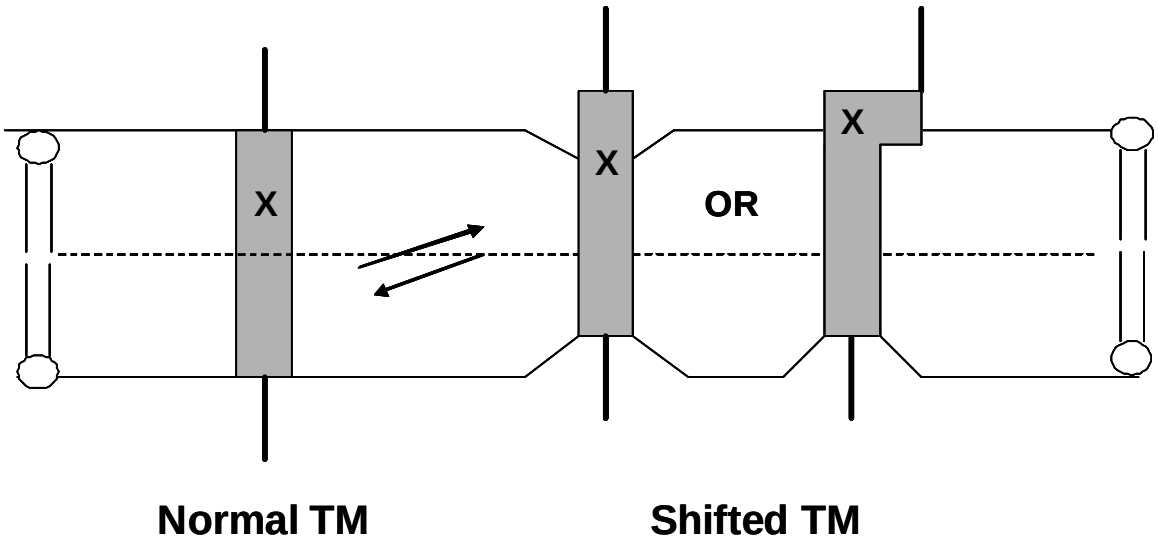

Figure 4.1: Helix transverse shift induced by a hydrophilic residue **X**. Shaded rectangles represent the helix and bold lines attached to the helix represent the juxtamembrane Lys residues. The dotted line signifies the lipid bilayer center.

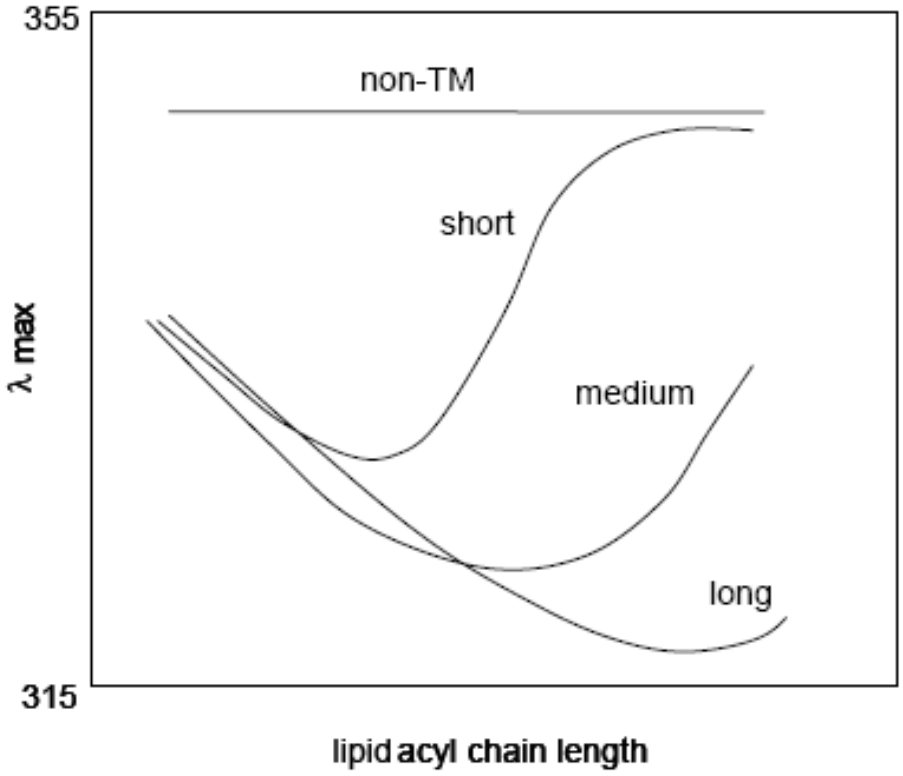

Figure 4.2: Effect of bilayers width upon the Trp emission λmax. Trp λmax dependence on lipid bilayers width can be used to determine the topography of peptides.

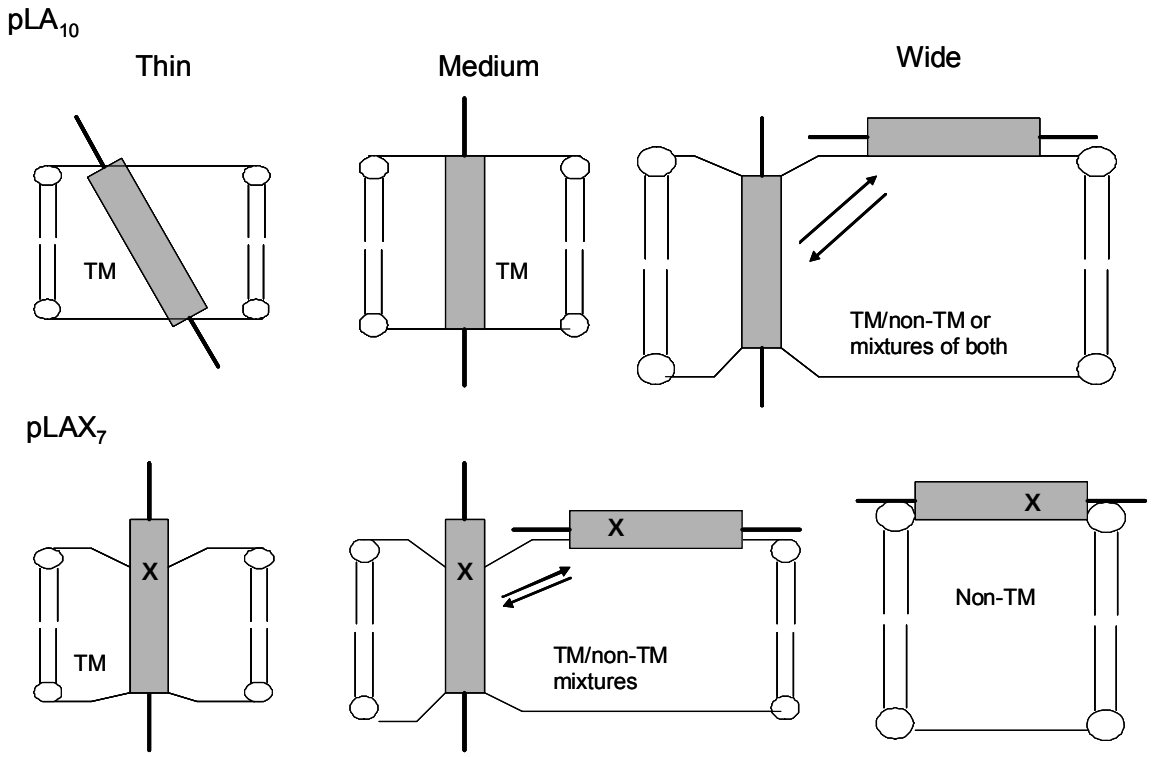

Figure 4.3: Schematic figures depicting the conformations of a long TM sequence and a short TM sequence in different bilayers thickness. The grey rectangle shows a normal TM helix (pLA) and grey rectangle with X represents a shortened TM helix as result of hydrophilic residue X (e.g. $pLAX_7$).

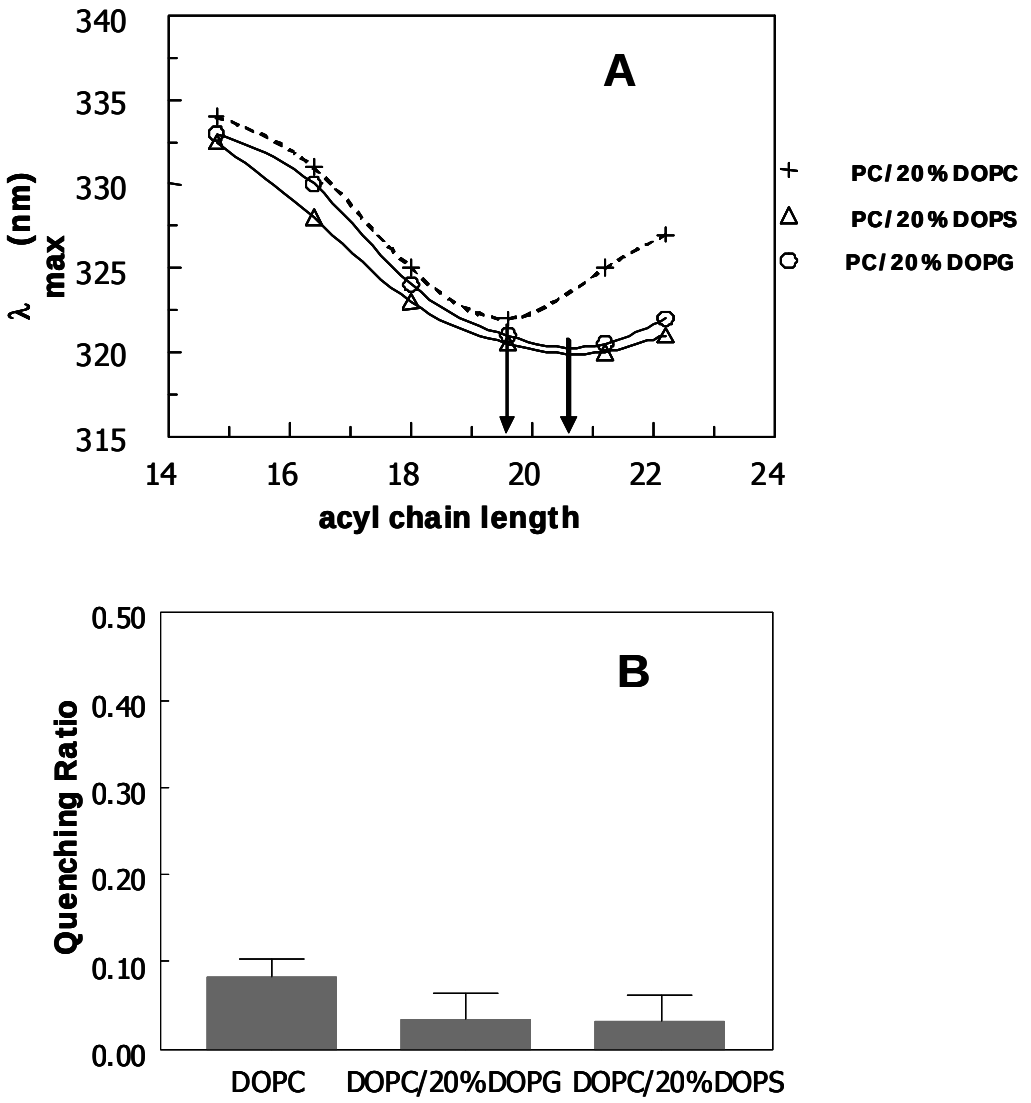

Figure 4.4: Effect of 20mol% anionic lipid upon the conformation of pLA peptide at pH 7.0. (A) Trp λmax dependence in lipid bilayer of different acyl chain lengths. (+) shows (80:20) mixtures of different length PC and DOPC. (O) shows (80:20) mixtures of different length PC and DOPG. (Δ) shows (80:20) mixtures of different length PC and DOPS. Arrow shows effective TM lengths in different lipid mixtures. (B) Trp fluorescence quenching ratio in different lipid mixtures. Samples contained 2μM peptide incorporated into 500 μM lipid vesicles suspended in PBS buffer.

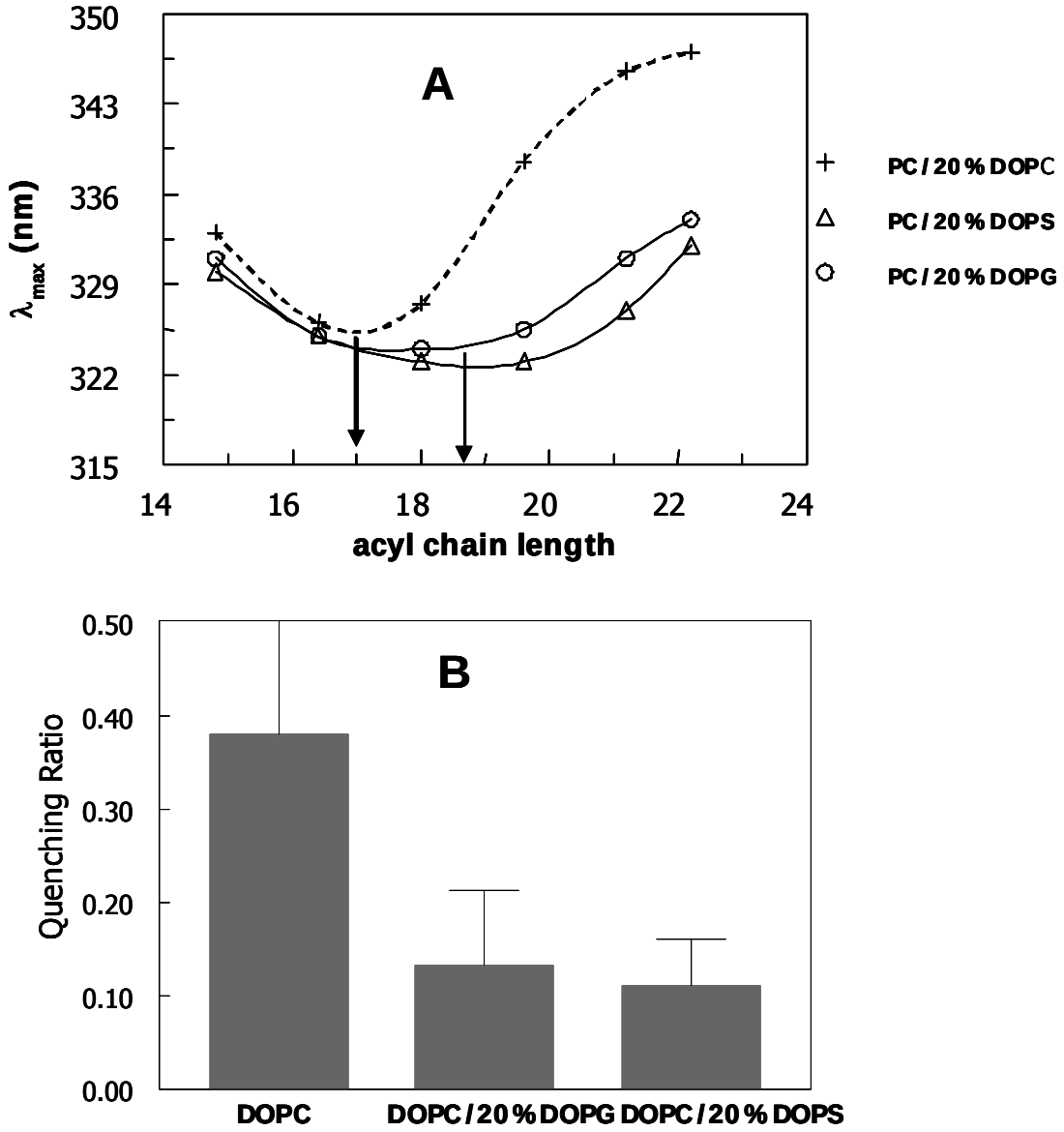

Figure 4.5: Effect of 20mol% anionic lipid upon the conformation of $pLAQ_7$ peptide at pH 7.0. (A) Trp λmax dependence in lipid bilayer of different acyl chain lengths. (+) shows (80:20) mixtures of different length PC and DOPC. (O) shows (80:20) mixtures of different length PC and DOPG. (Δ) shows (80:20) mixtures of different length PC and DOPS. Arrow shows effective TM lengths in different lipid mixtures. (B) Trp fluorescence quenching ratio in different lipid mixtures. Samples contained 2μM peptide incorporated into 500 μM lipid vesicles suspended in PBS buffer.

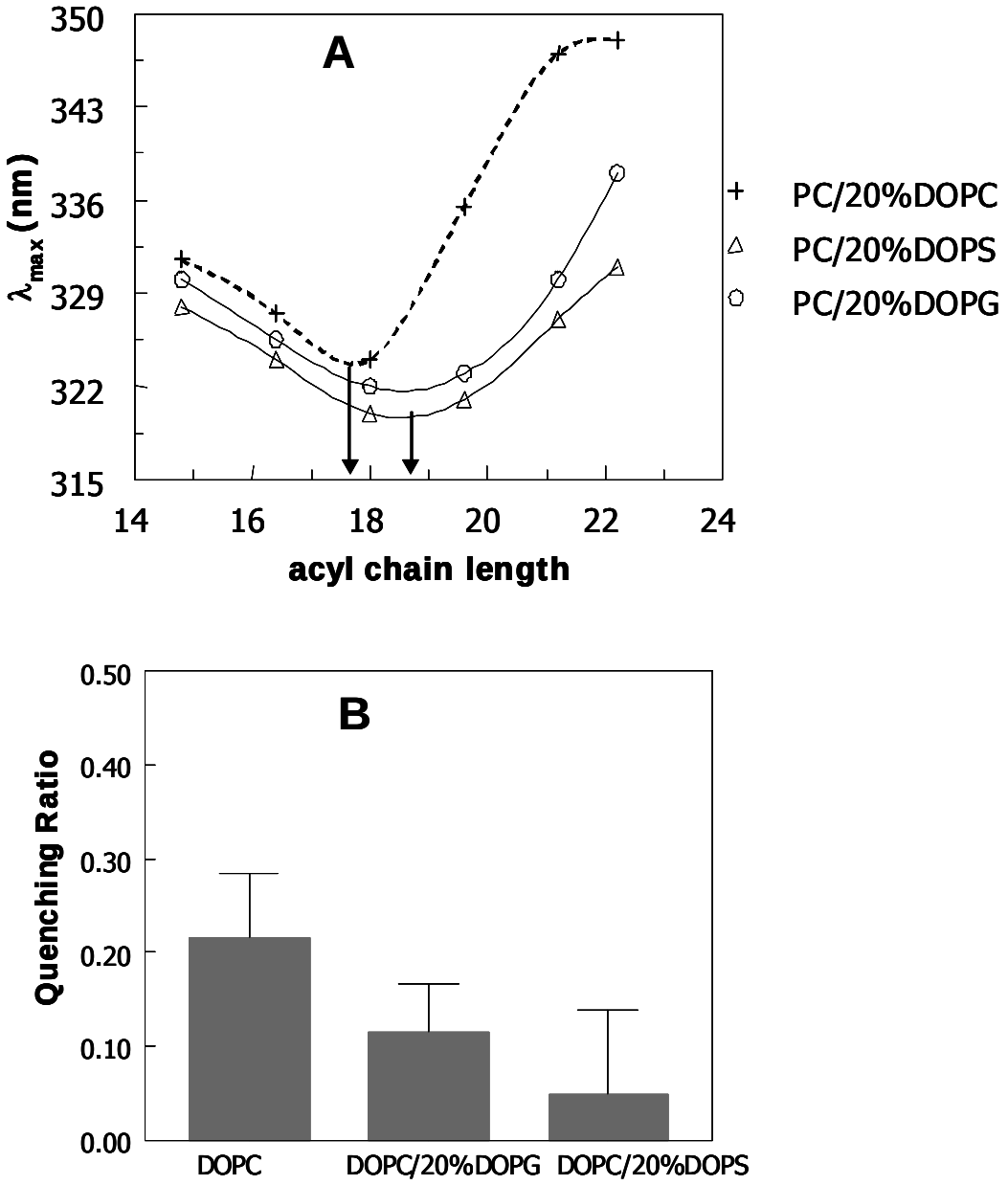

Figure 4.6: Effect of 20mol% anionic lipid upon the conformation of $pLAR_7$ peptide at pH 7.0. (A) Trp λmax dependence in lipid bilayer of different acyl chain lengths. (+) shows (80:20) mixtures of different length PC and DOPC. (O) shows (80:20) mixtures of different length PC and DOPG. (Δ) shows (80:20) mixtures of different length PC and DOPS. Arrow shows effective TM lengths in different lipid mixtures. (B) Trp fluorescence quenching ratio in different lipid mixtures. Samples contained 2μM peptide incorporated into 500 μM lipid vesicles suspended in PBS buffer.

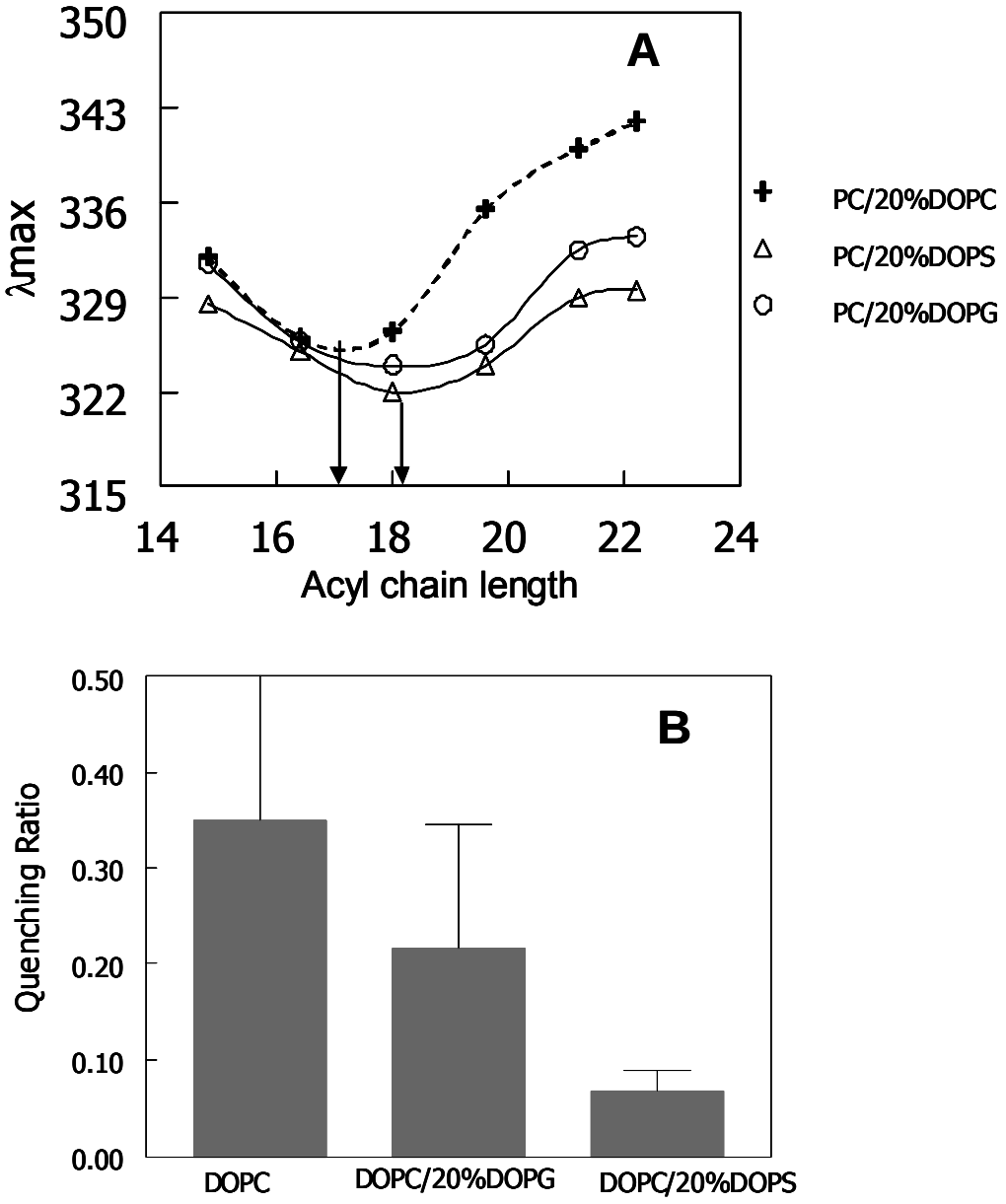

Figure 4.7: Effect of 20mol% anionic lipid upon the conformation of $pLAE_7$ peptide at pH 7.0. (A) Trp λmax dependence in lipid bilayer of different acyl chain lengths. (+) shows (80:20) mixtures of different length PC and DOPC. (O) shows (80:20) mixtures of different length PC and DOPG. (Δ) shows (80:20) mixtures of different length PC and DOPS. Arrow shows effective TM lengths in different lipid mixtures. (B) Trp fluorescence quenching ratio in different lipid mixtures. Samples contained 2μM peptide incorporated into 500 μM lipid vesicles suspended in PBS buffer.

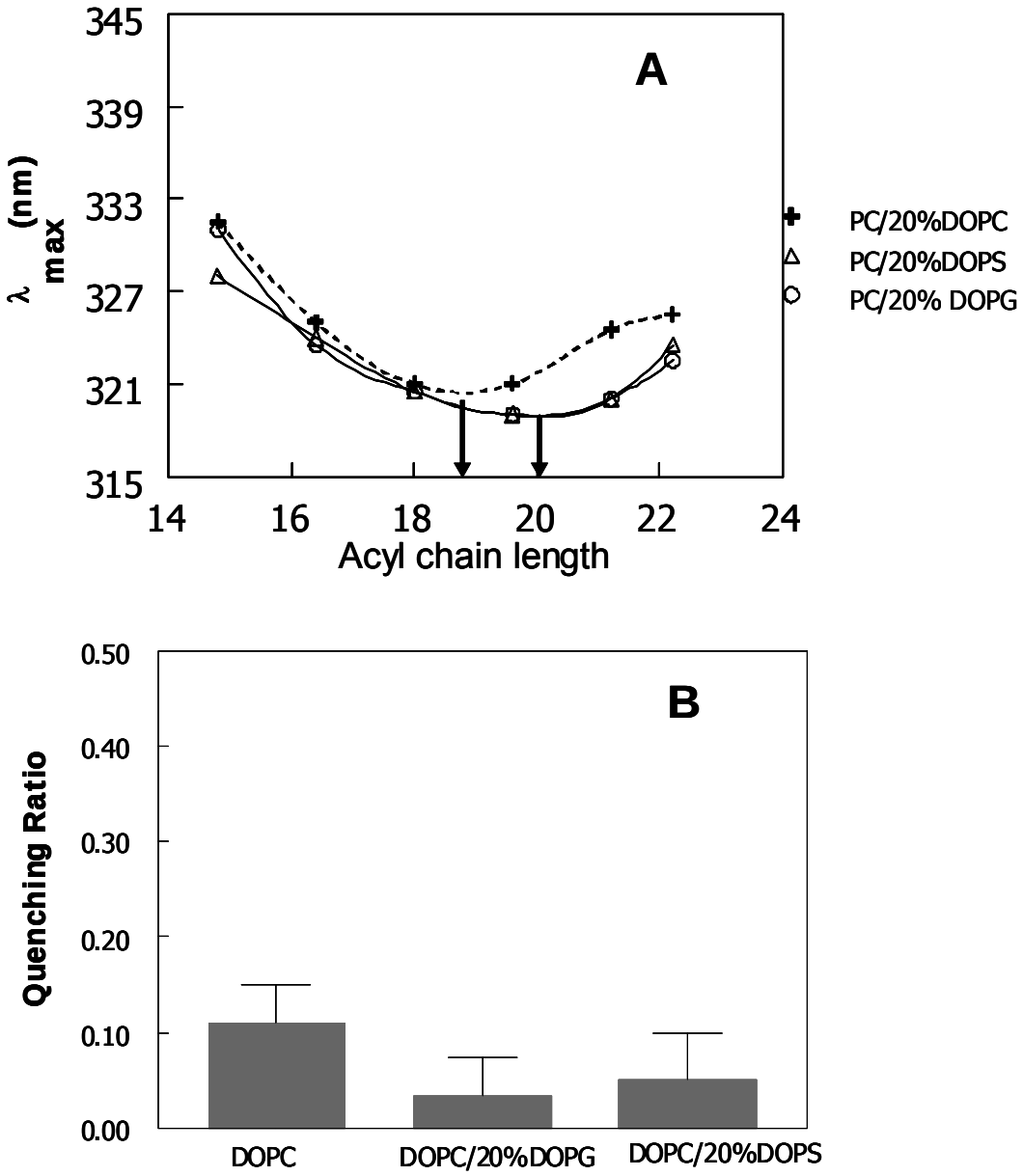

Figure 4.8:Effect of 20mol% anionic lipid upon the conformation of $pLAY_7$ peptide at pH 7.0. (A) Trp λmax dependence in lipid bilayer of different acyl chain lengths. (+) shows (80:20) mixtures of different length PC and DOPC. (O) shows (80:20) mixtures of different length PC and DOPG. (Δ) shows (80:20) mixtures of different length PC and DOPS. Arrow shows effective TM lengths in different lipid mixtures. (B) Trp fluorescence quenching ratio in different lipid mixtures. Samples contained 2μM peptide incorporated into 500 μM lipid vesicles suspended in PBS buffer.

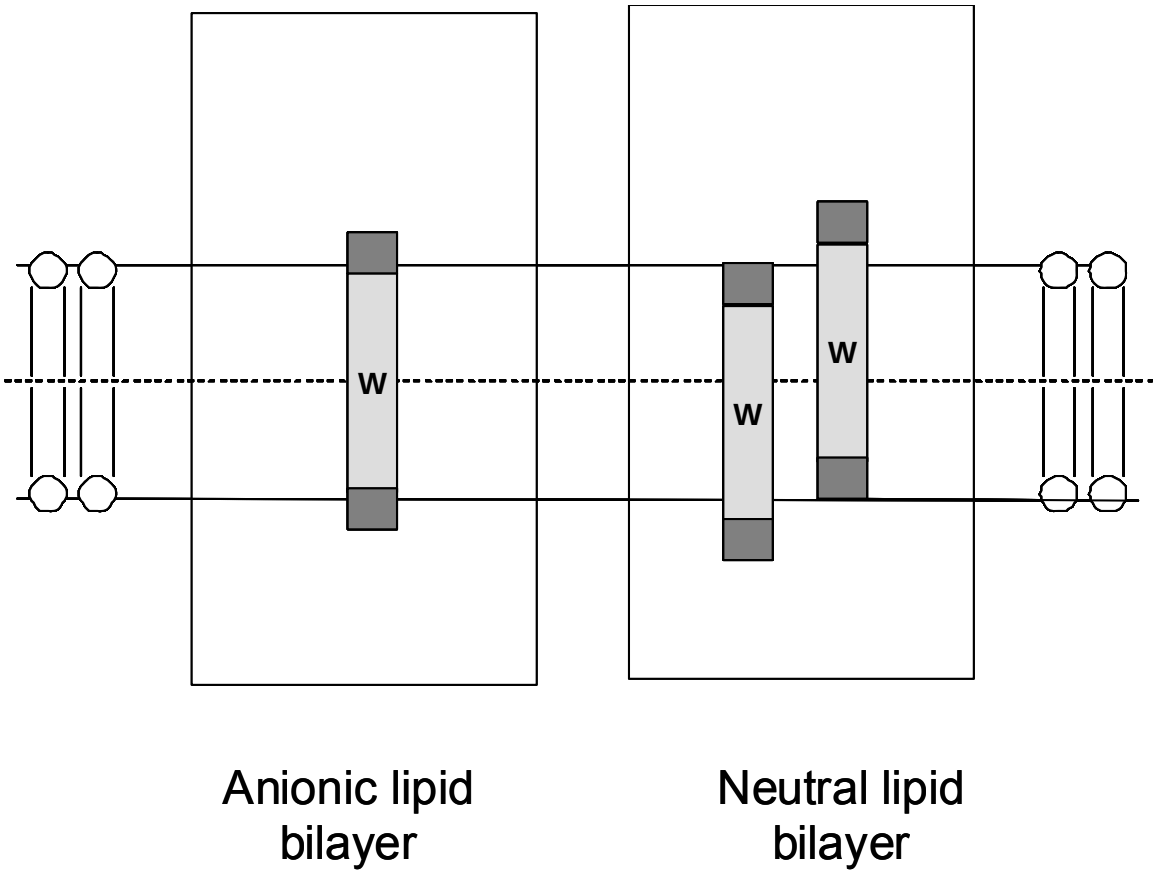

Figure 4.9: Schematic illustration of possible difference in anchoring of the TM state in uncharged PC bilayer (left) and negatively charged lipid bilayer (right). Membrane buried region of the TM helix is shown as grey shaded area and the dark grey area represents juxtamembrane (JM) residues at the bilayer interface. Trp position is denoted by W. Note the average Trp distance from the bilayer center is greater in neutral bilayer. In negatively charged bilayer Trp position is fixed at the bilayers due to better anchoring of the TM sequence. Distortion in lipid bilayer induced by peptide is not shown.

Chapter 5

ErbB2 receptor TM topography and anionic lipid

INTRODUCTION

The ErbB or epidermal growth factor receptor family is a family of four structurally related (ErbB1-ErbB4) receptor tyrosine kinases (RTK). The RTK's are involved in many cellular processes including recruitment and activation of signaling proteins [154; 155; 156 157; 158]. Like most RTKs, ErbB receptors are composed of a single α-helical transmembrane (TM) domain flanked by extracellular ligand-binding domain, and an intracellular tyrosine kinase domain [154; 155; 156]. These receptors are activated through binding of ligand to the extracellular domain. The binding induces receptor dimerization (or dimer rearrangement) (Figure 5.1) that leads to the activation of tyrosine kinase activity initiating an array of intracellular signaling pathways. The four receptors of the ErbB protein family can form many homo or heterodimers and possibly higher order oligomers in a ligand-dependant fashion, thus expanding the signaling diversity that can be induced by a single ligand[157; 159; 160; 161].

Proper control and precise coordination of the ErbB receptors is important as they regulate numerous critical biological outcomes including cellular growth and differentiation. It is well documented that excessive ErbB signaling, arising from receptor overexpression and or gene amplification, or by genetic alteration such as deletion and mutation, is a hallmark of a wide variety of solid tumors. For instance, ErbB2 is overexpressed in 20-30% of metastatic breast cancer cells[162; 163; 164]. Moreover, mutation of a single valine to glutamine at position 664 in the TM domain of neu, a rat homologue of the ErbB2 receptor has been shown to overactivate the receptor turning it into an oncogene [165]; [166]. Studies have demonstrated that glutamic acid mutation does not change the membrane association [166; 167] of the TM sequence and it is not clear how glu mutation leads to receptor activation. Earlier studies have suggested that mutation causes a conformational change in the receptor which leads to the receptor activation[168; 169]. An alternative model of receptor activation proposed increased receptor dimerization due to inter-receptor hydrogen bond formation by the protonated carboxylic group of glutamic acid residue [166; 167; 170; 171; 172]. However, the glu mutation had very little effect on dimerization in the human homologue of ErbB2 receptor as reported by the TOXCAT assay [173]. In addition, analysis of a range of neu proteins with mutations in TM domain

revealed that dimerization of the oncogenic form of ErbB2 receptor through its transmembrane domain may be important but not sufficient for its transforming activity[174]. Further studies using both computational and experimental methods proposed that the wild-type and mutant ErbB2 have different dimerization motifs based on the observation that both wild type and mutant ErbB2 have different membrane orientations [175; 176].

Unpublished studies from our lab using a peptide with the sequence of the ErbB2 TM domain (residues 656-680) investigated the structural consequences of the transforming mutations (glutamic acid, glutamine, aspartic acid) [165]on the ErbB2 TM segment. Using fluorescence techniques, it was shown that V664E mutation induced a transverse shift in the TM topography such that the E residue located closer to the bilayer surface, thereby shortening the membrane spanning segment from 24 residues observed for WT-ErbB2 to 17 residues in V664E mutant sequence (Figure 5.2). Other hydrophilic mutations (Q and D) at position 664 also altered the TM helix boundary. It was reported that while hydrophilic mutations like E664, Q664 and to a lesser degree D664 could activate the receptor, other mutations like G664, H664 and K664 had no transforming ability[165]. Thus, he transforming ability of these hydrophilic residues might be related to their helix shifting tendency. It is possible that the altered TM topography (e.g. a shifted-TM position) in the mutant ErbB2 can result in a rearrangement of the pre-existing dimers which can lead to receptor activation.

The intracellular juxtamembrane domain (JM), located between the transmembrane domain and the kinase domains, also has been suggested to play a vital role in receptor regulation and signaling specificity by protein kinase C and MAP kinase[177; 178; 179; 180]. When expressed in mammalian cell, a JM deletion mutant (ΔJM)in the ErbB intracellular domain failed to dimerize and autophosphorylate, indicating that JM domain is require for proper dimerization of the receptor[178; 179] The JM domain contains an abundance of positively charged basic amino acid residues in its N-terminal region and this is highly conserved feature among the ErbB family (Table 5.1)[178; 181]. It has been suggested that binding of the positively charged JM region to the membrane can

modulate signaling between the ligand binding domain and kinase domain[177; 182] A recent report by McLaughlin et al showed that peptide corresponding to JM region bind strongly to acidic lipid containing membrane and they proposed an electrostatic engine model for ErbB receptor activation[181] They postulated that the flexible JM and kinase domains bind electrostatically to the membrane surface preventing the kinase domains from close contact with each other. Ligand induced dimerization causes partial trans autophophorylation of ErbB leading to an increase in intracellular Ca2+ concentration which can activate calmodulin and the Ca2+/calmodulin complex then binds to JM region reversing its net charge and triggering the release of JM and kinase domains from membrane further facilitating the kinase domain dimerization. [181; 183].

Thus, it is important to understand the structural consequence of the interaction between the JM residues and membranes. We speculate that this interaction may be influenced by the transverse shift of the ErbB2 TM domain.

Goals of my studies in this chapter are as follows:

i. To define the effect of non-oncogenic hydrophilic mutations (Gly, His, Lys) at position 664 upon ErbB2 TM topography.
ii. To define how interaction between the juxtamembrane residues and anionic lipid membrane surface affects the topography of ErbB2-wt and ErbB2-mutant TM sequences.
iii. To define the relationship between JM-membrane interface and the helix shift. As noted above, a Gln (Q) at position 664 which is closer to the N-terminus of the ErbB2 TM sequence than the C-terminus induces a significant transverse shift in helix position. We investigated the helix shifting behavior of a Q placed at an analogous position near the C terminus. Since C terminus (unlike the N-terminus) contains the positively charged JM region, we wanted to determine if a Q-induced vertical shift in helix position toward the C terminus would be prevented in the presence of anionic lipid.

RESULTS

Topographical studies of membrane inserted ErbB2 V664X (X=hydrophilic residue) mutant peptides using fluorescence spectroscopy

To study the effect of a hydrophilic mutation at position 664 of the ErbB2 receptor, peptide sequences containing the TM domain of the rat homologue of ErbB2 receptor with a single Trp substitution at position 671 as fluorescent probe and with or without (WT) the hydrophilic mutation at position 664 were obtained. The general sequence was: Acetyl-
^{649}AEQRASPVTFIIATV**X**^{664}GVLLFL**W**LVVVVGILIKRRRKYK^{687} –amide
(membrane spanning segment is underlined). Fluorescence properties of the trp located within the hydrophobic sequence were employed to study the topographical behavior of these peptide sequences [43; 90]. Previously, the behavior of ErbB2 WT (X=V) and ErbB2 containing the transforming mutants (X=E,D,and Q) was studied in our lab (Shyam Krishnakumar unpublished result). To complete the story ErbB2 sequences with non-transforming hydrophilic mutations (X= G,H,K) were studied. First, the effect of bilayer width upon the trp emission λmax was used to define the conformation of the peptides in lipid bilayer. It has been shown that trp λmax is most blue shifted when there is a hydrophobic match between the lipid bilayer thickness and the length of the TM sequence [46; 50; 55; 74]. Trp emission λmax red shifts as result of hydrophobic mismatch in thinner and thicker bilayer. As a result, the shape of the trp λmax vs. lipid acyl chain length curve aids topography characterization and helps define the length of a TM segment (Figure 4.2).

Figure 5.3 shows λmax behavior of neu/ErbB2 WT and ErbB2 mutant peptides at pH 7.0. Results for WT, V664E, V664D and V664Q peptides from previous studies (Shyam Krishnakumar) were included in this figure for comparison purpose. New mutations introduced at position 664 of ErbB2 TM domain are: His, Lys and Gly. Replacing V at position 664 with G (V664G) gave a similar pattern of λmax vs. bilayer width curve as the WT sequence with a very blue shifted emission in DEuPC bilayers (22 carbon atoms acyl chain). This behavior is consistent with the putative TM segment of 23 hydrophobic residues of the ErbB2 TM segment spanning the lipid bilayer. The V664H

peptide shifted the λmax minimum to a thinner bilayer width (16 carbon atoms) similar to the other hydrophilic mutations V664E and V664D. This is characteristics behavior of a short TM helix where the hydrophilic residue forms the boundary of the inserted portion of the helix shortening the membrane spanning segment. These short TM helices are destabilized in wider lipid bilayer more easily as seen by the steep shape of the curve toward the right side of the plot (Figure 5.3). An intermediate pattern between that of V664H and V664G was observed for V664K peptide with λmax minimum in medium length bilayer (DOPC, 18 carbons chain).

In addition, the conformation of these peptides was studied by dual quenching method that measures the trp depth in the bilayer[43]. Two trp fluorescence quenchers are used in this method. One is10-doxylnonadecane (10-DN) is a membrane inserted quencher that preferentially quenches the fluorescence of membrane-buried trp and the other is acrylamide a water soluble quencher that mainly quenches the fluorescence of exposed trp. The ratio of acrylamide quenching to 10-DN quenching (Q ratio) responds linearly to the trp depth in the bilayer. A low Q ratio (<.1-.2) is characteristic of trp near or close to bilayer center while a high Q ratio (≥ 1) indicate a trp location near the bilayer surface. And an intermediate value for Q ratio is observed for peptides adopting a mixed orientation with shallow and deep trp depths, or for peptides adopting a shifted TM conformation with an intermediate trp depth[43].

The topological behavior of the ErbB2 mutant peptides observed in the different bilayer width study was confirmed by dual quenching assay (Figure 5.4). In this figure trp depth in both medium bilayer DOPC (18:1 carbon acyl chain) and wider bilayer DEuPC (22:1 carbon acyl chain) at pH 7.0 were reported for ErbB2 sequences. Again, quenching results for V664E, V664D and V664Q (unpublished study by Shyam Krishnakumar) were included in this figure so we could compare the results for all the hydrophilic mutations. The V664G non-oncogenic mutation had similar quenching result as WT ErbB2 which agrees with the λmax result in different bilayer widths. Both peptides had lower Q ratio in wider bilayers (striped bar) indicating a deep trp location in the wider bilayer and consistent with a long membrane spanning TM segment. All the hydrophilic

mutations except G had a shallower trp location in the wider bilayer (striped bar) and deeper trp location in medium width bilayer (solid bar). This pattern indicates a shorter TM length for sequences with D,H,K,Q,E residues than for the WT (V) and G containing peptides. This observation agrees with the λmax value in medium width bilayer (18 carbon chain) and wider bilayer (22 carbon chain).

Also, it should be noted that trp location in shorter shifted helices are different than the longer WT sequence. The trp671 location within the hydrophobic sequence is closer to the center of the DOPC bilayer for shifted sequences (residues 666-680) where the hydrophilic residues form the membrane boundary. But in the entire hydrophobic sequence (residues 656-680) trp is located off center within the sequence (Figure 5.5B). Originally trp was placed at position 669 which is at the center of the ErbB2 WT sequence. But as shown in figure 5.5A, trp 669 was near the bilayer surface when the peptide formed shifted conformation (as in ErbB2 mutants) making it difficult to distinguish between shifted-TM and non-TM conformation. Moving the trp position to 669 solved this problem. In 671 position, event though WT sequence formed a stable TM conformation in the DOPC vesicles (which may be tilted to minimize mismatch) the trp experiences a polar environment due to its nearness to the bilayer surface. Nevertheless, information regarding the length of the membrane spanning segment can be obtained from the relative difference in Q ratio between the 18 carbon acyl chain bilayer (DOPC) and 22 carbon acyl chain bilayer (DEuPC) .

Since H is an ionizable residue, the behavior of V664H mutation upon the ErbB2 conformation was studied under different pH conditions. Figure 5.6 shows the effect of bilayer width upon V664H trp λmax emission at pH 4,7, and 9. The results indicated that at V664H formed a shorter TM segment at pH 7.0 and 9.0 than pH 4.0. The similar pattern of λmax curve at pH 7.0 and 9.0 indicate that His is probably deprotonated at pH 7.0 (His pKa was not determined). Interestingly, the V664H sequence formed a more stable TM structure in DOPC bilayer at pH 4.0 contrary to the expectations since His bears a positive charge at this pH. This also evident from the quenching result where the

deepest trp location for V664H was in DOPC at pH 4.0 (Figure 6). Quenching ratio at (figure 5.7) at pH 4, 7, and 9 also agrees with the λmax data.

Effect of 20 mol% anionic lipid upon the topography of ErbB2 WT and mutant peptides

The ErbB2 transmembrane sequence used in our study contained a stretch of positively charged residues at the C-termini of the hydrophobic region. This juxtamembrane (JM) domain is highly conserved in the ErbB family[178]. In the previous chapter, I have reported that interaction between the anionic lipid headgroup and the positively charged flanking residues of the peptides (contained alternating Leu/Ala) can suppress transverse shift of these helices in anionic lipid containing vesicle. Unlike those poly-Leu-ala peptides the ErbB2 peptides have cationic residues only at one end. In order to investigate the affect of anionic lipid upon the shifted TM conformation of ErbB2 sequences containing oncogenic mutations, ErbB2 peptides were incorporated into 20mol% anionic lipid containing vesicles and their behavior were discerned by fluorescence assays.

The bilayer width dependence of Trp emission maximum due to hydrophobic mismatch is an important parameter for determining the length of the TM segment. Figure 5.8 compares the effect of bilayer width upon trp λmax emission of WT sequence between the PC containing vesicles (dashed line, PC/20%DOPC) and 20 mol% anionic lipid containing vesicles (solid lines) at pH 7.0. In order to make negatively charged bilayer 20mol% of 18 carbon chain length monounsaturated phosphatidylserine (PS) or phosphatidylglycerol were incorporated into monounsaturated phosphatidylcholine (PC) vesicles of different acyl chain lengths. WT peptide conformation was not effected by the presence of 20mol% DOPS or DOPG (Figure 5.8A) which is consistent with the TM stability of the WT sequence. This was further confirmed by quenching results (Figure 5.8B) where trp depth was similar in both uncharged (DOPC) and negatively charged vesicles [(80:20)DOPC/DOPS or DOPC/DOPG] at pH 7.0.

However, we observed a difference in the topography of a peptide with the V664E sequence between the zwitterionic and negatively charged vesicles (Figure 5.9). Oncogenic mutation V664E formed a short truncated TM helix in PC bilayers as evident from the trp λmax minimum near 16 carbon acyl chain bilayers (dashed line). This minimum shifted slightly toward thicker bilayers in the anionic lipid containing vesicles (solid lines). In addition, the λmax curve is more blue shifted in PS or PG containing vesicles than the PC vesicles in the negative mismatch region. These observations in combination with a slightly deeper Trp depth in PG/PS containing bilayer (Figure 5.9B) suggests some suppression of transverse shift by anionic lipid. To show that the enhanced TM stability in anionic lipid containing vesicles is not due to protonation of glu residue (which would decrease its hydrophobicity) these studies were also done at pH 9.0 (Figure 5.10). Results at pH 9.0 also showed blue shifted trp λmax and lower Q ratio for V664E when incorporated into 20mol% PS containing bilayer. So, the stability of V664E observed in anionic vesicle is not likely to be due to the glu ionization event.

When V664Q was incorporated into 20mol% PS containing vesicles a blue shift in λmax was observed relative to that in PC vesicles (Figure 5.11). The shape of the λmax did not change much in the presence of anionic lipid as seen for V664E peptide. The quenching result did not show any significant difference trp depth between DOPC and 20mol% DOPS containing vesicles. From these results, it is does not appear there is a large change in V664Q topography in the presence of anionic lipid.

Effect of ErbB2 C-terminal hydrophilic mutation upon the topography

To study the effect of a hydrophilic mutation near the C-terminus of the ErbB2 TM domain, we designed an ErbB2 TM sequence such that a valine residue at position 674 near the C-terminal end was replaced with a hydrophilic residue Q to mimic the position of the oncogenic Q mutation at the N-terminus side. Also, the W was moved to position 667 where it would be located near the middle of the shifted sequence if Q formed the membrane boundary at the C-terminus end. The resulting sequence is: Acetyl^{649}AEQRASP<u>VTFIIATVVGVW^{667}LFLILV</u>**Q**^{674}VVGILIKRRRKYK^{687}amide (potential shifted TM segment is underlined). Figure 5.12 shows the behavior of V674Q

and WT (original sequence) in different PC bilayer width at pH 7.0. The WT sequence TM structure exhibited a λmax minimum at 22 carbons bilayer whereas V674Q had a λmax at around 18 carbons bilayer indicating that V674 membrane spanning sequence length is shorter than the WT sequence. Unlike the WT sequence TM state of the V674Q peptide is destabilized in thicker bilayer as a result of hydrophobic mismatch, which is also a hallmark of short TM helices. The shifted conformation of V674Q peptide was also confirmed by directly measuring trp depth by fluorescence quenching. Figure 5.13 compares the trp quenching results for V664Q, WT and V674Q in medium bilayer (DOPC) and thicker bilayer (DEuPC) at pH 7.0. WT TM conformation is more stable in thicker bilayer as indicated by the smaller Q ratio in DEuPC. But both V664Q and V674Q TM conformations were more stable in thinner bilayers as they exhibited a small Q ratio in DOPC vesicles.

Effect of 20 mol% anionic lipid upon ErbB2-V674Q TM topography

To study the effect of anionic lipid we incorporated V674Q peptide into vesicles composed of 80:20 mol ratio of PC (various acyl chain lengths) and DOPS (18 carbons acyl chain length). The V674 peptide was also incorporated into vesicles composed of 80 mol% PC of different acyl chain lengths and 20 mol% DOPC as a control. The results of bilayer width variation upon V674Q trp λmax is shown in figure 5.14. There was a significant change in V674Q λmax minimum when incorporated into 20 mol% anionic lipid containing vesicles (Δ). The bilayer width at which V674 TM state was most stable shifted from 18 carbons acyl chain when incorporated into uncharged vesicles to a wider bilayer (~21 carbon acyl chain) in case of charged vesicles (Δ). The V674Q λmax minimum in DOPS containing vesicles is close to the WT λmax minimum in PC vesicles (+) indicating that in anionic lipid the V674Q peptide adopted a longer TM conformation which was more similar to WT peptide.

The quenching results in figure 5.15 provide more evidence of supporting these observations. In uncharged vesicles V674Q TM state was less stable in wider bilayers than it was in thinner bilayers as indicated by bigger Q ratio in DEuPC (striped bar) than

DOPC(solid bar). However, upon incorporation of 20% negatively charged lipid, the V674Q TM stability increased greatly in the thicker bilayer as judged by a very low Q ratio in the both DOPC and DEuPC vesicles.

DISCUSSION

Certain hydrophilic mutations within the TM domain of some tyrosine kinases have been associated with oncogenic transformation [184]. One well known example is mutation of a hydrophobic valine residue at position 664 to glutamate in neu protein a rat homologue of ErbB2 receptor. Bargmann and Weinberg have reported that while hydrophilic mutations such as Glu and Gln at position 664 in the TM domain of ErbB2 had a strong transforming ability and Asp had a moderate transforming ability [169]. Other hydrophilic mutations such as His,Lys and Gly showed no transforming ability[165]. An unpublished study (Shyam Krishnakumar) from our lab showed that activating mutation (V664E) in a peptide sequence containing the TM domain of neu/ErbB2 receptor altered the position of the TM helix within the membrane. Based on his observation that other transforming mutations (Q and D) also induced helix shift it was proposed that these shifted TM helices might alter the lateral helix association so as to promote receptor activation. Since, Glu,Gln and Asp have a higher propensity to alter a TM helix position than less hydrophilic Lys,His and Gly[90]it was believed that the transforming ability of these hydrophilic residues might be related to their ability to induce a shift in TM helix position which can in turn alter the lateral helix association.

In order to investigate this, peptide sequences with H664, K664 and G664 were studied. Replacing valine with glycine at position 664 did not change the conformation of the TM sequence. Lysine induced a moderate shift in TM helix position but less than the transforming mutations (E,Q,D)(Figure 5.3). This lesser shift may be because Lysine has a long positively charged side chain which can snorkel, burying the rest of the residue within the bilayer. Contrary to the expectations, His induced as much helix shift as an Asp or Glu at pH 7.0. At pH 7.0 His should be mostly uncharged so the TM state should be more stable at pH 7.0 or pH 9.0. But we observed that a His at pH 4.0 formed a more

stable TM conformation as shown by the blue shifted λmax and smaller quenching ratio (Figure 5.6 and 5.7). H664 peptide behavior in this case was different than predicted by other studies where His containing peptide sequences were more hydrophobic at high pH [42; 90]. So, V664H mutation proved to be an exception to our speculation that the TM helix shifting ability of these mutations are related to their transforming ability. Sharpe et al observed a significant structural rearrangement of the TM domain caused by V664 to E mutation in the ErbB2 receptor[184]. As I have reported V664H in spite of being a non-transforming mutation, was able to bring structural change in neu/ErbB2 TM domain. Hence, structural changes in the TM domain might only be one of the several steps that lead to the active dimer conformation. Besides causing structural rearrangement of the dimers activating mutations might affect the dimer interface or packing interactions between the ErbB2 homo or heterodimers, thus activating the receptor in a manner that can not occur with His mutation.

It is possible that neu gene favor a Glu/Gln residue at position 664 for specific helix-helix association mode that is important for receptor activation. For instance, only Glu and Gln which share a similar side chain are able to fully activate the neu oncogene, while Asp with a slightly smaller side chain shows weak activation[165].Thus, the interaction might be more favored by Glu/Gln residue than other hydrophilic residues with smaller or bigger side chains for steric reason.

Besides the TM domain, ErbB2 juxtamembrane (JM) domain (a region between the TM domain and kinase domain) might also play a vital role in the receptor activation. A cytoplasmic JM domain rich in positively charged residues (Arg, Lys) is found in all the ErbB family proteins[178; 181]. Since the cytoplasmic leaflet of the biological membranes contain negatively charged lipid it has been suggested that positively charged JM region should bind to membrane and be in a position to modulate receptor activation[177; 182; 183]. Knowledge concerning this interaction is scarce. Recent study by McLaughlin and colleagues have reported that peptide corresponding to the JM domain of ErbB1 bind strongly to PS containing vesicles whereas binding to the uncharged PC vesicles was weak[181].

We investigated the effect of ErbB2 JM-anionic lipid interaction on the topography of ErbB2-WT and mutant peptides. In previous chapters I have showed that anionic lipid and JM residue interaction greatly stabilized the TM conformation relative to the membrane surface bound non-TM states and shifted-TM states for hydrophobic sequences flanked by JM Lys residues. For WT and V664Q ErbB2 peptides we did not observe a large change in TM topography in the presence of 20mol% anionic lipid relative to that of zwitterionic vesicles. ErbB2 WT peptide already existed as stable TM conformation in uncharged bilayer so the topography was unaffected by the negative lipid. The V664E mutant had a blue shifted λmax and lower quenching ratio at pH 7.0 in the presence of anionic lipid indicating that TM state is more stable in these vesicles. This moderate increase in TM stability might be due to the protonation of E residue in anionic lipid containing vesicles at pH 7.0. We have shown that ionizable residues had higher pKa in anionic lipid bilayers than the uncharged bilayer in previous chapter. However, there was still a moderate increase in TM stability of V664E peptide in 20mol% DOPS containing vesicle at pH 9.0. In any case, unlike the diLys flanked shifted sequences (Chapter 4) suppression of ErbB2 helix transverse shift was minimal in the presence of physiological amount of anionic lipid. We attribute this to the lack of positively charged JM residues in the N terminus of the ErbB2 TM domain. Location of the hydrophilic mutation (664) in ErbB2 TM domain is closer to the N terminal end so the N-terminal side of the sequence gets pushed out of the membrane when helix shift occurs. Since N-terminus does have any net charge, anionic lipid should not prevent this type of helix shift. The minimal increase in TM stability observed for ErbB2 mutants in anionic vesicles might to due the better anchoring of positively charged C-terminus JM region in the negatively charged bilayer.

An interaction the ErbB2 peptide C-terminal JM domain and anionic lipid should reflect an actual protein lipid interaction in cell membranes. Anionic lipids are located primarily in the cytoplasmic leaflet of the cell membrane and cytoplasmic end of TM domains are often flanked by positively charged JM residues as is true for ErbB proteins. This JM-membrane interaction believed to modulate the TM helix orientation in

membranes[94; 95]. Despite our use of vesicles with symmetric distribution of anionic lipids ErbB2 peptides only interact with one face of the charged bilayer via its positively charged C-terminal region. We took advantage of that fact and investigated the structural consequence of introducing a hydrophilic Gln residue near at position 674 the C-terminal end of the ErbB2 peptide. This C-terminal Q residue was placed at similar distance from the membrane boundary as the N-terminal Q residue (664) and in both cases a V was replaced with a Q. We have found that C-terminal Q residue was able to induce a shift in TM helix position. Both V664Q and V674Q had a λmax minimum in about 18 carbon acyl chain lipid bilayers but V674Q Trp λmax was redder than V664Q, which might be due to different Trp depth. It was clear from the Trp λmax dependence of bilayer width pattern that like the V664 peptide, V674Q peptide TM length was much shorter than the WT peptide. Interestingly, the V674Q peptide TM length was longer in the 20mol% DOPS containing vesicle. In other words unlike the N-terminal Q peptide (V664Q), the C-terminal Q (V674Q) peptide TM helix was pushed back into the membrane by the anionic lipid. We propose that TM helix shift toward the cytoplasmic side of a membrane is prevented by strong interaction between N-terminal JM domain and anionic lipid headgroup (Figure 5.16). On the other hand, TM helix can shift toward the lumenal side of the membrane (e.g. toward N-terminal side in case of ErbB2). This could have other important implications for TM regions shift in response to external factors or polar mutants.

Table 5.1: ErbB family proteins share a highly conserved basic/amphipathic membrane anchoring region corresponding to residues 645-660 in the JM region of human ErbB1. Basic residues are highlighted in bold.

RRRHIV**RKR**TL**RR**LLQ	ErbB1
KRRQQ**K**I**RK**YTM**RR**LLQ	ErbB2
RG**RR**IQN**KR**AM**RR**YLE**R**	ErbB3
RRRKSI**KKKR**AL**RR**FLET	ErbB4

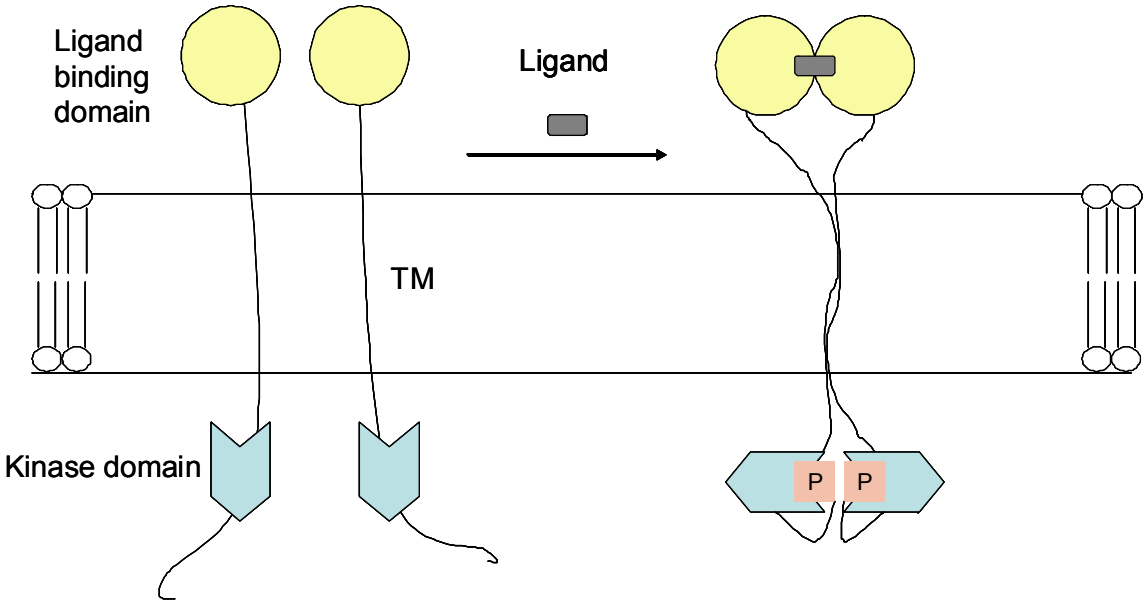

Figure 5.1: Schematic representation of ErbB activation model. Two ErbB monomers are colored same. Yellow circle depicts the extracellular ligand binding domain which is connected to kinase domain (blue shape) by a transmembrane helix. Activation occurs when ligand binds to extracellular domain leading to dimerization which brings the kinase domain closer resulting in transphorylation. Some ErbB's exist as dimers and ligand binding believe to rearrange the dimer conformation which lead to the receptor activation. But it is omitted for simplicity.

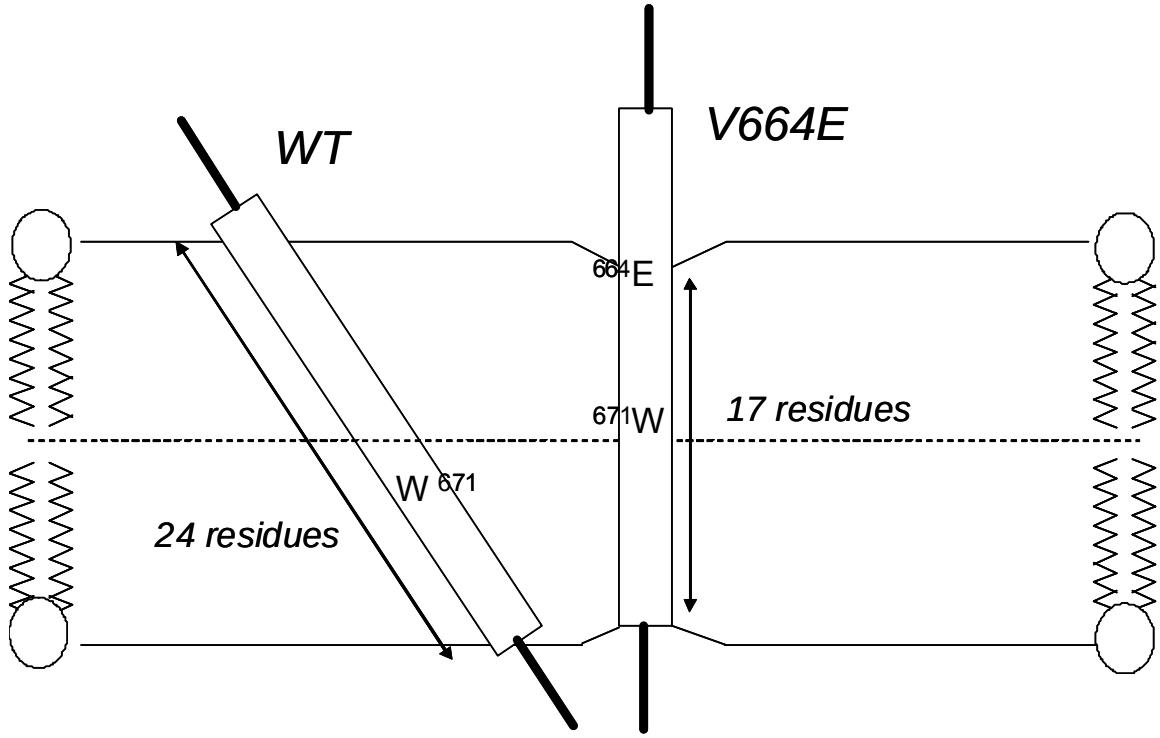

Figure 5.2: Schematic depiction of helix transverse shift induced by V664E mutation in ErbB2 TM helix. Trp position in the sequence is denoted by W.

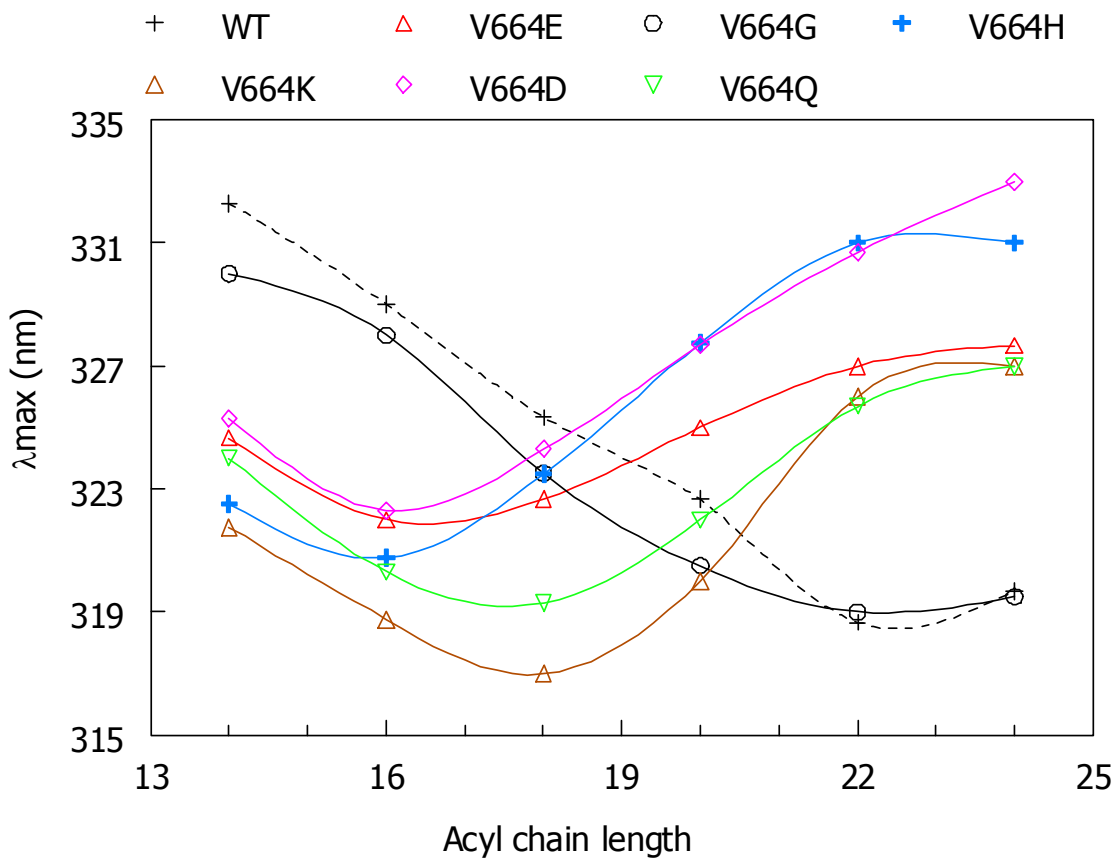

Figure 5.3: Effect of lipid bilayer width upon Trp emission λmax for neu/ErbB2 mutants and WT peptides at pH 7.0. The WT, V664E, V664D, and V664Q result from the work of Shyam Krishnakumar are included here for comparison. Sample contained 2μM peptide incorporated into 500μM lipid dispersed in PBS buffer at pH 7.0. The values shown here are average of 2-6 samples.

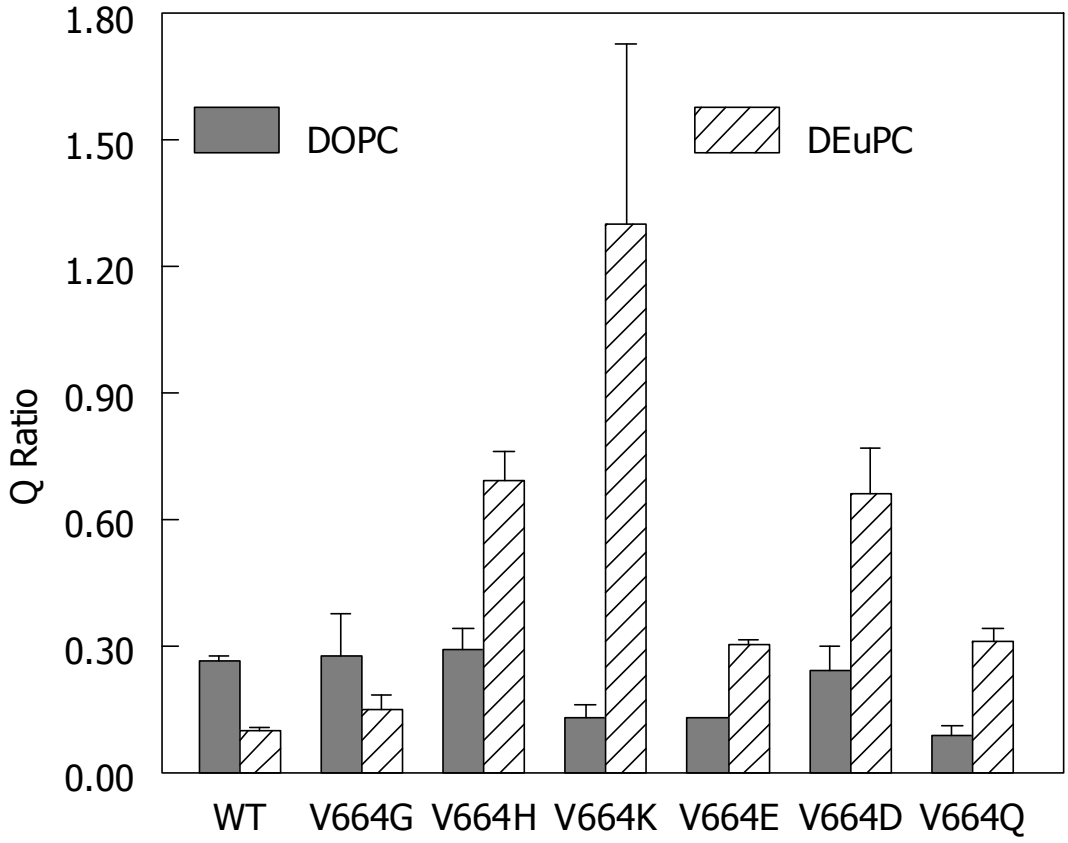

Figure 5.4: Quenching ratios for ErbB2 mutant and wild type peptide in DOPC (filled bar) and DEuPC(striped bar) vesicles at pH 7.0. Results for V664E, V664D and V664Q were from previous study (Krishnakumar) and shown here for comparison. Sample contained 2μM peptide incorporated into 500μM lipid dispersed in PBS buffer at pH 7.0

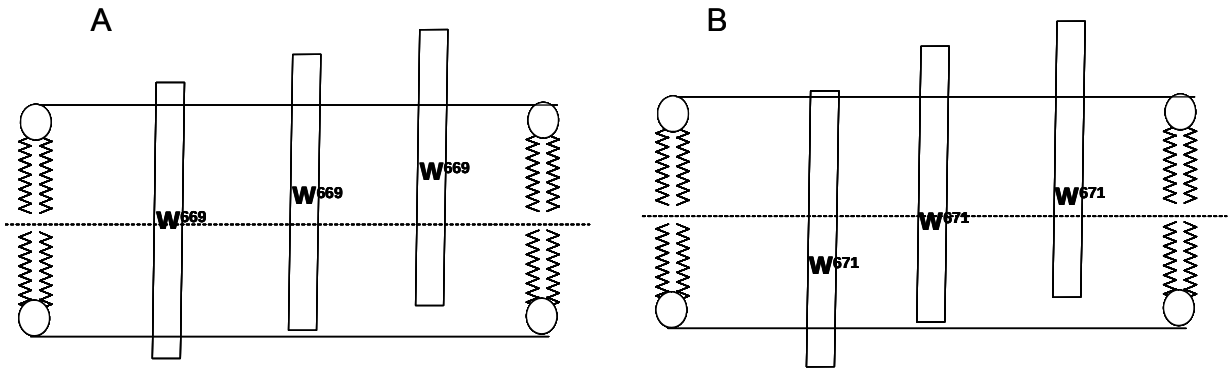

Figure 5.5: Effect of different Trp location within the TM segment of ErbB2 peptide. (A) position 669 (B) position 671. Clear rectangles represent TM helix. Dotted line shows lipid bilayers center.

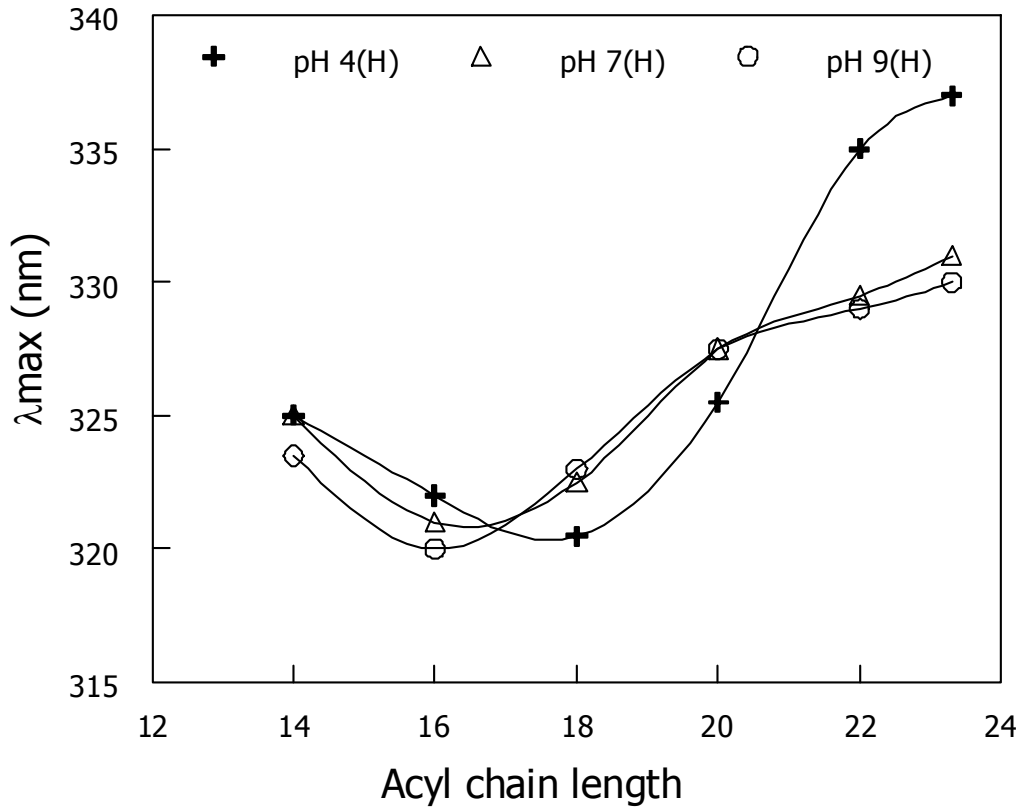

Figure 5.6: Effect of lipid bilayer width upon Trp emission λmax for ErbB2 V664H peptides at pH 4(+), pH 7.0(Δ) and pH 9.0(O). Sample contained 2μM peptide incorporated into 500μM lipid dispersed in PBS buffer. The values shown here are average of 2-6 samples.

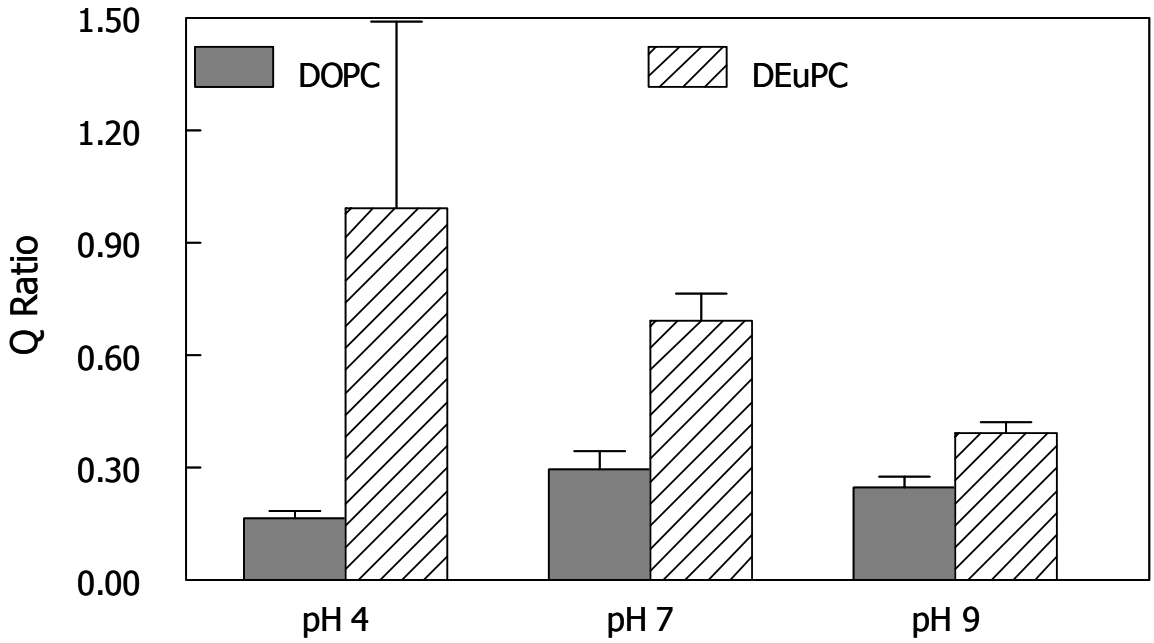

Figure 5.7: Quenching ratio of ErbB2 V664H peptide in DOPC (filled bar) and DEuPC (striped bar) at pH 4.0, pH 7.0, and pH 9.0. Sample contained 2μM peptide incorporated into 500μM lipid dispersed in PBS buffer.

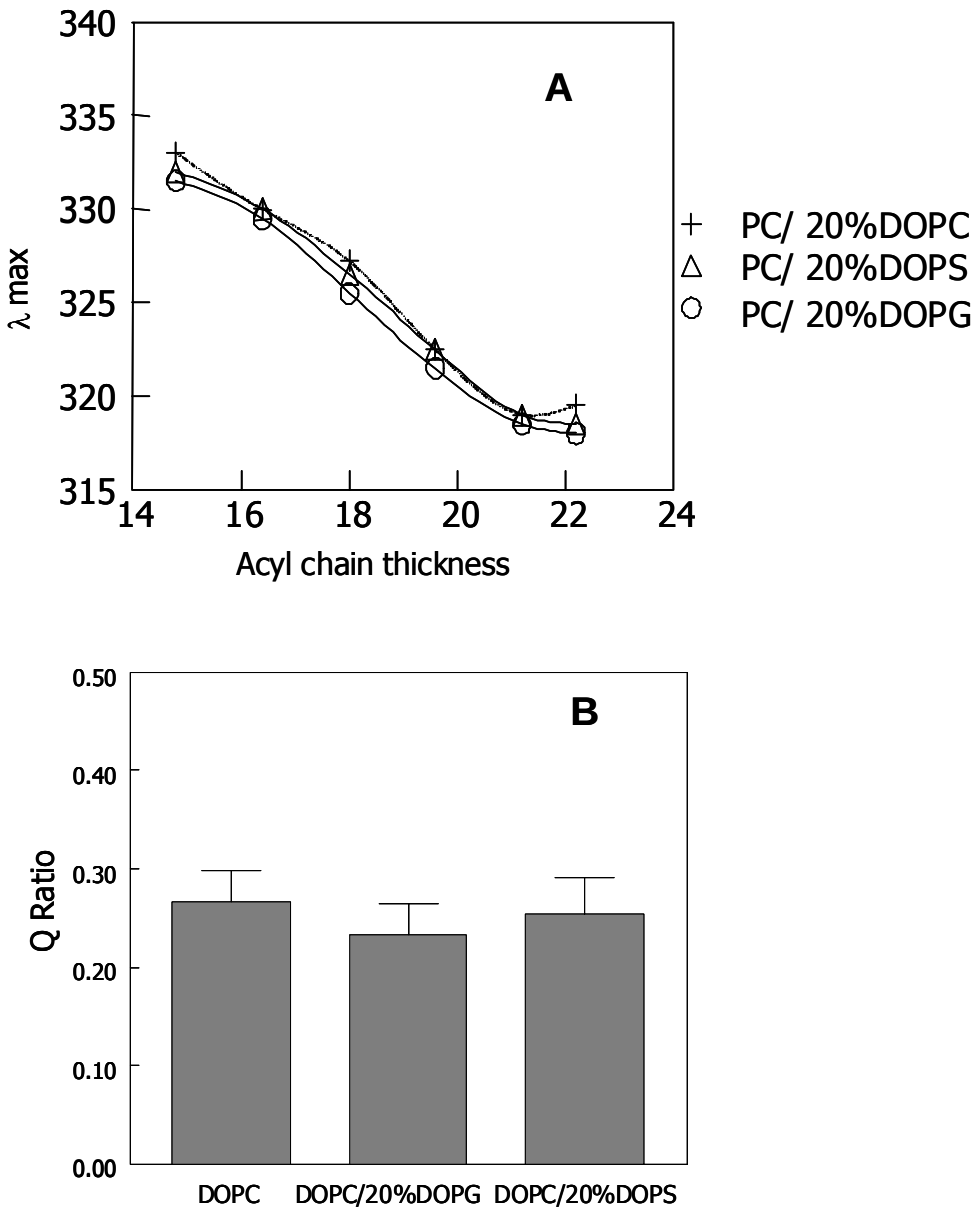

Figure 5.8: Effect of 20mol% anionic lipid upon the conformation of ErbB2-WT peptide at pH 7.0. (A) Trp λmax dependence in lipid bilayer of different acyl chain lengths. + shows (80:20) mixtures of different length PC and DOPC. O shows (80:20) mixtures of different length PC and DOPG. Δ shows (80:20) mixtures of different length PC and DOPS. (B) Trp fluorescence quenching ratio in different lipid mixtures. Samples contained 2μM peptide incorporated into 500 μM lipid suspended in PBS buffer.

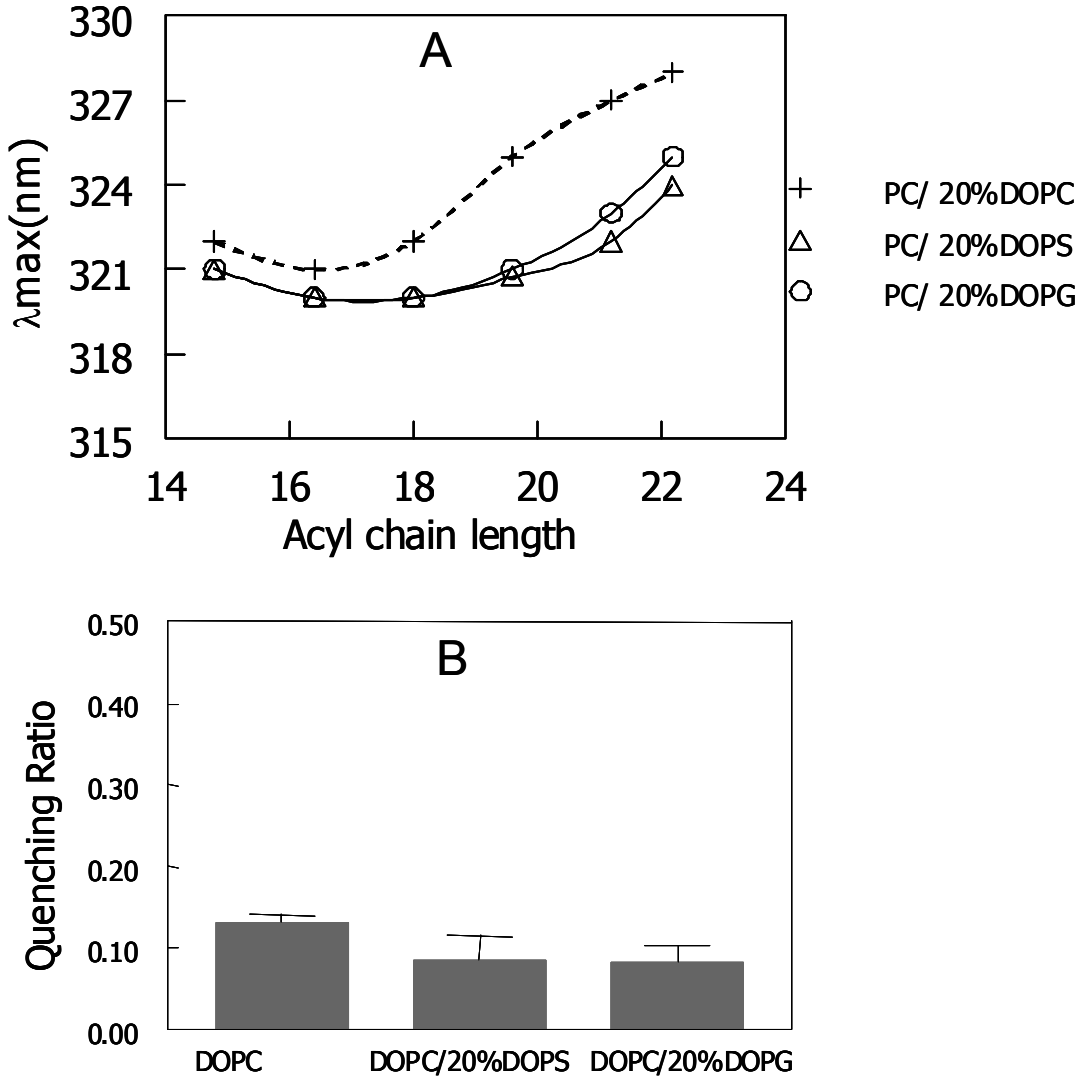

Figure 5.9: Effect of 20mol% anionic lipid upon the conformation of V664E peptide at pH 7.0. (A) Trp λmax dependence in lipid bilayer of different acyl chain lengths. + shows (80:20) mixtures of different length PC and DOPC. O shows (80:20) mixtures of different length PC and DOPG. Δ shows (80:20) mixtures of different length PC and DOPS. (B) Trp fluorescence quenching ratio in different lipid mixtures. Samples contained 2μM peptide incorporated into 500 μM lipid suspended in PBS buffer.

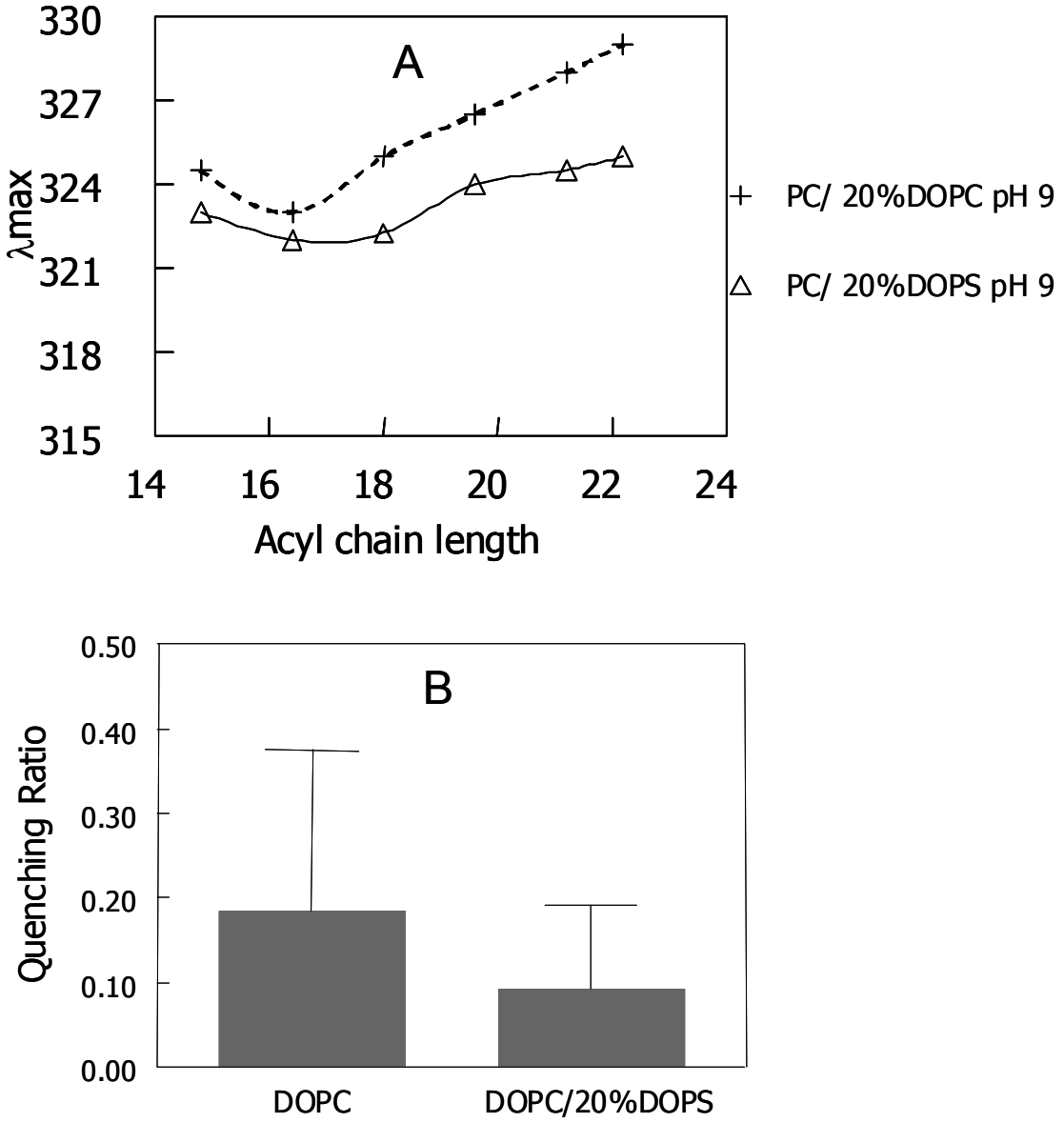

Figure 5.10: Effect of 20mol% anionic lipid upon the conformation of V664E peptide at pH 9.0. (A) Trp λmax dependence in lipid bilayer of different acyl chain lengths. + shows (80:20) mixtures of different length PC and DOPC. Δ shows (80:20) mixtures of different length PC and DOPS. (B) Trp fluorescence quenching ratio in different lipid mixtures. Samples contained 2μM peptide incorporated into 500 μM lipid suspended in PBS buffer.

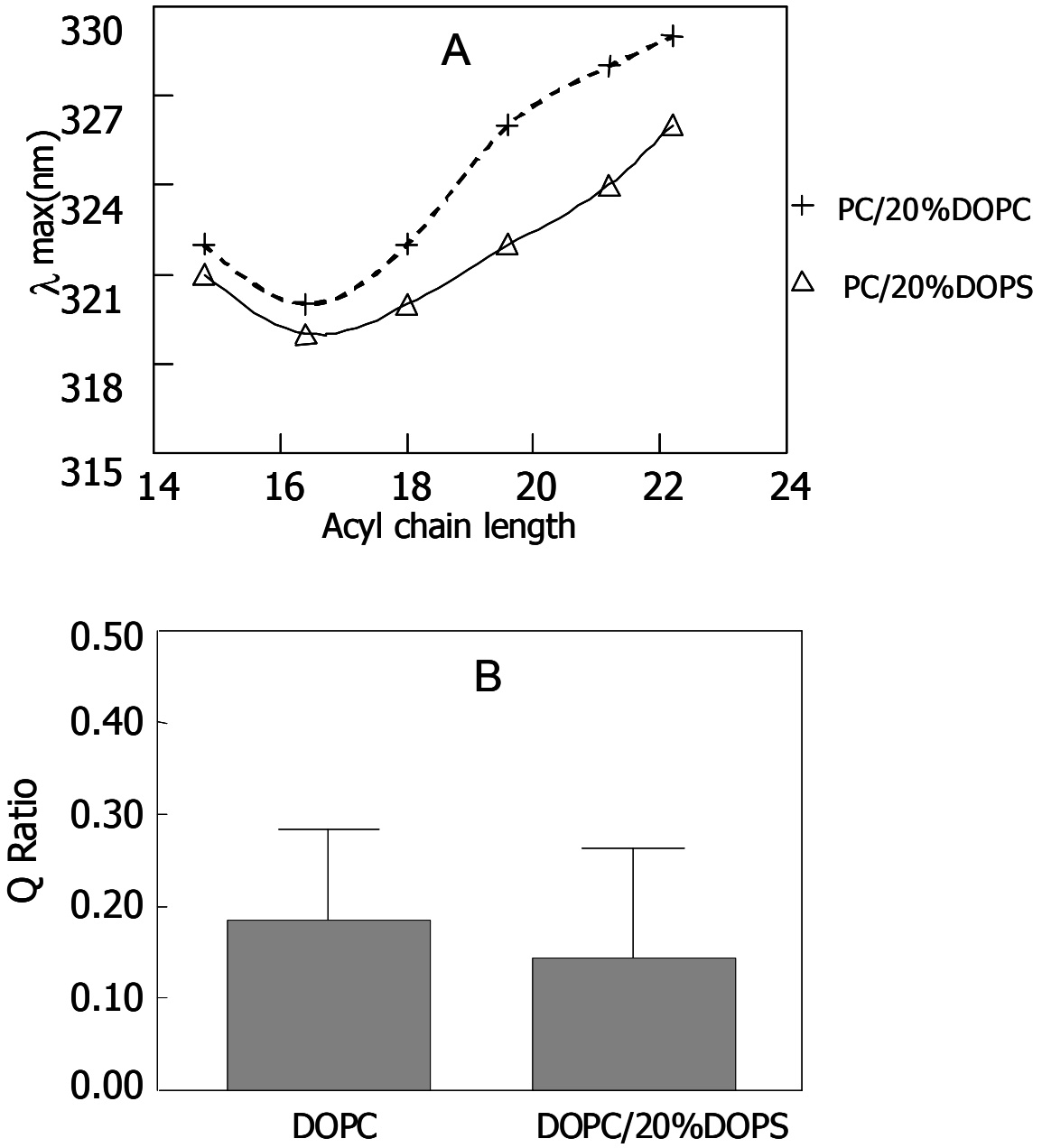

Figure 5.11: Effect of 20mol% anionic lipid upon the conformation of V664Q peptide at pH 7.0. (A) Trp λmax dependence in lipid bilayer of different acyl chain lengths. + shows (80:20) mixtures of different length PC and DOPC. Δ shows (80:20) mixtures of different length PC and DOPS. (B) Trp fluorescence quenching ratio in different lipid mixtures. Samples contained 2μM peptide incorporated into 500 μM lipid suspended in PBS buffer

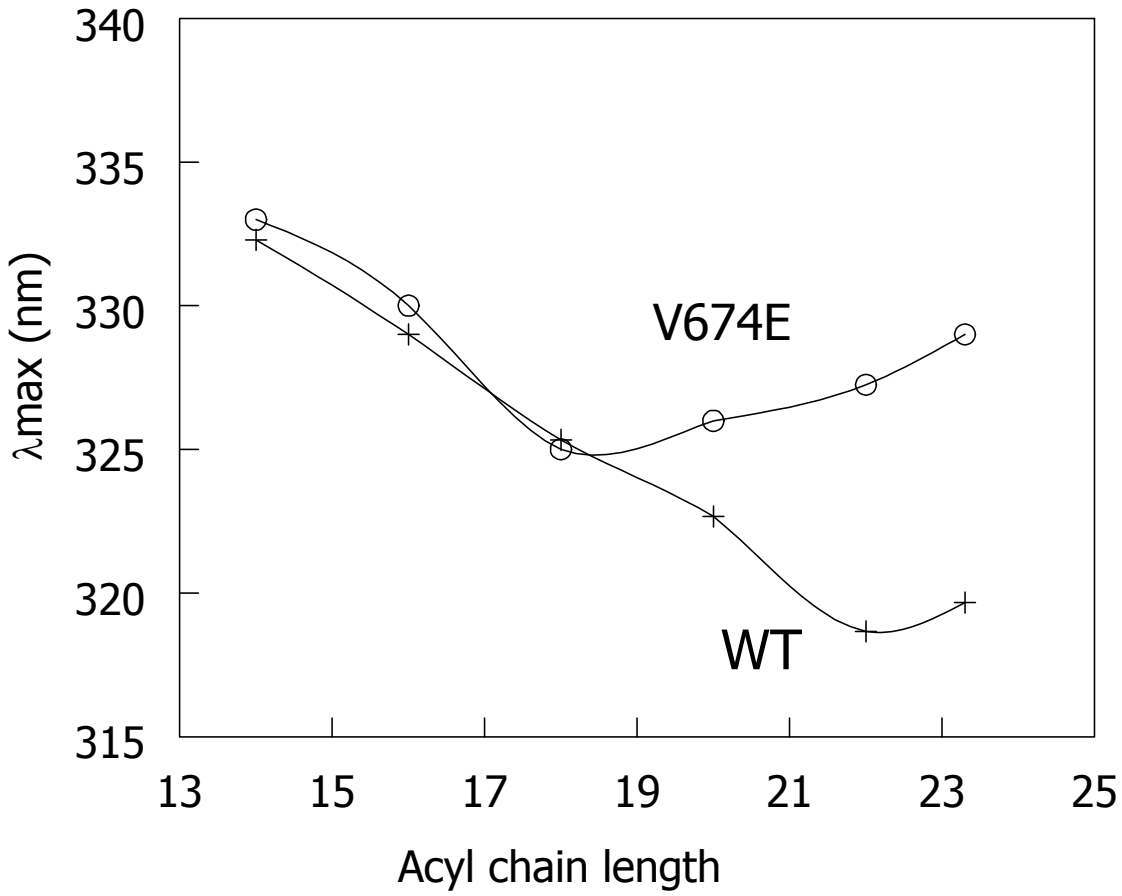

Figure 5.12: Effect of bilayer width upon Trp λmax emission of V674Q peptide at pH 7.0. WT result is shown here for comparison. Samples contained 2μM peptide incorporated into 500 μM lipid suspended in PBS buffer

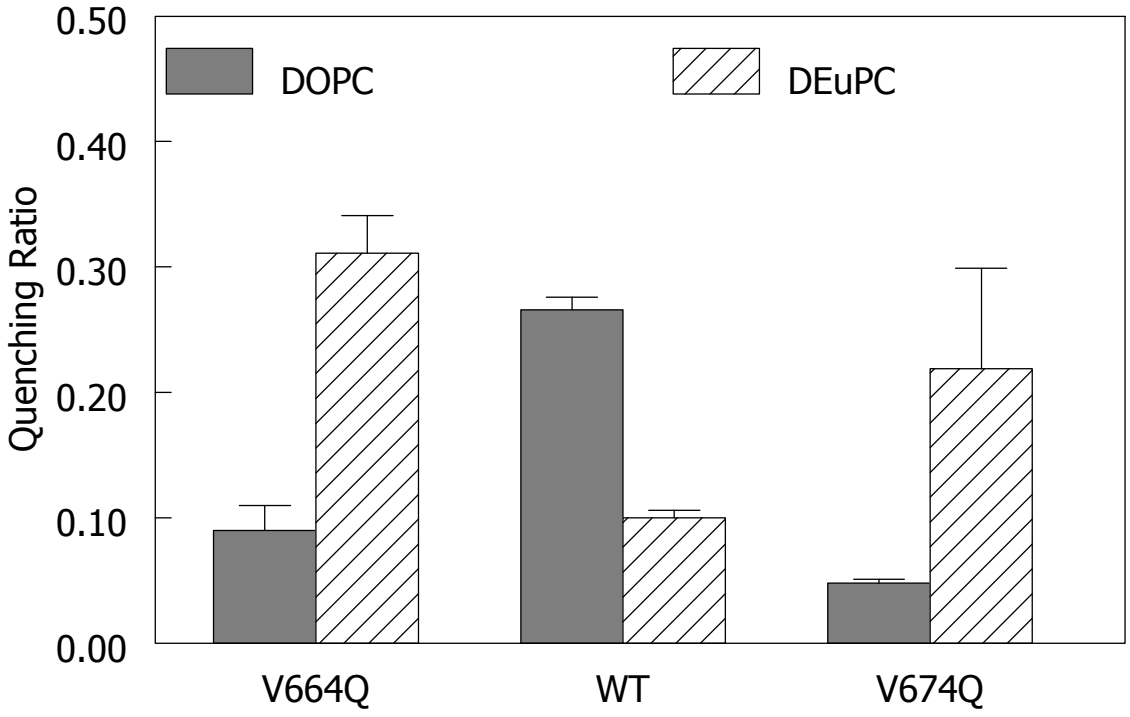

Figure 5.13: Quenching results of ErbB2 WT, N-terminal Q mutant (V664Q) and C-terminal Q mutant (V674Q) in DOPC (solid bars) and DEuPC (striped bars) at pH 7.0. Results for ErbB2 WT and V664Q peptides are included here for comparison. Samples contained 2μM peptide incorporated into 500 μM lipid suspended in PBS buffer

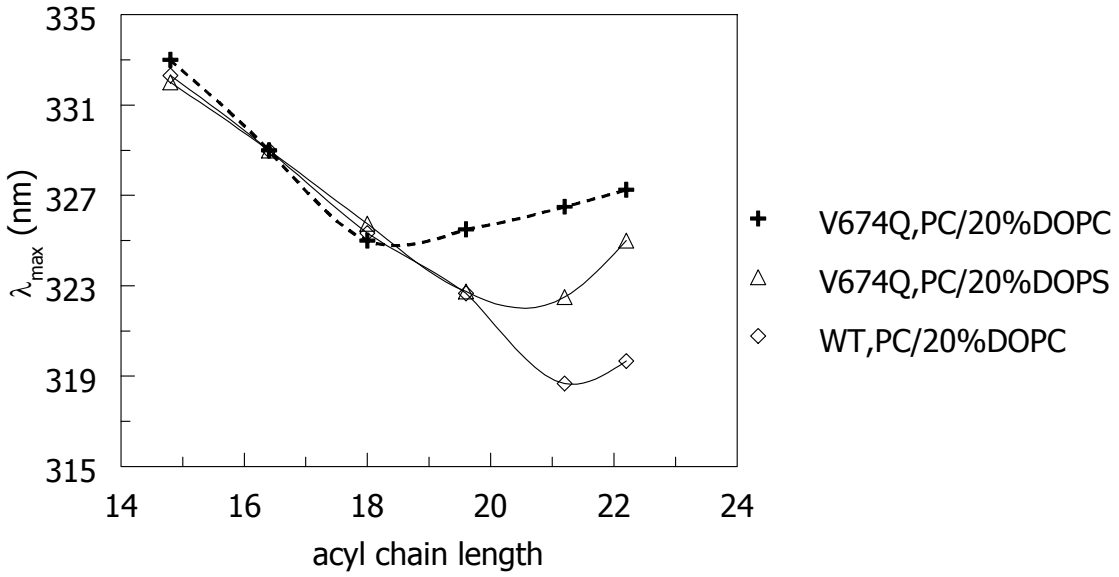

Figure 5.14: Trp λmax dependence in lipid bilayer of different acyl chain lengths at pH 7.0. + shows (80:20) mixtures of different length PC and DOPC. Δ represents (80:20) mixtures of different length PC and DOPS. Result for WT peptide in (80:20) mixtures of different length PC and DOPC for comparison. Samples contained 2μM peptide incorporated into 500 μM lipid suspended in PBS buffer

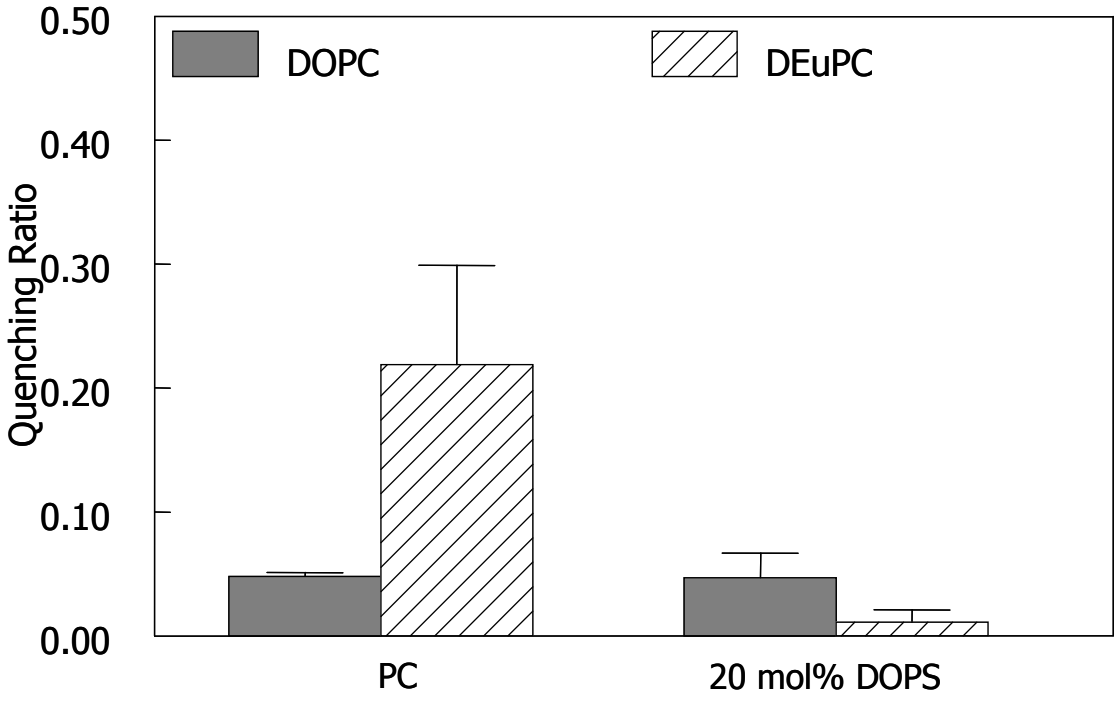

Figure 5.15: Quenching ratio of V674Q in neutral vesicles (PC) and negatively charged vesicles (80:20, mol:mol, DOPC:DOPS) of different bilayer thickness at pH 7.0. Samples contained 2μM peptide incorporated into 500 μM lipid suspended in PBS buffer

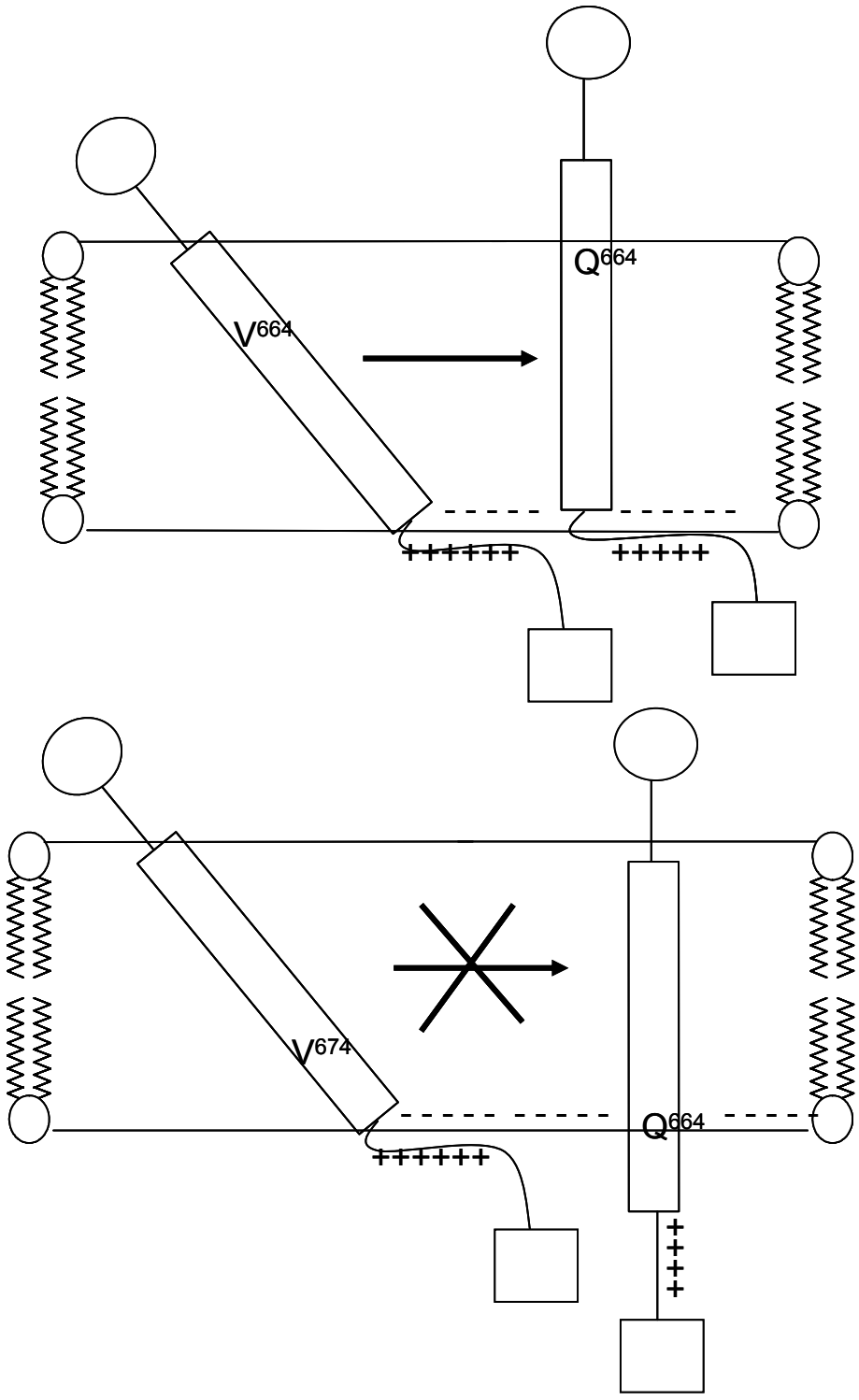

Figure 5.16: Schematic showing transverse TM helix shift toward the lumenal and cytoplasmic side of membranes. Rectangles represent ErbB2 TM helix. Circle shows the extracellular domain and square shows intracellular domain.

FUTURE DIRECTIONS

Effect of other types of anionic lipids on the topography of membrane inserted hydrophobic α-helices

I have reported that anionic lipids, such as, phosphatidylserine (PS) and phosphatidylglycerol (PG) which are an integral part of the cell membranes, stabilized the TM conformations of hydrophobic helices relative to non-TM or shifted-TM topography through a specific headgroup-cationic juxtamembrane (JM) residue interaction. There are also other types of negatively charged lipid in the cell membrane. Cardiolipin (CL) is an integral part of inner mitochondrial membrane constituting about 20% of the total lipid where it has been known to be involved in mitochondrial function. It has been seen in some bacterial membrane[185].Unlike other lipids it has four fatty acyl chains and -2 net negative charges. Another anionic phospoholipid that is a major part of cell membrane is phophatidic acid (PA). PA is the smallest of the phospholipids it can exist in two ionization sates with net -1 or net -2 charges as phophatidate. PA plays a vital role in many physiological events including regulation of protein and lipid phosphorylation, activation of oxidative process and modulation of membrane trafficking through direct interaction with the proteins[186]. Having smaller headgoups than more conventional phospholipids like PS or PG, cardiolipin and PA might interact differently with the polybasic or the charged region of the protein. Studies of Artificial hydrophobic helices with positively charged JM residues in CL or PA containing lipid bilayer would help in the understanding of real protein-lipid interaction.

ErbB2 receptor studies: Effect of hydrophilic mutations upon the helix-helix interaction between ErbB2 and ErbB3

Since neu/ErbB2 receptor function as dimers the effect of hydrophilic mutation upon the dimerization can be important. ErbB2 preferentially forms heterodimers with ErbB3 among other ErbB receptors. Fluorescence energy transfer or FRET can be used to study this ErbB2/ErbB3 dimerization. ErbB2 TM sequence used in the study already

contains a Trp residue which can be used as a donar molecule for FRET studies. Since dansyl chloride is a good acceptor for Trp fluorescence, peptides corresponding to the ErbB3/ ErbB2 TM segment with dansyl label can be synthesized from Anaspec. Amount of FRET from each hydrophilic mutation could be applied to measure the extent of homo/heterodimerization. It has been proposed that oncogenicity of the Glu^{664} mutation arise from its ability to form more stable dimers than the WT sequence. Using FRET we could measure the relative stability of WT and mutant ErbB2 dimers at physiological pH to confirm this hypothesis.

REFERENCES

1. Wallin, E. & von Heijne, G. (1998). Genome-wide analysis of integral membrane proteins from eubacterial, archaean, and eukaryotic organisms. *Protein Sci* **7**, 1029-38.
2. Lenard, J. & Singer, S. J. (1966). Protein Conformation in Cell Membrane Preparations as Studied by Optical Rotatory Dispersion and Circular Dichroism. *Proc Natl Acad Sci U S A* **56**, 1828-1835.
3. Wallach, D. F., Zahler,P.H. (1966). Protein conformations in cellular membranes. *PNAS* **56**, 1552-1559.
4. Henderson, R. & Unwin, P. N. (1975). Three-dimensional model of purple membrane obtained by electron microscopy. *Nature* **257**, 28-32.
5. Blobel, G. & Dobberstein, B. (1975). Transfer of proteins across membranes. II. Reconstitution of functional rough microsomes from heterologous components. *J Cell Biol* **67**, 852-62.
6. Schatz, G. & Dobberstein, B. (1996). Common principles of protein translocation across membranes. *Science* **271**, 1519-26.
7. White, S. H. & Wimley, W. C. (1999). Membrane protein folding and stability: physical principles. *Annu Rev Biophys Biomol Struct* **28**, 319-65.
8. Zhan, H., Oh, K. J., Shin, Y. K., Hubbell, W. L. & Collier, R. J. (1995). Interaction of the isolated transmembrane domain of diphtheria toxin with membranes. *Biochemistry* **34**, 4856-63.
9. Dempsey, C. E. (1990). The actions of melittin on membranes. *Biochim Biophys Acta* **1031**, 143-61.
10. Seddon, A. C., P;Booth,PJ. (2004). Membrane proteins, lipids and detergents: not just a soap opera. *Biochym.Biophys.Acta* **1666**
105-117.
11. Wiener, M. W., SH. (1992). Structure of a fluid dioleoylphosphatidylcholine bilayer determined by joint refinement of x-ray and neutron diffraction data. III. Complete structure. *Biophys.J.* **61**, 434-447.
12. Wang, Y., Malenbaum, S. E., Kachel, K., Zhan, H., Collier, R. J. & London, E. (1997). Identification of shallow and deep membrane-penetrating forms of diphtheria toxin T domain that are regulated by protein concentration and bilayer width. *J Biol Chem* **272**, 25091-8.
13. Kachel, K., Ren, J., Collier, R. J. & London, E. (1998). Identifying transmembrane states and defining the membrane insertion boundaries of hydrophobic helices in membrane-inserted diphtheria toxin T domain. *J Biol Chem* **273**, 22950-6.
14. Petosa, C., Collier, R. J., Klimpel, K. R., Leppla, S. H. & Liddington, R. C. (1997). Crystal structure of the anthrax toxin protective antigen. *Nature* **385**, 833-8.
15. Shepard, L. A., Heuck, A. P., Hamman, B. D., Rossjohn, J., Parker, M. W., Ryan, K. R., Johnson, A. E. & Tweten, R. K. (1998). Identification of a membrane-spanning domain of the thiol-activated pore-forming toxin Clostridium

perfringens perfringolysin O: an alpha-helical to beta-sheet transition identified by fluorescence spectroscopy. *Biochemistry* **37**, 14563-74.
16. Tilley, S. J., Orlova, E. V., Gilbert, R. J., Andrew, P. W. & Saibil, H. R. (2005). Structural basis of pore formation by the bacterial toxin pneumolysin. *Cell* **121**, 247-56.
17. Malenbaum, S. E., Merrill, A. R. & London, E. (1998). Membrane-inserted colicin E1 channel domain: a topological survey by fluorescence quenching suggests that model membrane thickness affects membrane penetration. *J Nat Toxins* **7**, 269-90.
18. Antignani, A. & Youle, R. J. (2006). How do Bax and Bak lead to permeabilization of the outer mitochondrial membrane? *Curr Opin Cell Biol* **18**, 685-9.
19. Wattenberg, B. & Lithgow, T. (2001). Targeting of C-terminal (tail)-anchored proteins: understanding how cytoplasmic activities are anchored to intracellular membranes. *Traffic* **2**, 66-71.
20. Gringhuis, S. I., Papendrecht-van der Voort, E.,Leow, A., Levarht, N.E.W.,Breedveld, F.C., Verweij, C.L. . (2002). Effect of Redox Balance Alterations on Cellular Localization of LAT and Downstream T-Cell Receptor Signaling Pathways. *Mol.Cell.Biol.* **22**, 400-411.
21. Fujita, K., Krishnakumar, S. S., Franco, D., Paul, A. V., London, E. & Wimmer, E. (2007). Membrane topography of the hydrophobic anchor sequence of poliovirus 3A and 3AB proteins and the functional effect of 3A/3AB membrane association upon RNA replication. *Biochemistry* **46**, 5185-99.
22. Huang, H. W. (2006). Molecular mechanism of antimicrobial peptides: the origin of cooperativity. *Biochim Biophys Acta* **1758**, 1292-302.
23. Zhao, G. & London, E. (2006). An amino acid "transmembrane tendency" scale that approaches the theoretical limit to accuracy for prediction of transmembrane helices: relationship to biological hydrophobicity. *Protein Sci* **15**, 1987-2001.
24. Popot, J., Engelman,D.M. (2000). Helical protein folding, stability, and evolution. *Annu.Ev.Biochem* **69**, 881-922.
25. Killian, J. A. (2003). Synthetic peptides as models for intrinsic membrane proteins. *FEBS Lett* **555**, 134-8.
26. Hunt, J. F., Rath, P., Rothschild, K. J. & Engelman, D. M. (1997). Spontaneous, pH-dependent membrane insertion of a transbilayer alpha-helix. *Biochemistry* **36**, 15177-92.
27. Lewis, R. N., Liu, F., Krivanek, R., Rybar, P., Hianik, T., Flach, C. R., Mendelsohn, R., Chen, Y., Mant, C. T., Hodges, R. S. & McElhaney, R. N. (2007). Studies of the minimum hydrophobicity of alpha-helical peptides required to maintain a stable transmembrane association with phospholipid bilayer membranes. *Biochemistry* **46**, 1042-54.
28. Bechinger, B. (1996). Towards membrane protein design: pH-sensitive topology of histidine-containing polypeptides. *J Mol Biol* **263**, 768-75.
29. Aisenbrey, C., Kinder, R., Goormaghtigh, E., Ruysschaert, J. M. & Bechinger, B. (2006). Interactions involved in the realignment of membrane-associated helices. An investigation using oriented solid-state NMR and attenuated total reflection Fourier transform infrared spectroscopies. *J Biol Chem* **281**, 7708-16.

30. Bechinger, B. (2001). Membrane insertion and orientation of polyalanine peptides: a (15)N solid-state NMR spectroscopy investigation. *Biophys J* **81**, 2251-6.
31. Vogt, B., Ducarme, P., Schinzel, S., Brasseur, R. & Bechinger, B. (2000). The topology of lysine-containing amphipathic peptides in bilayers by circular dichroism, solid-state NMR, and molecular modeling. *Biophys J* **79**, 2644-56.
32. Bechinger, B., Ruysschaert, J. M. & Goormaghtigh, E. (1999). Membrane helix orientation from linear dichroism of infrared attenuated total reflection spectra. *Biophys J* **76**, 552-63.
33. Aisenbrey, C., Goormaghtigh, E., Ruysschaert, J. M. & Bechinger, B. (2006). Translocation of amino acyl residues from the membrane interface to the hydrophobic core: thermodynamic model and experimental analysis using ATR-FTIR spectroscopy. *Mol Membr Biol* **23**, 363-74.
34. Wu, Y., Huang, H. W. & Olah, G. A. (1990). Method of oriented circular dichroism. *Biophys J* **57**, 797-806.
35. Mykhailiuk, P. K., Afonin, S., Palamarchuk, G. V., Shishkin, O. V., Ulrich, A. S. & Komarov, I. V. (2008). Synthesis of trifluoromethyl-substituted proline analogues as 19F NMR labels for peptides in the polyproline II conformation. *Angew Chem Int Ed Engl* **47**, 5765-7.
36. Burck, J., Roth, S., Wadhwani, P., Afonin, S., Kanithasen, N., Strandberg, E. & Ulrich, A. S. (2008). Conformation and membrane orientation of amphiphilic helical peptides by oriented circular dichroism. *Biophys J* **95**, 3872-81.
37. Ladokhin, A. S. (1999). Analysis of protein and peptide penetration into membranes by depth-dependent fluorescence quenching: theoretical considerations. *Biophys J* **76**, 946-55.
38. Ren, J., Kachel, K., Kim, H., Malenbaum, S. E., Collier, R. J. & London, E. (1999). Interaction of diphtheria toxin T domain with molten globule-like proteins and its implications for translocation. *Science* **284**, 955-7.
39. Rosconi, M. P. & London, E. (2002). Topography of helices 5-7 in membrane-inserted diphtheria toxin T domain: identification and insertion boundaries of two hydrophobic sequences that do not form a stable transmembrane hairpin. *J Biol Chem* **277**, 16517-27.
40. London, E. (1982). Investigation of membrane structure using fluorescence quenching by spin-labels. A review of recent studies. *Mol Cell Biochem* **45**, 181-8.
41. Ladokhin, A. S., Isas, J. M., Haigler, H. T. & White, S. H. (2002). Determining the membrane topology of proteins: insertion pathway of a transmembrane helix of annexin 12. *Biochemistry* **41**, 13617-26.
42. Liu, L. P. & Deber, C. M. (1997). Anionic phospholipids modulate peptide insertion into membranes. *Biochemistry* **36**, 5476-82.
43. Caputo, G. A. & London, E. (2003). Using a novel dual fluorescence quenching assay for measurement of tryptophan depth within lipid bilayers to determine hydrophobic alpha-helix locations within membranes. *Biochemistry* **42**, 3265-74.
44. Hessa, T., Kim, H., Bihlmaier, K., Lundin, C., Boekel, J., Andersson, H., Nilsson, I., White, S. H. & von Heijne, G. (2005). Recognition of transmembrane helices by the endoplasmic reticulum translocon. *Nature* **433**, 377-81.

45. Hessa, T., White, S. H. & von Heijne, G. (2005). Membrane insertion of a potassium-channel voltage sensor. *Science* **307**, 1427.
46. Caputo, G. A. & London, E. (2004). Position and ionization state of Asp in the core of membrane-inserted alpha helices control both the equilibrium between transmembrane and nontransmembrane helix topography and transmembrane helix positioning. *Biochemistry* **43**, 8794-806.
47. Lew, S., Ren, J. & London, E. (2000). The effects of polar and/or ionizable residues in the core and flanking regions of hydrophobic helices on transmembrane conformation and oligomerization. *Biochemistry* **39**, 9632-40.
48. Landolt-Marticorena, C., Williams, K. A., Deber, C. M. & Reithmeier, R. A. (1993). Non-random distribution of amino acids in the transmembrane segments of human type I single span membrane proteins. *J Mol Biol* **229**, 602-8.
49. Ulmschneider, M. B. & Sansom, M. S. (2001). Amino acid distributions in integral membrane protein structures. *Biochim Biophys Acta* **1512**, 1-14.
50. Caputo, G. A. & London, E. (2003). Cumulative effects of amino acid substitutions and hydrophobic mismatch upon the transmembrane stability and conformation of hydrophobic alpha-helices. *Biochemistry* **42**, 3275-85.
51. Hessa, T., Meindl-Beinker, N. M., Bernsel, A., Kim, H., Sato, Y., Lerch-Bader, M., Nilsson, I., White, S. H. & von Heijne, G. (2007). Molecular code for transmembrane-helix recognition by the Sec61 translocon. *Nature* **450**, 1026-30.
52. Jiang, Y., Ruta, V., Chen, J., Lee, A. & MacKinnon, R. (2003). The principle of gating charge movement in a voltage-dependent K+ channel. *Nature* **423**, 42-8.
53. Aires, J. R., Pechere, J. C., Van Delden, C. & Kohler, T. (2002). Amino acid residues essential for function of the MexF efflux pump protein of Pseudomonas aeruginosa. *Antimicrob Agents Chemother* **46**, 2169-73.
54. Subramaniam, S., Greenhalgh, D. A. & Khorana, H. G. (1992). Aspartic acid 85 in bacteriorhodopsin functions both as proton acceptor and negative counterion to the Schiff base. *J Biol Chem* **267**, 25730-3.
55. Ren, J., Lew, S., Wang, J. & London, E. (1999). Control of the transmembrane orientation and interhelical interactions within membranes by hydrophobic helix length. *Biochemistry* **38**, 5905-12.
56. Zhang, Y. P., Lewis, R. N., Hodges, R. S. & McElhaney, R. N. (1992). Interaction of a peptide model of a hydrophobic transmembrane alpha-helical segment of a membrane protein with phosphatidylcholine bilayers: differential scanning calorimetric and FTIR spectroscopic studies. *Biochemistry* **31**, 11579-88.
57. Zhang, Y. P., Lewis, R. N., Hodges, R. S. & McElhaney, R. N. (1992). FTIR spectroscopic studies of the conformation and amide hydrogen exchange of a peptide model of the hydrophobic transmembrane alpha-helices of membrane proteins. *Biochemistry* **31**, 11572-8.
58. Krishnakumar, S. S. & London, E. (2007). Effect of sequence hydrophobicity and bilayer width upon the minimum length required for the formation of transmembrane helices in membranes. *J Mol Biol* **374**, 671-87.
59. Hammond, K., Caputo, G. A. & London, E. (2002). Interaction of the membrane-inserted diphtheria toxin T domain with peptides and its possible implications for chaperone-like T domain behavior. *Biochemistry* **41**, 3243-53.

60. Lewis, R. N., Zhang, Y. P., Hodges, R. S., Subczynski, W. K., Kusumi, A., Flach, C. R., Mendelsohn, R. & McElhaney, R. N. (2001). A polyalanine-based peptide cannot form a stable transmembrane alpha-helix in fully hydrated phospholipid bilayers. *Biochemistry* **40**, 12103-11.
61. Nilsson, I., Johnson, A. E. & von Heijne, G. (2003). How hydrophobic is alanine? *J Biol Chem* **278**, 29389-93.
62. Wimley, W. C. & White, S. H. (1996). Experimentally determined hydrophobicity scale for proteins at membrane interfaces. *Nat Struct Biol* **3**, 842-8.
63. Chen, H. & Kendall, D. A. (1995). Artificial transmembrane segments. Requirements for stop transfer and polypeptide orientation. *J Biol Chem* **270**, 14115-22.
64. Kuroiwa, T., Sakaguchi, M., Mihara, K. & Omura, T. (1991). Systematic analysis of stop-transfer sequence for microsomal membrane. *J Biol Chem* **266**, 9251-5.
65. Sui, H., Han, B. G., Lee, J. K., Walian, P. & Jap, B. K. (2001). Structural basis of water-specific transport through the AQP1 water channel. *Nature* **414**, 872-8.
66. Dutzler, R., Campbell, E. B., Cadene, M., Chait, B. T. & MacKinnon, R. (2002). X-ray structure of a ClC chloride channel at 3.0 A reveals the molecular basis of anion selectivity. *Nature* **415**, 287-94.
67. Whitley, P., Grahn, E., Kutay, U., Rapoport, T. A. & von Heijne, G. (1996). A 12-residue-long polyleucine tail is sufficient to anchor synaptobrevin to the endoplasmic reticulum membrane. *J Biol Chem* **271**, 7583-6.
68. Bretscher, M. S. & Munro, S. (1993). Cholesterol and the Golgi apparatus. *Science* **261**, 1280-1.
69. Munro, S. (1995). A comparison of the transmembrane domains of Golgi and plasma membrane proteins. *Biochem Soc Trans* **23**, 527-30.
70. Munro, S. (1995). An investigation of the role of transmembrane domains in Golgi protein retention. *Embo J* **14**, 4695-704.
71. Webb, R. J., East, J. M., Sharma, R. P. & Lee, A. G. (1998). Hydrophobic mismatch and the incorporation of peptides into lipid bilayers: a possible mechanism for retention in the Golgi. *Biochemistry* **37**, 673-9.
72. Adams, G. A. & Rose, J. K. (1985). Structural requirements of a membrane-spanning domain for protein anchoring and cell surface transport. *Cell* **41**, 1007-15.
73. Juad, S., Fernandez-Vidal, M.,Nilsson, I.M.,Meindl-Beinker,N.M.,Hubner,N.,von Heijne,G.,White,S.H. (2008). Insertion of Short Transmembrane Helices by the Sec61 Translocon. *Nature.Struct.Mol.Biol.*
74. Ren, J., Lew, S., Wang, Z. & London, E. (1997). Transmembrane orientation of hydrophobic alpha-helices is regulated both by the relationship of helix length to bilayer thickness and by the cholesterol concentration. *Biochemistry* **36**, 10213-20.
75. Falke, J. J. & Hazelbauer, G. L. (2001). Transmembrane signaling in bacterial chemoreceptors. *Trends Biochem Sci* **26**, 257-65.
76. Miller, A. F. & Falke, J. J. (2004). Chemotaxis receptors and signaling. *Adv Protein Chem* **68**, 393-444.

77. Hughson, A. G. & Hazelbauer, G. L. (1996). Detecting the conformational change of transmembrane signaling in a bacterial chemoreceptor by measuring effects on disulfide cross-linking in vivo. *Proc Natl Acad Sci U S A* **93**, 11546-51.
78. Armulik, A., Nilsson, I., von Heijne, G. & Johansson, S. (1999). Determination of the border between the transmembrane and cytoplasmic domains of human integrin subunits. *J Biol Chem* **274**, 37030-4.
79. Han, X., Mihailescu, M. & Hristova, K. (2006). Neutron diffraction studies of fluid bilayers with transmembrane proteins: structural consequences of the achondroplasia mutation. *Biophys J* **91**, 3736-47.
80. Gupta-Rossi, N., Six, E., LeBail, O., Logeat, F., Chastagner, P., Olry, A., Israel, A. & Brou, C. (2004). Monoubiquitination and endocytosis direct gamma-secretase cleavage of activated Notch receptor. *J Cell Biol* **166**, 73-83.
81. Abrami, L., Kunz, B., Iacovache, I. & van der Goot, F. G. (2008). Palmitoylation and ubiquitination regulate exit of the Wnt signaling protein LRP6 from the endoplasmic reticulum. *Proc Natl Acad Sci U S A* **105**, 5384-9.
82. Smith, J., Su, X., El-Maghrabi, R., Stahl, P. D. & Abumrad, N. A. (2008). Opposite regulation of CD36 ubiquitination by fatty acids and insulin: effects on fatty acid uptake. *J Biol Chem* **283**, 13578-85.
83. Kukar, T. L., Ladd, T. B., Bann, M. A., Fraering, P. C., Narlawar, R., Maharvi, G. M., Healy, B., Chapman, R., Welzel, A. T., Price, R. W., Moore, B., Rangachari, V., Cusack, B., Eriksen, J., Jansen-West, K., Verbeeck, C., Yager, D., Eckman, C., Ye, W., Sagi, S., Cottrell, B. A., Torpey, J., Rosenberry, T. L., Fauq, A., Wolfe, M. S., Schmidt, B., Walsh, D. M., Koo, E. H. & Golde, T. E. (2008). Substrate-targeting gamma-secretase modulators. *Nature* **453**, 925-9.
84. Lichtenthaler, S. F., Beher, D., Grimm, H. S., Wang, R., Shearman, M. S., Masters, C. L. & Beyreuther, K. (2002). The intramembrane cleavage site of the amyloid precursor protein depends on the length of its transmembrane domain. *Proc Natl Acad Sci U S A* **99**, 1365-70.
85. Murphy, M. P., Hickman, L. J., Eckman, C. B., Uljon, S. N., Wang, R. & Golde, T. E. (1999). gamma-Secretase, evidence for multiple proteolytic activities and influence of membrane positioning of substrate on generation of amyloid beta peptides of varying length. *J Biol Chem* **274**, 11914-23.
86. Chin, C. N. & von Heijne, G. (2000). Charge pair interactions in a model transmembrane helix in the ER membrane. *J Mol Biol* **303**, 1-5.
87. Monne, M., Nilsson, I., Johansson, M., Elmhed, N. & von Heijne, G. (1998). Positively and negatively charged residues have different effects on the position in the membrane of a model transmembrane helix. *J Mol Biol* **284**, 1177-83.
88. Monne, M. & von Heijne, G. (2001). Effects of 'hydrophobic mismatch' on the location of transmembrane helices in the ER membrane. *FEBS Lett* **496**, 96-100.
89. Braun, P. & von Heijne, G. (1999). The aromatic residues Trp and Phe have different effects on the positioning of a transmembrane helix in the microsomal membrane. *Biochemistry* **38**, 9778-82.
90. Krishnakumar, S. S. & London, E. (2007). The control of transmembrane helix transverse position in membranes by hydrophilic residues. *J Mol Biol* **374**, 1251-69.

91. de Vrije, G. J., Batenburg, A. M., Killian, J. A. & de Kruijff, B. (1990). Lipid involvement in protein translocation in Escherichia coli. *Mol Microbiol* **4**, 143-50.
92. de Kruijff, B. (1994). Anionic phospholipids and protein translocation. *FEBS Lett* **346**, 78-82.
93. Lad, M. D., Birembaut, F., Clifton, L. A., Frazier, R. A., Webster, J. R. & Green, R. J. (2007). Antimicrobial peptide-lipid binding interactions and binding selectivity. *Biophys J* **92**, 3575-86.
94. von Heijne, G. (1986). Net N-C charge imbalance may be important for signal sequence function in bacteria. *J Mol Biol* **192**, 287-90.
95. von Heijne, G. (1989). Control of topology and mode of assembly of a polytopic membrane protein by positively charged residues. *Nature* **341**, 456-8.
96. Andersson, H. & von Heijne, G. (1994). Positively charged residues influence the degree of SecA dependence in protein translocation across the E. coli inner membrane. *FEBS Lett* **347**, 169-72.
97. Lerch-Bader, M., Lundin, C., Kim, H., Nilsson, I. & von Heijne, G. (2008). Contribution of positively charged flanking residues to the insertion of transmembrane helices into the endoplasmic reticulum. *Proc Natl Acad Sci U S A* **105**, 4127-32.
98. Lew, S., Caputo, G. A. & London, E. (2003). The effect of interactions involving ionizable residues flanking membrane-inserted hydrophobic helices upon helix-helix interaction. *Biochemistry* **42**, 10833-42.
99. Ozdirekcan, S., Rijkers, D. T., Liskamp, R. M. & Killian, J. A. (2005). Influence of flanking residues on tilt and rotation angles of transmembrane peptides in lipid bilayers. A solid-state 2H NMR study. *Biochemistry* **44**, 1004-12.
100. Strandberg, E., Ozdirekcan, S., Rijkers, D. T., van der Wel, P. C., Koeppe, R. E., 2nd, Liskamp, R. M. & Killian, J. A. (2004). Tilt angles of transmembrane model peptides in oriented and non-oriented lipid bilayers as determined by 2H solid-state NMR. *Biophys J* **86**, 3709-21.
101. Strandberg, E., Morein, S., Rijkers, D. T., Liskamp, R. M., van der Wel, P. C. & Killian, J. A. (2002). Lipid dependence of membrane anchoring properties and snorkeling behavior of aromatic and charged residues in transmembrane peptides. *Biochemistry* **41**, 7190-8.
102. van der Wel, P. C., Strandberg, E., Killian, J. A. & Koeppe, R. E., 2nd. (2002). Geometry and intrinsic tilt of a tryptophan-anchored transmembrane alpha-helix determined by (2)H NMR. *Biophys J* **83**, 1479-88.
103. Killian, J. A. & von Heijne, G. (2000). How proteins adapt to a membrane-water interface. *Trends Biochem Sci* **25**, 429-34.
104. de Planque, M. R., Boots, J. W., Rijkers, D. T., Liskamp, R. M., Greathouse, D. V. & Killian, J. A. (2002). The effects of hydrophobic mismatch between phosphatidylcholine bilayers and transmembrane alpha-helical peptides depend on the nature of interfacially exposed aromatic and charged residues. *Biochemistry* **41**, 8396-404.
105. Choma, C., Gratkowski, H., Lear, J. D. & DeGrado, W. F. (2000). Asparagine-mediated self-association of a model transmembrane helix. *Nat Struct Biol* **7**, 161-6.

106. Zhou, F. X., Cocco, M. J., Russ, W. P., Brunger, A. T. & Engelman, D. M. (2000). Interhelical hydrogen bonding drives strong interactions in membrane proteins. *Nat Struct Biol* **7**, 154-60.
107. Gratkowski, H., Lear, J. D. & DeGrado, W. F. (2001). Polar side chains drive the association of model transmembrane peptides. *Proc Natl Acad Sci U S A* **98**, 880-5.
108. Zhou, F. X., Merianos, H. J., Brunger, A. T. & Engelman, D. M. (2001). Polar residues drive association of polyleucine transmembrane helices. *Proc Natl Acad Sci U S A* **98**, 2250-5.
109. Dawson, J. P., Weinger, J. S. & Engelman, D. M. (2002). Motifs of serine and threonine can drive association of transmembrane helices. *J Mol Biol* **316**, 799-805.
110. Dawson, J. P., Melnyk, R. A., Deber, C. M. & Engelman, D. M. (2003). Sequence context strongly modulates association of polar residues in transmembrane helices. *J Mol Biol* **331**, 255-62.
111. Hildebrand, P. W., Preissner, R. & Frommel, C. (2004). Structural features of transmembrane helices. *FEBS Lett* **559**, 145-51.
112. van Meer, G. (1989). Lipid traffic in animal cells. *Annu Rev Cell Biol* **5**, 247-75.
113. Montecucco, C., Smith, G. A., Dabbeni-sala, F., Johannsson, A., Galante, Y. M. & Bisson, R. (1982). Bilayer thickness and enzymatic activity in the mitochondrial cytochrome c oxidase and ATPase complex. *FEBS Lett* **144**, 145-8.
114. Caffrey, M. & Feigenson, G. W. (1981). Fluorescence quenching in model membranes. 3. Relationship between calcium adenosinetriphosphatase enzyme activity and the affinity of the protein for phosphatidylcholines with different acyl chain characteristics. *Biochemistry* **20**, 1949-61.
115. Goforth, R. L., Chi, A. K., Greathouse, D. V., Providence, L. L., Koeppe, R. E., 2nd & Andersen, O. S. (2003). Hydrophobic coupling of lipid bilayer energetics to channel function. *J Gen Physiol* **121**, 477-93.
116. Mitra, K., Ubarretxena-Belandia, I., Taguchi, T., Warren, G. & Engelman, D. M. (2004). Modulation of the bilayer thickness of exocytic pathway membranes by membrane proteins rather than cholesterol. *Proc Natl Acad Sci U S A* **101**, 4083-8.
117. Lew, S. & London, E. (1997). Simple procedure for reversed-phase high-performance liquid chromatographic purification of long hydrophobic peptides that form transmembrane helices. *Anal Biochem* **251**, 113-6.
118. Wang, X., Bogdanov, M. & Dowhan, W. (2002). Topology of polytopic membrane protein subdomains is dictated by membrane phospholipid composition. *EMBO J* **21**, 5673-81.
119. Xie, J., Bogdanov, M., Heacock, P. & Dowhan, W. (2006). Phosphatidylethanolamine and monoglucosyldiacylglycerol are interchangeable in supporting topogenesis and function of the polytopic membrane protein lactose permease. *J Biol Chem* **281**, 19172-8.
120. Giddings, K. S., Johnson, A. E. & Tweten, R. K. (2003). Redefining cholesterol's role in the mechanism of the cholesterol-dependent cytolysins. *Proc Natl Acad Sci U S A* **100**, 11315-20.
121. Killian, J. A. (1998). Hydrophobic mismatch between proteins and lipids in membranes. *Biochim Biophys Acta* **1376**, 401-15.

122. Killian, J. A. & Nyholm, T. K. (2006). Peptides in lipid bilayers: the power of simple models. *Curr Opin Struct Biol* **16**, 473-9.
123. van Duyl, B. Y., Meeldijk, H., Verkleij, A. J., Rijkers, D. T., Chupin, V., de Kruijff, B. & Killian, J. A. (2005). A synergistic effect between cholesterol and tryptophan-flanked transmembrane helices modulates membrane curvature. *Biochemistry* **44**, 4526-32.
124. Liu, F., Lewis, R. N., Hodges, R. S. & McElhaney, R. N. (2004). Effect of variations in the structure of a polyleucine-based alpha-helical transmembrane peptide on its interaction with phosphatidylethanolamine Bilayers. *Biophys J* **87**, 2470-82.
125. Tsui, F. C., Ojcius, D. M. & Hubbell, W. L. (1986). The intrinsic pKa values for phosphatidylserine and phosphatidylethanolamine in phosphatidylcholine host bilayers. *Biophys J* **49**, 459-68.
126. MacDonald, R. C., Simon, S. A. & Baer, E. (1976). Ionic influences on the phase transition of dipalmitoylphosphatidylserine. *Biochemistry* **15**, 885-91.
127. Maltseva, E., Shapovalov, V. L., Mohwald, H. & Brezesinski, G. (2006). Ionization state and structure of l-1,2-dipalmitoylphosphatidylglycerol monolayers at the liquid/air interface. *J Phys Chem B* **110**, 919-26.
128. Koynova, R. & Caffrey, M. (1998). Phases and phase transitions of the phosphatidylcholines. *Biochim Biophys Acta* **1376**, 91-145.
129. Voglino, L., McIntosh, T. J. & Simon, S. A. (1998). Modulation of the binding of signal peptides to lipid bilayers by dipoles near the hydrocarbon-water interface. *Biochemistry* **37**, 12241-52.
130. Kachel, K., Asuncion-Punzalan, E. & London, E. (1995). Anchoring of tryptophan and tyrosine analogs at the hydrocarbon-polar boundary in model membrane vesicles: parallax analysis of fluorescence quenching induced by nitroxide-labeled phospholipids. *Biochemistry* **34**, 15475-9.
131. Yau, W. M., Wimley, W. C., Gawrisch, K. & White, S. H. (1998). The preference of tryptophan for membrane interfaces. *Biochemistry* **37**, 14713-8.
132. Egashira, M., Gorbenko, G., Tanaka, M., Saito, H., Molotkovsky, J., Nakano, M. & Handa, T. (2002). Cholesterol modulates interaction between an amphipathic class A peptide, Ac-18A-NH2, and phosphatidylcholine bilayers. *Biochemistry* **41**, 4165-72.
133. Saito, H., Miyako, Y., Handa, T. & Miyajima, K. (1997). Effect of cholesterol on apolipoprotein A-I binding to lipid bilayers and emulsions. *J Lipid Res* **38**, 287-94.
134. Arbuzova, A., Wang, L., Wang, J., Hangyas-Mihalyne, G., Murray, D., Honig, B. & McLaughlin, S. (2000). Membrane binding of peptides containing both basic and aromatic residues. Experimental studies with peptides corresponding to the scaffolding region of caveolin and the effector region of MARCKS. *Biochemistry* **39**, 10330-9.
135. Makovitzki, A., Avrahami, D. & Shai, Y. (2006). Ultrashort antibacterial and antifungal lipopeptides. *Proc Natl Acad Sci U S A* **103**, 15997-6002.
136. Sitaram, N. & Nagaraj, R. (1999). Interaction of antimicrobial peptides with biological and model membranes: structural and charge requirements for activity. *Biochim Biophys Acta* **1462**, 29-54.

137. Valiyaveetil, F. I., Zhou, Y. & MacKinnon, R. (2002). Lipids in the structure, folding, and function of the KcsA K+ channel. *Biochemistry* **41**, 10771-7.
138. Gohil, V. M., Hayes, P., Matsuyama, S., Schagger, H., Schlame, M. & Greenberg, M. L. (2004). Cardiolipin biosynthesis and mitochondrial respiratory chain function are interdependent. *J Biol Chem* **279**, 42612-8.
139. Zhang, M., Mileykovskaya, E. & Dowhan, W. (2005). Cardiolipin is essential for organization of complexes III and IV into a supercomplex in intact yeast mitochondria. *J Biol Chem* **280**, 29403-8.
140. Powl, A. M., East, J. M. & Lee, A. G. (2005). Heterogeneity in the binding of lipid molecules to the surface of a membrane protein: hot spots for anionic lipids on the mechanosensitive channel of large conductance MscL and effects on conformation. *Biochemistry* **44**, 5873-83.
141. Lee, A. G. (2005). How lipids and proteins interact in a membrane: a molecular approach. *Mol Biosyst* **1**, 203-12.
142. Heijne, G. V. (1986). The distribution of positively charged residues in bacterial inner membrane proteins correlates with the trans-membrane topology. *EMBO J* **5**, 3021-3027.
143. van Klompenburg, W., Nilsson, I., von Heijne, G. & de Kruijff, B. (1997). Anionic phospholipids are determinants of membrane protein topology. *EMBO J* **16**, 4261-6.
144. Borochov, H. & Shinitzky, M. (1976). Vertical displacement of membrane proteins mediated by changes in microviscosity. *Proc Natl Acad Sci U S A* **73**, 4526-30.
145. Lau, T. L., Dua, V. & Ulmer, T. S. (2008). Structure of the integrin alphaIIb transmembrane segment. *J Biol Chem* **283**, 16162-8.
146. Briggs, M. S., Cornell, D. G., Dluhy, R. A. & Gierasch, L. M. (1986). Conformations of signal peptides induced by lipids suggest initial steps in protein export. *Science* **233**, 206-8.
147. Tamm, L. K. (1991). Membrane insertion and lateral mobility of synthetic amphiphilic signal peptides in lipid model membranes. *Biochim Biophys Acta* **1071**, 123-48.
148. Backlund, B. M., Wikander, G., Peeters, T. L. & Graslund, A. (1994). Induction of secondary structure in the peptide hormone motilin by interaction with phospholipid vesicles. *Biochim Biophys Acta* **1190**, 337-44.
149. Lakey, J. H., Parker, M. W., Gonzalez-Manas, J. M., Duche, D., Vriend, G., Baty, D. & Pattus, F. (1994). The role of electrostatic charge in the membrane insertion of colicin A. Calculation and mutation. *Eur J Biochem* **220**, 155-63.
150. Mikhaleva, N. I., Kalinin, A. E., Molotkovsky Yu, G. & Nesmeyanova, M. A. (1997). Interaction of the E. coli alkaline phosphatase precursor with model phospholipid membranes. *Biochemistry (Mosc)* **62**, 184-90.
151. Yeung, T., Terebiznik, M., Yu, L., Silvius, J., Abidi, W. M., Philips, M., Levine, T., Kapus, A. & Grinstein, S. (2006). Receptor activation alters inner surface potential during phagocytosis. *Science* **313**, 347-51.
152. Yeung, T., Gilbert, G. E., Shi, J., Silvius, J., Kapus, A. & Grinstein, S. (2008). Membrane phosphatidylserine regulates surface charge and protein localization. *Science* **319**, 210-3.

153. Shahidullah, K. & London, E. (2008). Effect of lipid composition on the topography of membrane-associated hydrophobic helices: stabilization of transmembrane topography by anionic lipids. *J Mol Biol* **379**, 704-18.
154. Citri, A. & Yarden, Y. (2006). EGF-ERBB signalling: towards the systems level. *Nat Rev Mol Cell Biol* **7**, 505-16.
155. Marmor, M. D., Skaria, K. B. & Yarden, Y. (2004). Signal transduction and oncogenesis by ErbB/HER receptors. *Int J Radiat Oncol Biol Phys* **58**, 903-13.
156. Olayioye, M. A., Neve, R. M., Lane, H. A. & Hynes, N. E. (2000). The ErbB signaling network: receptor heterodimerization in development and cancer. *Embo J* **19**, 3159-67.
157. Schlessinger, J. (2000). Cell signaling by receptor tyrosine kinases. *Cell* **103**, 211-25.
158. Mi, L. Z., Grey, M. J., Nishida, N., Walz, T., Lu, C. & Springer, T. A. (2008). Functional and structural stability of the epidermal growth factor receptor in detergent micelles and phospholipid nanodiscs. *Biochemistry* **47**, 10314-23.
159. Li, E. & Hristova, K. (2006). Role of receptor tyrosine kinase transmembrane domains in cell signaling and human pathologies. *Biochemistry* **45**, 6241-51.
160. Fantl, W. J., Johnson, D. E. & Williams, L. T. (1993). Signalling by receptor tyrosine kinases. *Annu Rev Biochem* **62**, 453-81.
161. van der Geer, P., Hunter, T. & Lindberg, R. A. (1994). Receptor protein-tyrosine kinases and their signal transduction pathways. *Annu Rev Cell Biol* **10**, 251-337.
162. Blume-Jensen, P. & Hunter, T. (2001). Oncogenic kinase signalling. *Nature* **411**, 355-65.
163. Robertson, S. C., Tynan, J. A. & Donoghue, D. J. (2000). RTK mutations and human syndromeswhen good receptors turn bad. *Trends Genet* **16**, 265-71.
164. Bublil, E. M. & Yarden, Y. (2007). The EGF receptor family: spearheading a merger of signaling and therapeutics. *Curr Opin Cell Biol* **19**, 124-34.
165. Bargmann, C. I. & Weinberg, R. A. (1988). Oncogenic activation of the neu-encoded receptor protein by point mutation and deletion. *Embo J* **7**, 2043-52.
166. Gullick, W. J., Bottomley, A. C., Lofts, F. J., Doak, D. G., Mulvey, D., Newman, R., Crumpton, M. J., Sternberg, M. J. & Campbell, I. D. (1992). Three dimensional structure of the transmembrane region of the proto-oncogenic and oncogenic forms of the neu protein. *Embo J* **11**, 43-8.
167. Weiner, D. B., Liu, J., Cohen, J. A., Williams, W. V. & Greene, M. I. (1989). A point mutation in the neu oncogene mimics ligand induction of receptor aggregation. *Nature* **339**, 230-1.
168. Brandt-Rauf, P. W., Rackovsky, S. & Pincus, M. R. (1990). Correlation of the structure of the transmembrane domain of the neu oncogene-encoded p185 protein with its function. *Proc Natl Acad Sci U S A* **87**, 8660-4.
169. Bargmann, C. I., Hung, M. C. & Weinberg, R. A. (1986). Multiple independent activations of the neu oncogene by a point mutation altering the transmembrane domain of p185. *Cell* **45**, 649-57.
170. Sternberg, M. J. & Gullick, W. J. (1989). Neu receptor dimerization. *Nature* **339**, 587.

171. Sternberg, M. J. & Gullick, W. J. (1990). A sequence motif in the transmembrane region of growth factor receptors with tyrosine kinase activity mediates dimerization. *Protein Eng* **3**, 245-8.
172. Smith, S. O., Smith, C. S. & Bormann, B. J. (1996). Strong hydrogen bonding interactions involving a buried glutamic acid in the transmembrane sequence of the neu/erbB-2 receptor. *Nat Struct Biol* **3**, 252-8.
173. Mendrola, J. M., Berger, M. B., King, M. C. & Lemmon, M. A. (2002). The single transmembrane domains of ErbB receptors self-associate in cell membranes. *J Biol Chem* **277**, 4704-12.
174. Burke, C. L., Lemmon, M. A., Coren, B. A., Engelman, D. M. & Stern, D. F. (1997). Dimerization of the p185neu transmembrane domain is necessary but not sufficient for transformation. *Oncogene* **14**, 687-96.
175. Beevers, A. J. & Kukol, A. (2006). The transmembrane domain of the oncogenic mutant ErbB-2 receptor: a structure obtained from site-specific infrared dichroism and molecular dynamics. *J Mol Biol* **361**, 945-53.
176. Samna Soumana, O., Aller, P., Garnier, N. & Genest, M. (2005). Transmembrane peptides from tyrosine kinase receptor. Mutation-related behavior in a lipid bilayer investigated by molecular dynamics simulations. *J Biomol Struct Dyn* **23**, 91-100.
177. Hunter, T., Ling, N. & Cooper, J. A. (1984). Protein kinase C phosphorylation of the EGF receptor at a threonine residue close to the cytoplasmic face of the plasma membrane. *Nature* **311**, 480-3.
178. Thiel, K. W. & Carpenter, G. (2007). Epidermal growth factor receptor juxtamembrane region regulates allosteric tyrosine kinase activation. *Proc Natl Acad Sci U S A* **104**, 19238-43.
179. Aifa, S., Aydin, J., Nordvall, G., Lundstrom, I., Svensson, S. P. & Hermanson, O. (2005). A basic peptide within the juxtamembrane region is required for EGF receptor dimerization. *Exp Cell Res* **302**, 108-14.
180. Segatto, O., Lonardo, F., Wexler, D., Fazioli, F., Pierce, J. H., Bottaro, D. P., White, M. F. & Di Fiore, P. P. (1991). The juxtamembrane regions of the epidermal growth factor receptor and gp185erbB-2 determine the specificity of signal transduction. *Mol Cell Biol* **11**, 3191-202.
181. McLaughlin, S., Smith, S. O., Hayman, M. J. & Murray, D. (2005). An electrostatic engine model for autoinhibition and activation of the epidermal growth factor receptor (EGFR/ErbB) family. *J Gen Physiol* **126**, 41-53.
182. Ullrich, A., Coussens, L., Hayflick, J. S., Dull, T. J., Gray, A., Tam, A. W., Lee, J., Yarden, Y., Libermann, T. A., Schlessinger, J. & et al. (1984). Human epidermal growth factor receptor cDNA sequence and aberrant expression of the amplified gene in A431 epidermoid carcinoma cells. *Nature* **309**, 418-25.
183. Sato, T., Pallavi, P., Golebiewska, U., McLaughlin, S. & Smith, S. O. (2006). Structure of the membrane reconstituted transmembrane-juxtamembrane peptide EGFR(622-660) and its interaction with Ca2+/calmodulin. *Biochemistry* **45**, 12704-14.
184. Sharpe, S., Barber, K. R. & Grant, C. W. (2000). Val(659)-->Glu mutation within the transmembrane domain of ErbB-2: effects measured by (2)H NMR in fluid phospholipid bilayers. *Biochemistry* **39**, 6572-80.

185. Pfeiffer, K., Gohil, V., Stuart, R. A., Hunte, C., Brandt, U., Greenberg, M. L. & Schagger, H. (2003). Cardiolipin stabilizes respiratory chain supercomplexes. *J Biol Chem* **278**, 52873-80.
186. Kraft, C. A., Garrido, J. L., Fluharty, E., Leiva-Vega, L. & Romero, G. (2008). Role of phosphatidic acid in the coupling of the extracellular-signal regulated kinase (ERK) cascade. *J Biol Chem*.